Sand2001-0054
Unlimited Release
Printed January 2001

Tectonic Setting and Characteristics of Natural Fractures in Mesaverde and Dakota Reservoirs of the San Juan Basin, New Mexico and Colorado

John C. Lorenz and Scott P. Cooper
Geophysical Technology Department
Sandia National Laboratories
P.O. Box 5800
Albuquerque, NM 87185-0750

Abstract

A set of vertical extension fractures, striking N-S to NNE-SSW but with local variations, is present in both the outcrop and subsurface in both Mesaverde and Dakota sandstones. Additional sets of conjugate shear fractures have been recognized in outcrops of Dakota strata and may be present in the subsurface. However, the deformation bands prevalent locally in outcrops in parts of the basin as yet have no documented subsurface equivalent. The immature Mesaverde sandstones typically contain relatively long, irregular extension fractures, whereas the quartzitic Dakota sandstones contain short, sub-parallel, closely spaced, extension fractures, and locally conjugate shear planes as well. Outcrops typically display secondary cross fractures which are rare in the subsurface, although oblique fractures associated with local structures such as the Hogback monocline may be present in similar subsurface structures.

Spacings of the bed-normal extension fractures are approximately equal to or less than the thicknesses of the beds in which they formed, in both outcrop and subsurface. Fracture intensities increase in association with faults, where there is a gradation from intense fracturing into fault breccia. Bioturbation and minimal cementation locally inhibited fracture development in both formations, and the vertical limits of fracture growth are typically at bedding/lithology contrasts. Fracture mineralizations have been largely dissolved or replaced in outcrops, but local examples of preserved mineralization show that the quartz and calcite common to subsurface fractures were originally present in outcrop fractures.

North-south trending compressive stresses created by southward indentation of the San Juan dome area (where Precambrian rocks are exposed at an elevation of 14,000 ft) and northward indentation of the Zuni uplift, controlled Laramide-age fracturing. Contemporaneous right-lateral transpressive wrench motion due to northeastward translation of the basin was both concentrated at the basin margins (Nacimiento uplift and Hogback monocline on east and west edges respectively) and distributed across the strata depth.

Table of Contents

1.0 Introduction.....7
1.1 Purpose of Study.....7
1.2 Location and General Geology.....7
1.3 Previous Work.....10
1.4 Technical Approach.....12

2.0 Tectonic Setting.....13
2.1 Tectonic Elements – Introduction.....13
2.2 San Juan Basin – Central/Inner Basin.....14
2.3 Chaco Slope.....15
2.4 Zuni Uplift.....16
2.5 Gallup Sag.....16
2.6 Acoma Sag.....17
2.7 Defiance Uplift.....17
2.8 Four Corners Platform.....17
2.9 San Juan Uplift.....17
2.10 Archuleta Anticlinorium.....18
2.11 Nacimiento Uplift.....19
2.12 Rio Puerco Fault Zone.....19
2.13 Hogback monocline.....22

3.0 Tectonic Model.....22
3.1 Introduction.....22
3.2 Laramide Tectonics.....22
3.3 Major Structural Elements – San Juan and Zuni Uplifts.....25
3.4 Minor Structural Elements.....28
3.5 Kinematic Model of Stresses and Structural Elements.....30
3.6 Predictions of Fracture Trends.....30

4.0 Outcrop Fracture Descriptions.....32
4.1 Introduction.....32
4.2 Indenter Margins.....32
4.2.1 Southern Margin.....32
4.2.2 Northern Margin.....35
4.3 Wrench Boundaries.....37
4.3.1 Farmington Area.....38
4.3.2 Ute Dome.....39
4.3.3 Nacimiento uplift.....41
4.4 Corners.....41
4.4.1 Archuleta Anticlinorium.....41
4.4.2 The Rio Puerco Fault Zone.....43
4.5 Summary: Distributions of Fracture Intensity and Orientation in Outcrop.....46

5.0 Core Fracture Descriptions.....48
5.1 Introduction.....48
5.2 Characteristics of Fractures in Core.....50
5.2.1 Mesaverde Cores.....50
5.2.2 Dakota Cores.....56
5.3 Core Fracture Summary.....60

6.0 Comparison of Subsurface and Outcrop Fracture Characteristics.....61

7.0 Subsurface Stresses.....62

8.0 Probable Effects of Fractures on Reservoirs.....62
8.1 Introduction.....62
8.2 Permeability Anisotropy.....63
8.3 Influence of Matrix Porosity and Permeability on Fracture Related Permeability Anisotropy.....63
8.4 Summary.....64

9.0 Recommendations for Future Work.....64

10.0 Conclusions.....65

11.0 Acknowledgements.....66

12.0 References.....66

List of Figures

Figure 1: Map of the San Juan Basin.....8
Figure 2: Structure contour map on the base of the Dakota Sandstone.....9
Figure 3: Structure contour map of the San Juan basin.....10
Figure 4: Stratigraphic nomenclature chart.....11
Figure 5: Tectonic elements.....14
Figure 6: Map of the southern San Juan basin.....15
Figure 7: Photograph of bedding-parallel shear.....18
Figure 8:Tectonic map of the Nacimiento uplift.....20
Figure 9: Tectonic map of the Rio Puerco Fault Zone.....21
Figure 10: Map illustrating NE-yielding of the Colorado Plateau.....23
Figure 11: Map of the Colorado Plateau.....24
Figure 12: Seismic lines across the Hogback monocline.....26
Figure 13: Faults and slip-line field southern San Juan Basin.....27
Figure 14: Seismic lines across the Archuleta anticlinorium.....28-29
Figure 15: Tectonic fracture model of the San Juan basin.....31
Figure 16: Fracture map of the Dalton Pass quadrangle.....33
Figure 17: Rose diagram of fracture orientations at Chaco Canyon.....34
Figure 18: Rose diagram of fracture orientations at Cerro Negro.....35

Figure 19: Rose diagram of fracture orientations at Animas Mountain.....36
Figure 20: Fracture map on the Hogback monocline.....39
Figure 21: Rose diagram of fracture orientations at Ute Dome.....40
Figure 22: Rose diagram of fracture orientations at Heron Lake.....42
Figure 23: Photograph of extension fractures at Heron Lake.....42
Figure 24: Rose diagram of fracture orientations near San Ysidro.....43
Figure 25: Models of conjugate shears near San Ysidro.....44-45
Figure 26: Rose diagrams of fracture orientations around the San Juan basin.....47
Figure 27: Map showing locations of measured core.....49
Figure 28: Photograph of calcite mineralization.....50
Figure 29: Photograph of parallel natural fractures.....51
Figure 30: Photograph of natural and induced fractures.....51
Figure 31: Photograph of fracture terminations.....52
Figure 32: Photograph of an irregular extension fracture.....53
Figure 33: Photograph of extension fractures limited by bedding and lithology.....54
Figure 34: Photograph of an unfractured, bioturbated facies.....54
Figure 35: Photograph of core from a deviated well.....56
Figure 36: Photograph of mineralized extension fractures.....57
Figure 37: Photograph of stylolite-related fractures.....57
Figure 38: Photograph of fault breccia.....58
Figure 39: Photograph of large mineralized fractures.....59
Figure 40: Photograph of parallel natural fractures.....59

1.0 INTRODUCTION

1.1 Purpose of study

This work was undertaken in order to provide a geologic framework for reservoir-engineering studies. Specifically, this report provides a characterization of the natural fractures in the natural-gas bearing, sandstone reservoirs of the Mesaverde and Dakota intervals in the San Juan basin of northwestern New Mexico. The questions addressed here concern the origins, orientations, distributions, intensities of natural fractures, and their effects on hydrocarbon reservoirs.

Although the study has been quantitative wherever possible, most of the answers provided to the questions listed above have been qualitative. This is due to the indirect nature of the outcrop data and to the widely-spaced nature of the subsurface data. There are valid questions concerning how well outcrop fracture characteristics can be extrapolated into the subsurface, and how adequate a four-inch diameter core sample is for characterizing many square miles of rock. Development of an understanding of the origins of the San Juan basin fracture system, as an additional task to describing the specifically observable fracture characteristics, has assisted in overcoming some of these limitations. This understanding, or tectonic model, has provided a basis for qualitative extrapolations of fracture characteristics between wells and from outcrops to subsurface.

1.2 Location and General Geology

The San Juan basin of northwestern New Mexico and southwestern Colorado is asymmetric, with the synclinal hinge offset to the northeast of the geographic center of the basin (Figure 1). The Cretaceous Mesaverde and Dakota strata of concern to this report dip gently to the north and northeast over most of the basin. Dips are reversed at the northwest-trending structural hinge of the basin, near the Colorado-New Mexico state line, and dip more steeply back to the southwest in the northern third of the basin (Figure 2).

The inner part of the San Juan basin, approximately delineated by the outcrop belt of the Pictured Cliffs sandstone (Figure 3), contains most of the hydrocarbon production. This domain is separated from the peripheral areas of the basin such as the Four Corners platform and Chama Embayment, on the west and northeast margins respectively, by a seemingly continuous hogback of steeply-dipping strata that is nearly 240 miles long. The Hogback also marks the northern limit of the entire basin. The southern margin of the basin can be separated into an external/peripheral zone of very low dip and the inner, producing basin, approximately along the outcrop of the Cliff House sandstone.

The tectonic elements that ring the inner basin to form the Hogback monocline, and that controlled stresses and thus the fracturing in the basin, are described in detail in a following section. However, it may be noted here that we believe that the structural continuity of this monocline rim is more apparent and coincidental than real. Moreover, our observations suggest that the present configuration of the basin developed during right-lateral, continental-scale wrench faulting along disparate elements of the eastern and western margins of the inner basin,

in combination with north-south directed indentation of basement-cored uplifts at the northern and southern basin margins, during Laramide time. This contrasts with the apparent but misleading inward-directed thrust-fault indentation along the superficially continuous, curvilinear hogback on the north, west and east margins of the basin.

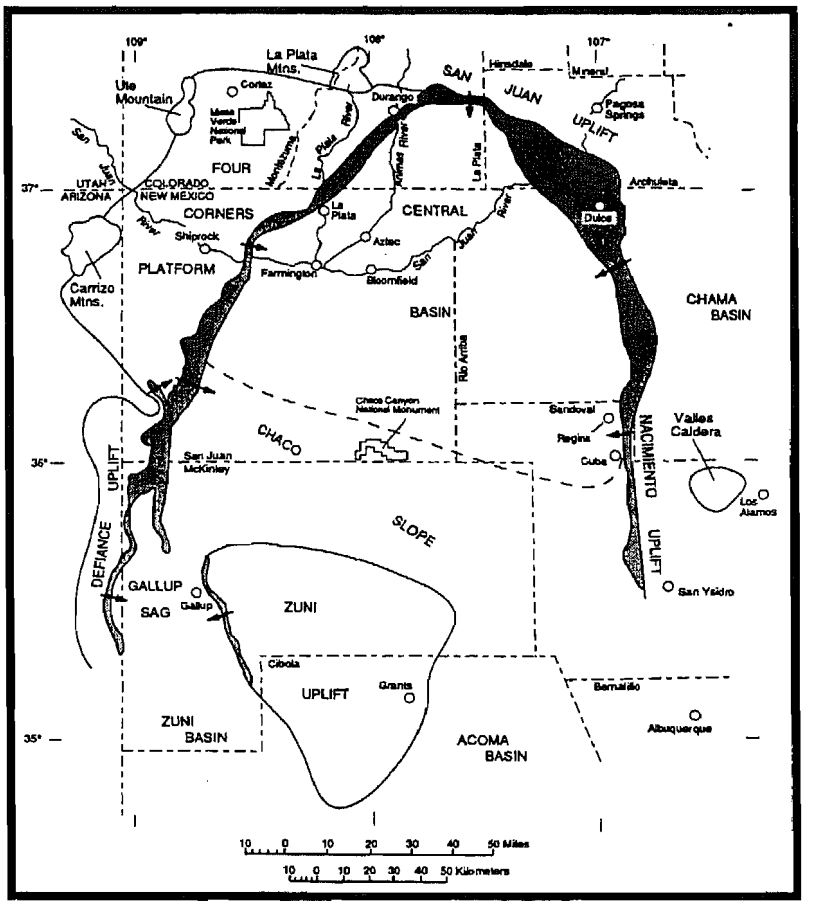

Figure 1: Index map showing the structural elements of the San Juan Basin. Areas of steep dip (monoclines) are shown as patterned areas with the direction of dip indicated by arrows; long dashed line separates the Chaco Slope from the Central Basin and is drawn approximately where the Pictured Cliffs Sandstone is subaerially exposed (modified from Fassett, 1989).

The fractured strata of the Mesaverde and Dakota formations studied for this report crop out at the margins of the basin. Outcrop exposures range from excellent to totally covered in this high desert to mountainous basin. Many outcrops are inaccessible due to ownership and/or topography concerns. The Cretaceous strata extend into the subsurface to depths as great as 8000 ft across the basin, where they have been penetrated by thousands of natural gas wells. Most of these wells were drilled as minimum-cost operations and typically the only geologic information available for them consists of a few basic logs, none useful for fracture identification. Cored wells are rare: what cores exist are unoriented and are typically slabbed with the butts thrown away. Most of the cores studied for this report were originally stored at the Amoco core warehouse in Tulsa, OK. The cores were later bequeathed to the New Mexico Library of Subsurface Data in Socorro, NM, as the Amoco core facility was being dismantled.

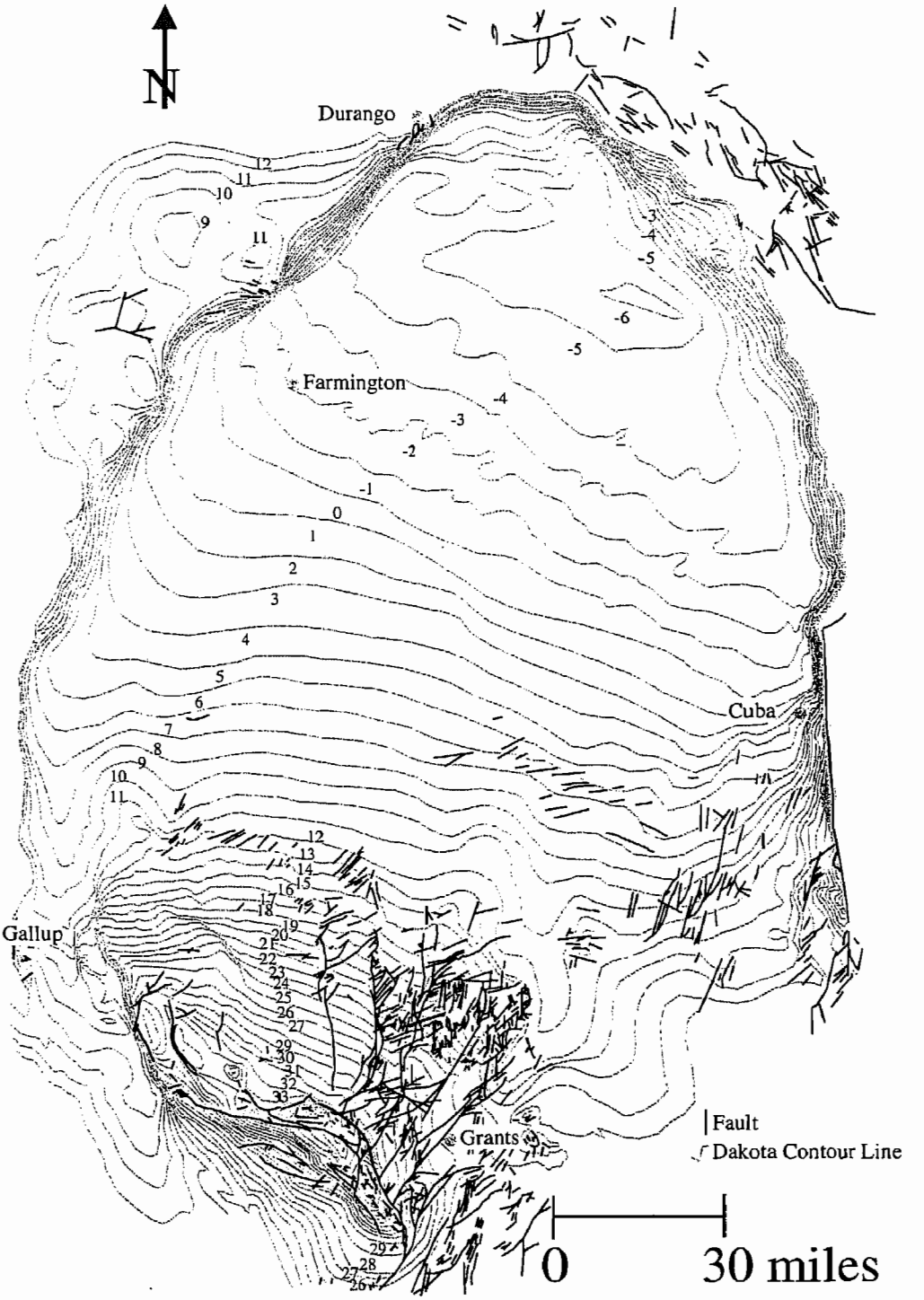

Figure 2: Structure contour map drawn on the base of the Dakota Sandstone. Contour intervals are in meters X100 (modified after Thaden and Zech, 1984).

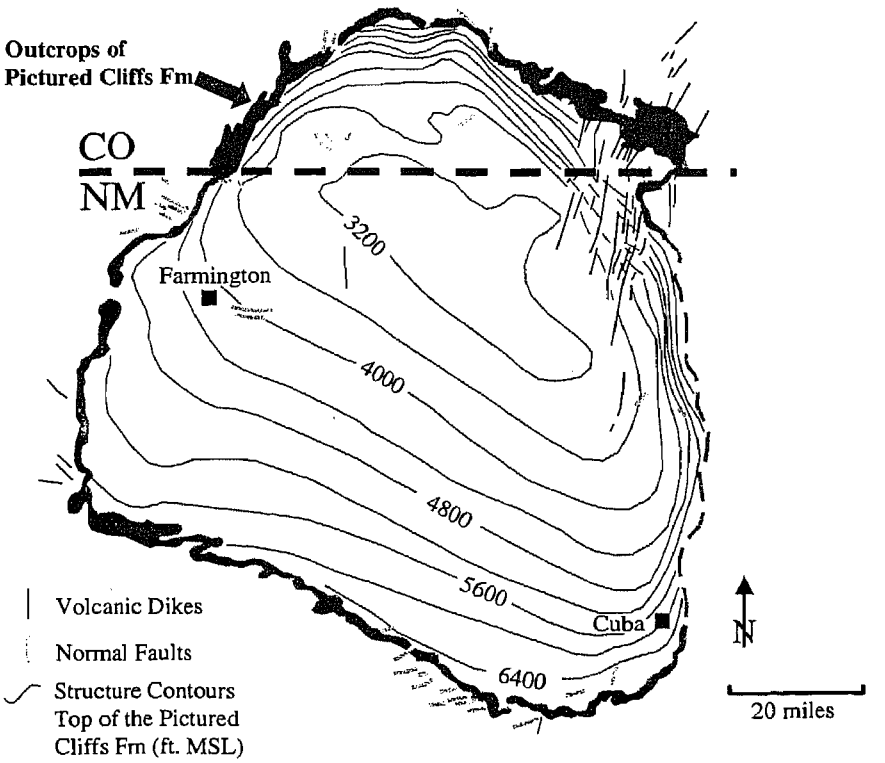

Figure 3: Generalized structure map of the San Juan basin.

Although coalbed methane is also an important resource in the San Juan basin, the fractured Mesaverde and Dakota reservoirs reported on here are sandstone. The component sands are typically very fine to fine-grained and reasonably well sorted. Sandstones of the Mesaverde interval are relatively immature whereas Dakota sandstones are typically very mature, almost quartzites. Cementation varies as well: the Dakota sandstones are commonly very well cemented with siliceous cement except where bioturbation has mixed clays into the sandstones. Mesaverde sandstones are less well cemented, typically with authigenic clay and calcite. This difference in original and diagenetic composition resulted in significantly different mechanical properties, and thus in different fracture characteristics in the two intervals.

A variable and poorly constrained thickness of Tertiary overburden has been stripped from the surface of the basin. As much as 8000 ft of overburden may have been removed from northern parts of the basin (Bond, 1984), the previous deep burial and resulting high overburden stress accounting for the horizontal stylolites that are locally common in many of the Dakota sandstones.

1.3 Previous Work

The Cretaceous stratigraphy of this basin (Figure 4) is reasonably well constrained. Numerous excellent studies have been published addressing this aspect of the San Juan basin geology (e.g., Fassett et al., 1990; Fassett and Hinds, 1971; Owen, 1966; Owen and Siemers, 1977; Turner-Peterson, 1989; Molenaar, 1977; 1988; Ayers et al., 1991). These studies have provided a framework for the fracture studies presented here.

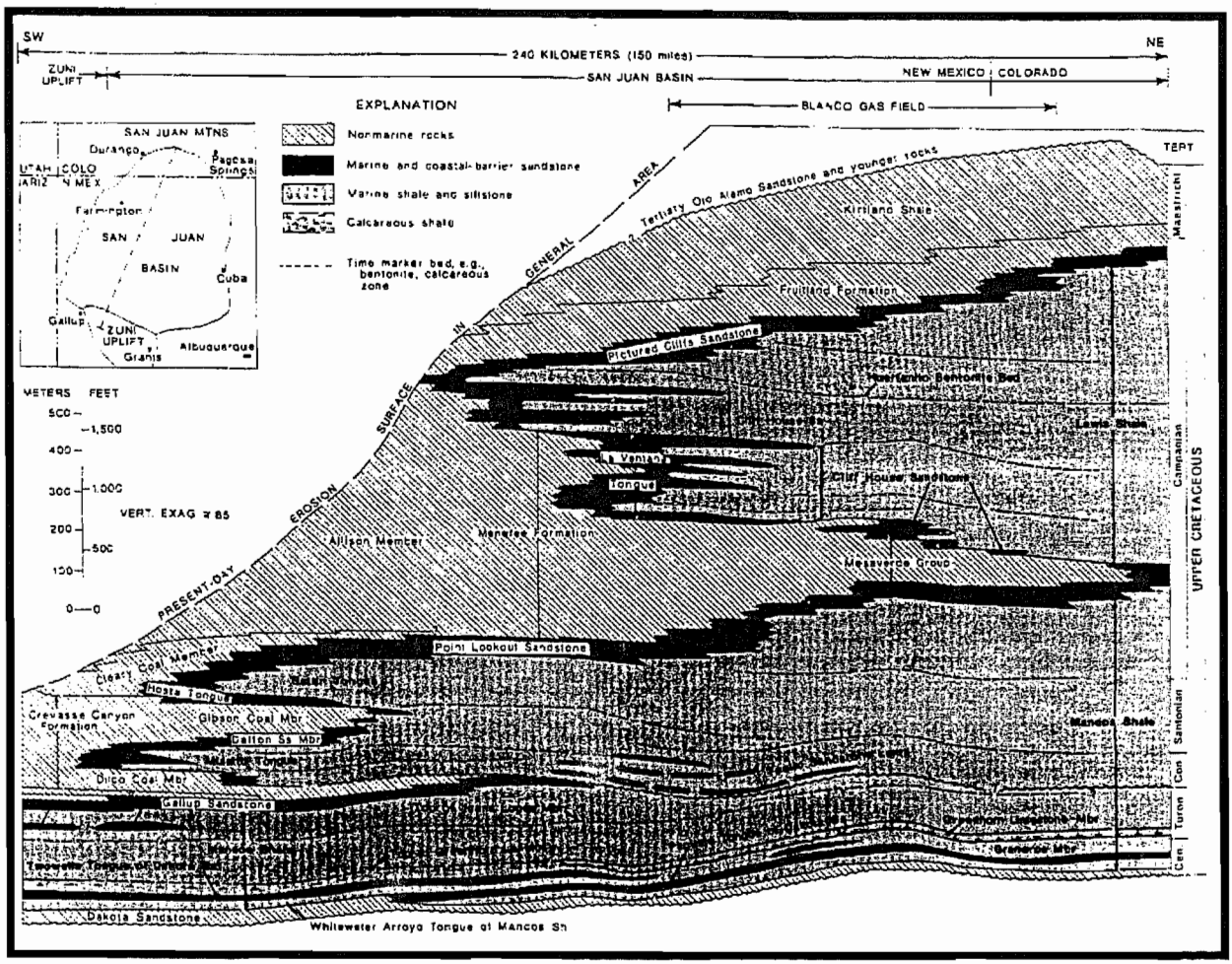

Figure 4: Stratigraphic nomenclature of the San Juan Basin illustrated in cross section from the Zuni uplift to the San Juan uplift (from Molenaar, 1988)

Most previously published structural studies associated with the San Juan basin have either focused on the specific tectonic elements bounding the basin (e.g., the Nacimiento uplift: Woodward, 1987; Baltz, 1967), or have dealt with the basin as a sub-unit within the Colorado Plateau (e.g., Chapin and Cather, 1981; Cather, 1999). Taylor and Huffman (1988; 1998) have published several seismic sections across the monoclines that bound the inner basin, and these suggest locally significant thrust indentation and overhang at the basin margins. As described below, we suggest that these geometries may be explained by transpressional wrench faulting.

Previous studies of the natural fractures in the San Juan basin have been primarily descriptive, and have concentrated on fractures in outcrops of Mesaverde strata, both in the coals (cleats) and in the sandstones (e.g., Whitehead, 1997; Tremain et al., 1991; Laubach, 1992). These studies have suggested that fractures in Mesaverde strata cropping out in the northern part of the basin trend NW-SE to NNW-SSE, whereas fractures in the surface strata at the southern edge of the basin trend N-S to NNE-SSW.

These studies have typically mixed natural fracture orientations from coal cleats and natural fractures in sandstones, thereby obscuring regional tectonic interpretations. As noted by Condon, (1988, 1997), coal cleats strike oblique to the fractures in adjacent sandstones more often than not, and thus the two systems should be separated for the purposes of tectonic reconstructions.

Kelley (1957) and Kelley and Clinton (1960), as part of their aerial-photo study of fractures on the Colorado Plateau, noted that several irregular domains of relatively uniform fracture strikes were visible in the San Juan basin at the scale of air-photo interpretation. The scale of their study did not permit detailed examination and assessment of the fractures at ground level. Tremain et al. (1991) have also proposed boundaries for fracture domains in the San Juan basin based on outcrop work, their domains not coinciding with Kelley and Clinton's domains. Whitehead (1997) has suggested that many of the fractures in outcrops, particularly on the Chaco Slope, are due entirely to surficial, valley-wall processes.

Other published sources of descriptive fracture data include an obscure set of reports sponsored by the old Atomic Energy Commission, which investigated fracture controls on uranium distribution (e.g., Gilkey, 1953), and several of the USGS geologic quadrangle maps that cover areas along the southern edge of the basin. Among the few fracture studies that both described and interpreted fractures are two papers by Condon (1988, 1997), which concern fractures in the strata along the basin-bounding monoclines on the northern and northwestern sides of the basin.

The observations of the San Juan basin fractures reported here are compatible with most of these early findings, though we offer slightly different interpretations. We suggest that the outcrop fracture domains described by previous authors and extrapolated across the basin may be spurious, as we feel that they are both too broad and based on a mixed data set of coal cleats and sandstone fractures that formed at different times.

Previous subsurface studies have inferred fractures in the local reservoirs based on several indirect criteria including seismic associations with faults (e.g., TerBest, 1997; DuChene, 1989), anomalous production (e.g., Emmendorfer, 1992; Gorham et al., 1979, Ouenes et al., 1998) or enhanced injectivity (e.g., Hawkins et al., 1977). The fracture patterns are typically assumed to have been caused by or at least enhanced by flexures. However, few actual subsurface fracture data have been published to date. Ortega and Marrett (2000) have published Mesaverde microfracture data for three wells in the central part of the basin, while Lorenz et al. (1999) presented a preliminary synthesis of the tectonic framework of the basin that was based primarily on measured fracture characteristics in Dakota core. The following interpretations build on the Lorenz et al. conclusions, expanding them to encompass Mesaverde reservoirs.

1.4 Technical Approach

The questions of fracture origins, orientations, distributions, intensities, and effects on reservoirs were addressed through a combination of outcrop and subsurface study supported by a literature search. Outcrops of Mesaverde and Dakota strata around the rim of the San Juan basin were located and assessed for their potential contribution to fracture characterization and

interpretations of fracture origin. The outcrops studied are on public lands; numerous other outcrops that might also have contributed to this study were inaccessible due to locations on private or tribal lands (much of the western part of the basin). Other well-exposed outcrops were inaccessible due to steep topography or cover (most common in the northern part of the basin). Fracture characteristics such as orientation, spacing, length, mineralization, surface ornamentation, and geometric relationships to local structure were noted, though not all criteria were displayed at each outcrop. These data were amassed in field notes and distilled into the rose diagrams and descriptions presented below.

The subsurface data source for this study consisted almost exclusively of core. Typical available cores were the slabbed ribbons of four-inch diameter archived cores. Unfortunately, much of the information contained in the core butts, and inherent in being able to lock adjacent core pieces together to form lengths of core (see Lorenz and Hill, 1991), had been lost long before this study began. Few in situ core orientations were available, thus the in situ fracture orientations could only rarely be reconstructed. The important core fractures were photographed, and a qualitative estimate was made of fracture intensity and distribution. Fracture characteristics such as mineralization, vertical termination locations, surface ornamentations, and orientations relative to the in situ stress indications provided by petal fractures, were noted. The data were compiled on core logs and distilled into the verbal descriptions given below.

In addition to the core and outcrop studies, a literature search was made in order to provide the background for a synthesis of the fractures within the context of the local and regional structures and tectonics. That synthesis is provided in the Tectonic Model section.

2.0 TECTONIC SETTING

2.1 Tectonic Elements – Introduction

Although the inner parts of the San Juan basin appear to be relatively without structure other than gentle, regional dips, there are significant tectonic elements that surround the basin and that acted in concert to produce not only the present basin configuration but also fractures in the reservoirs. The major structures surrounding the basin are described here, along with their documented tectonic dynamics. In addition to these structures, the basement underlying the basin contains numerous geologically old faults that were reactivated in concert with activity of the basin-margin structures, although the effects of that reactivation on the overlying stratigraphic column are poorly known.

The San Juan basin is situated between the San Juan uplift to the north, the Zuni uplift to the south, the Defiance uplift to the west, the Nacimiento uplift to the east, and the Archuleta anticlinorium to the northeast (Figure 5). Although less important to tectonic reconstructions, other structural elements of the San Juan basin include the Four Corners platform, the Chaco slope, the Central basin, the Rio Puerco fault zone, the Acoma sag, and the Gallup sag. The Hogback monocline is the demarcation between the Four Corners platform and the inner basin.

The major tectonic elements around the basin as well as the basin itself are largely the result of deformation during the Laramide orogeny (Kirk and Condon, 1986). The Laramide

orogeny lasted from about 75 to 35 million years ago, starting during the latest Cretaceous and continuing into the Eocene (Dickinson and Snyder, 1978; Chapin and Cather, 1983; Bird, 1998). Some of these structures were reactivated during Tertiary rifting associated with the Rio Grande rift, including the Rio Puerco fault zone and the Nacimiento uplift (Kelley, 1957; Slack and Campbell, 1976; Woodward, 1987).

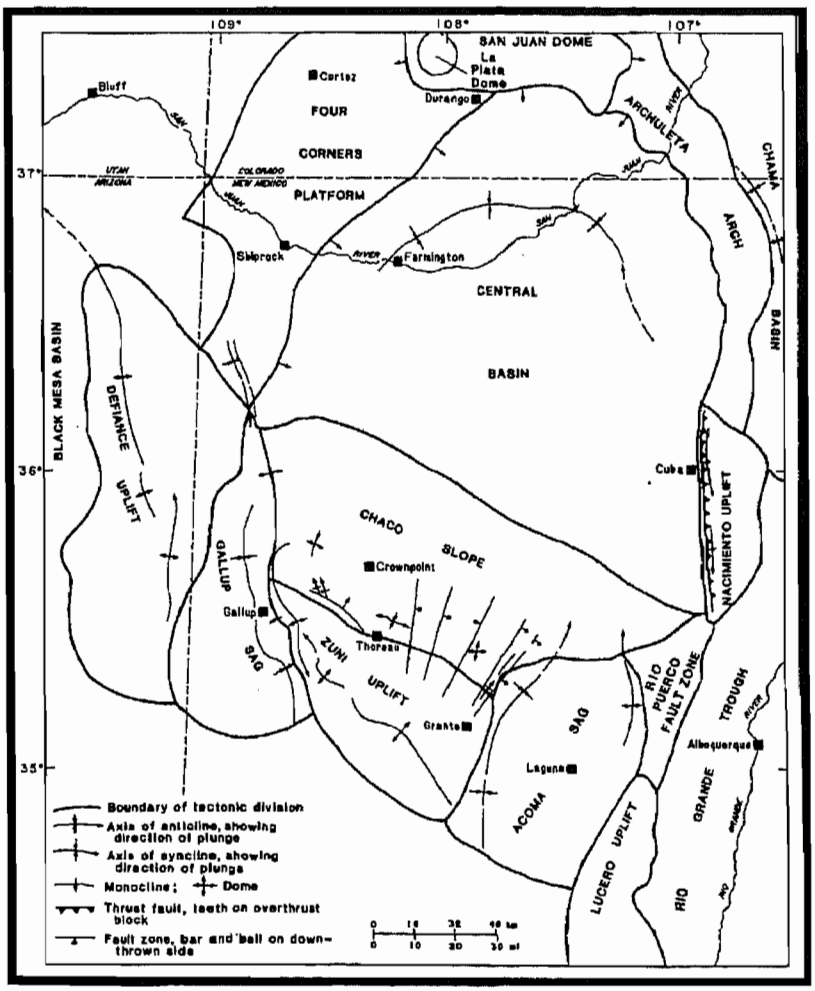

Figure 5: Tectonic elements of the San Juan basin area (modified from Kirk and Condon (1986) after Kelley (1963).

2.2 San Juan Basin – Central/Inner Basin

The central or inner part of the San Juan basin covers an area of approximately 7500 square miles and has a diameter of roughly 100 miles (Fassett, 1989). The basin is asymmetric with the northwest-striking axis of the basin nearer to the northeastern rim. Dips along the monoclines which surround the basin on the west, north and eastern sides generally range between 20°-40°, whereas dips along the remainder of the basin range from less than 1° up to 2° (Fassett, 1989). Near-vertical to overturned beds are recorded at specific locations, particularly along the Nacimiento uplift at the eastern edge of the San Juan basin (Baltz, 1967).

The inner basin is underlain by Proterozoic crystalline basement with numerous ancient faults trending NE-SW and NW-SE (Taylor and Huffman, 1998). Fault spacing, where known, is on the order of 4-10 miles. These faults have been reactivated at various times and in various fashions through geologic history, although only the vertical component of motion can be seen on seismic lines. Some have been reactived as thrust faults, and it is likely that the Hogback monocline, thrusted at depth (Taylor and Huffman, 1988) overlies a family of some of the more important basement faults. Small folds and anticlines, a few tens of feet in relief, are apparent on structure contour maps of the inner basin where well spacing is close enough to delineate them and where three-dimensional seismic data are available.

2.3 Chaco Slope

The Chaco slope is the passive structural transition between the Zuni uplift and the inner basin. It is an area of relatively gentle northward dip, variable between 2°–10° to the north or northeast. Several deformational events have broadly folded and faulted the sedimentary rock units within this area, the main one being Laramide indentation from the south by the Zuni uplift (Chamberlin and Anderson, 1989). The current character of the Chaco slope is related to uplifting during the Laramide orogeny. Fault intensity increases from west to east across the slope, reaching a maximum just opposite the northeastern corner of the Zuni uplift. The few faults in the western half have only minor offsets. Fault strike also varies from northerly in the western section to northeasterly in the eastern section of the slope (Figure 6) (Kirk and Condon, 1986).

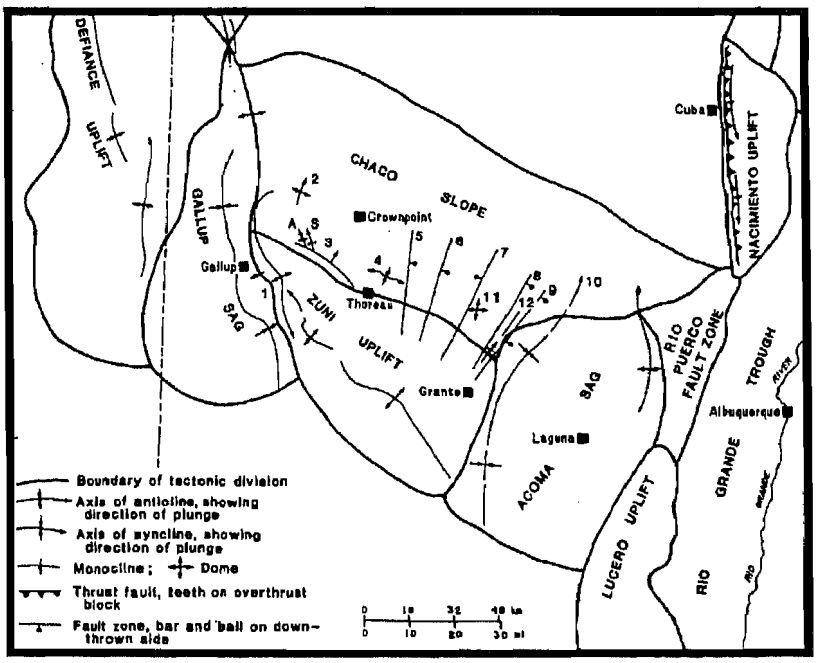

Figure 6: Structures along the southern San Juan basin area; A = anticline, S = syncline, 1 = Nutria monocline, 2 = Coyote Canyon anticline, 3 = Pinedale monocline, 4 = Mariano Lake-Ruby Wells anticline, 5 = Bluewater fault zone, 6 = Big Draw fault zone, 7 = Ambrosia fault zone, 8 = San Mateo fault zone, 9 = San Rafael fault zone, 10 = McCartys syncline, 11 = Ambrosia dome, 12 = McCartys arch (modified from Kirk and Condon (1986) after Kelley (1963)).

2.4 Zuni Uplift

The Zuni uplift is a deceptively small tectonic unit that played a major role in fracturing of the Cretaceous strata in the San Juan basin. This northwest-striking asymmetric uplift has its steepest limb along the southwestern edge, with only minor structures marking its northern border with the San Juan basin. It is 70 miles long and 35 miles wide with 8,000 ft of structural relief between the highest parts of the uplift and the base of the adjacent Gallup sag. Over 13,000 ft of structural relief exists between the uplift and the deepest part of the San Juan basin approximately 140 miles to the northeast (Kelley, 1955; Woodward and Callender, 1977).

With the exception of some small-scale monoclines, the Zuni uplift merges, with a gradual dip, with the Chaco slope to the north. Bedding dips average between 3° and 10° to the NE along the northeastern boundary. This area is broken by numerous north to northeast striking faults with straight-line segments from 18-30 miles long, including the San Rafael, San Mateo, Ambrosia, Big Draw and Bluewater fault zones. A smaller, less pervasive set of faults, striking northeast to east-northeast, is situated between or branches off from the larger faults (Kelley, 1967; Thaden and Zech, 1984). The Nutria monocline marks the western margin of the uplift and is 32 miles long by 1-2 miles wide. The monocline has dips ranging from low to slightly overturned (Kelley, 1967).

The Zuni uplift has had a compound tectonic history, going back at least as far as the late Paleozoic time when Pennsylvanian strata thickened north of the Zuni uplift indicating contemporaneous differential movement (Jentgen, 1977). Uplift in the Jurassic is recognized by depositional patterns within the Morrison (Kirk and Condon, 1986), by an unconformity at the base of the Dakota Sandstone, and by folds below that unconformity (Hilpert, 1969; Santos and Turner-Peterson, 1986). The present configuration of the Zuni uplift was essentially achieved during the Laramide orogeny (Kirk and Condon, 1986; Chamberlin and Anderson, 1989).

Chamberlin and Anderson (1989) suggest that the Zuni uplift is the result of Laramide indentation-extrusion tectonics. The indenter in this case was the rigid El Morro gravity high, which was interpreted to be a Precambrian igneous belt, that was pushed northward into the San Juan basin, with large slivers of material shoved aside to the east and west by the indentation. Indentation action also extruded the core of the Zuni uplift vertically and to the northwest, forming the Nutria monocline. The authors suggest as much as 3 miles of left-lateral slip along the western margin of the El Morro gravity high near Fence Lake, an indication of the order of magnitude of indentation.

2.5 Gallup Sag

The Gallup Sag lies west of the Nutria monocline, between the Zuni uplift and the Defiance uplift. The sag, a passive remnant between two highs, is approximately 70 miles long by 8-28 miles wide (Kelley and Clinton, 1960; Kelley, 1967). Kelley (1967) describes the sag as a narrow embayment extending from the San Juan Basin southward to where it gradually merges with the Mogollon slope. The synclinal axis of the sag is nearer to Nutria monocline (i.e. the western side of the Zuni Uplift), suggesting, as does the asymmetric Acoma sag on the opposite side of the Zuni uplift, that the uplift was thrust over and onto adjacent pieces of the crust. The

Gallup sag plunges gently, approximately 60 ft per mile, to the north and has a relatively flat bottom (Sears, 1925; Kelley, 1967).

2.6 Acoma Sag

The Acoma sag is another passive unit, bounded by the Zuni uplift to the west, the Chaco slope to the northwest, the Rio Puerco fault zone to the northeast, and the Lucero uplift to the southeast. The sag is approximately 25 miles wide by 50 miles long (Kelley, 1957). The synclinal axis of the sag is near the eastern border of the Zuni uplift. The structural axis of the sag, known as McCartys syncline, plunges very gently to the north, and has been intruded by the volcanics of Mount Taylor.

2.7 Defiance Uplift

The Defiance uplift is peripheral to the San Juan basin on the west side, and consists of a north-striking asymmetric uplift with the steepest limb along the eastern edge. The uplift is 95 miles long by 35 miles wide. The eastern limb is defined by the Defiance monocline, which dips 20°-90° to the east. The sinuosity of the monocline is due to several southeast plunging anticlinal and synclinal cross-folds, including the Lukachukai monocline (Kelley, 1967; Woodward and Callender, 1977), that give the Defiance monocline an en echelon character indicating a component of right-lateral movement (Kelley, 1967; Woodward and Callender, 1977).

2.8 Four Corners Platform

The area west of the Hogback monocline and between the Defiance and the San Juan uplifts is termed the Four Corners platform (Kelley, 1950). The platform forms the northwestern boundary of the San Juan basin at the Hogback monocline. While the monocline has approximately 4,000 ft of structural relief (Woodward and Callender, 1977), there is very little topographical relief within the platform itself: the platform is a relatively flat and wide feature (Kelley, 1950; Thaden and Zech, 1984). The boundary between the platform and the inner basin is marked by several anticlines and domes, such as Ute Dome and Barker Dome, suggesting that the boundary is the result of wrench faulting along an irregular fault.

2.9 San Juan Uplift

The San Juan uplift or 'dome', lying immediately north of the San Juan basin, is inferred here to have been a major structural component of the San Juan tectonic system. However, it has been partially obscured by Tertiary volcanism, and, like the Zuni uplift, it is deceptively small. This structure is roughly circular and approximately 60 miles in diameter. Structural relief from the top of the uplift to the deepest portions of the basin is approximately 20,000 ft. This occurs over a distance of approximately 35 miles, but much of it (11,500 ft) is taken up across a much shorter distance within the Hogback monocline, where dips range up to 90° but are generally between 40°-60°.

The Needle Mountains are situated along the southwestern edge of the San Juan uplift and are a Laramide-age structure (Steven, 1975; Kelley, 1957). Orientation of sedimentary

structures within the braided fluvial Ojo Alamo Sandstone of early Tertiary age indicate south (Sikkink, 1986) to southeastern (Powell, 1973) flow, away from this developing uplift (Fassett, 1991; Steven, 1975). Volcanic activity at the San Juan volcanic center during Tertiary time has covered much of the San Juan uplift with volcanic and volcaniclastic strata, although Steven (1975) suggests that the central Precambrian core of the Needle Mountains stood as a series of hills that were never completely covered. The volcanic rocks spread around the uplift and covered the northern part of the San Juan basin, where the stratigraphically equivalent upper part of the Animas Formation is composed of course-grained sandstones and conglomerates with numerous volcanic clasts. This formation is as much as 2700 ft thick in the northern part of the basin and may represent continued subsidence along the northern edge of the San Juan basin during deposition (Fassett, 1991).

Although poorly exposed, small east-west striking, southward-verging thrust faults have been mapped in the surface and subsurface (e.g., Taylor and Huffman, 1998) on the southern side of the San Juan Dome. Our field studies have documented southward-directed bedding-plane slip (Figure 7) in Jurassic strata north of Durango. The fact that Precambrian crystalline strata are now exposed at the surface at an altitude of over 14,000 ft suggests that this Laramide uplift was not unlike the larger Uinta uplift (where Precambrian strata have been elevated to only some 13,000 ft). We suggest that it was indented southward into the San Juan basin, forming the east-west trending section of the Hogback monocline, and was a major source of compressive stress far out into the basin.

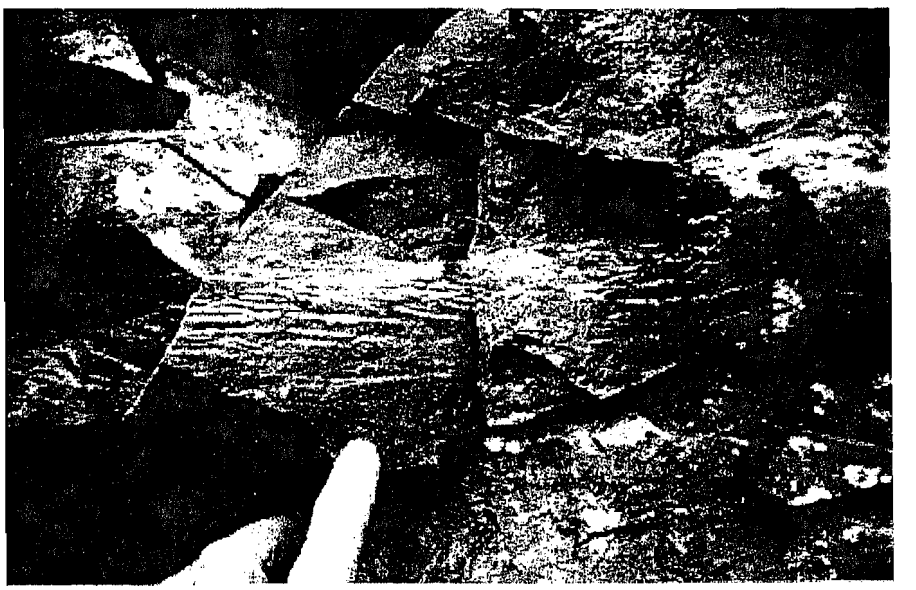

Figure 7: Southward-directed bedding-plane parallel shear in Jurassic strata, Hidden Valley north of Durango, Colorado.

2.10 Archuleta Anticlinorium

The generally north-striking Archuleta anticlinorium is a series of broad, northwest-striking, parallel folds that delineate the amorphous northeastern boundary of the San Juan basin. There is approximately 13,000 ft of structural relief between the highest portion of the

anticlinorium and the San Juan Basin, but only 1,500 ft of relief relative to the Chama basin to the east. Exceptions to the northwest-striking folds exist near Tierra Amarilla where fold axes strike west northwestward (Muehlberger, 1967; Woodward and Callender, 1977). Small, elevated blocks of Precambrian crystalline rock are present on the northeastern margin of the Chama basin, but their function in the tectonic system of the San Juan basin is unclear.

2.11 Nacimiento Uplift

The Nacimiento uplift is formed by a series of north-striking tilted Precambrian blocks, sticking up like a sore thumb at the southeastern edge of the San Juan basin, with at least 10,000 ft of total structural relief relative to the adjacent basin. North-striking normal faults parallel to the main Nacimiento front delineate smaller tilted blocks. Different segmented blocks are separated by faults striking east-west, northeast and northwest (Woodward et al., 1972). These faults are interpreted to have taken up some of the differential movement between individual fault blocks (Woodward and Callender, 1977). The northern end of the uplift is essentially a faulted anticline that plunges 10-20° to the north to merge with the Archuleta anticlinorium. The southern limit of the uplift consists of smaller folds that die out to the south (Slack, 1973).

The Nacimiento uplift has had a compound history. The first period of major uplift was associated with the Laramide orogeny, consisting of two phases. An early phase of right-lateral motion is recorded by remnants of NNW-SSE striking en echelon folding along the western margin of the uplift (Figure 8) (Baltz, 1967; Woodward et al., 1972; Woodward et al., 1992). Right lateral offset along the western margin of the Nacimiento uplift at this time has been interpreted to be on the order of 2-3 miles (Woodward et al., 1992; Baltz, 1967). The early phase was followed by transpressive, right-lateral wrench faulting during later Laramide time, leading to overthrusting in the sedimentary units and minor overhang immediately west of the uplift (Woodward et al., 1972; Woodward, 1983; Woodward, 1987). Secondary reactivation of the uplift occurred during late Tertiary time and was associated with extensional faulting along the Rio Grande rift (Kelley, 1957; Woodward, 1987).

2.12 Rio Puerco Fault Zone

The southern end of the Nacimiento uplift transitions abruptly into the Rio Puerco fault zone (Figure 9). Slack and Campbell (1976) describe three major structures within this zone, from north to south these are: 1) northwest striking en echelon folds, 2) northeast striking en echelon normal faults and 3) the Ignacio-Lucero monocline.

The en echelon folds extend along the western edge of the Nacimiento uplift, striking from 135-315° to 160-340°. Some folds near the southern plunging area of the Nacimiento uplift strike 350° to 5°. Slack and Campbell (1976) suggest these en echelon folds as well as the en echelon faults are the result of right lateral wrench movement, the total amount of offset being probably less than 1.5 miles. The wrench related structures are related to an early phase of Laramide deformation wherein right-lateral deformation was induced by north-northeast directed stresses (Slack and Campbell, 1976).

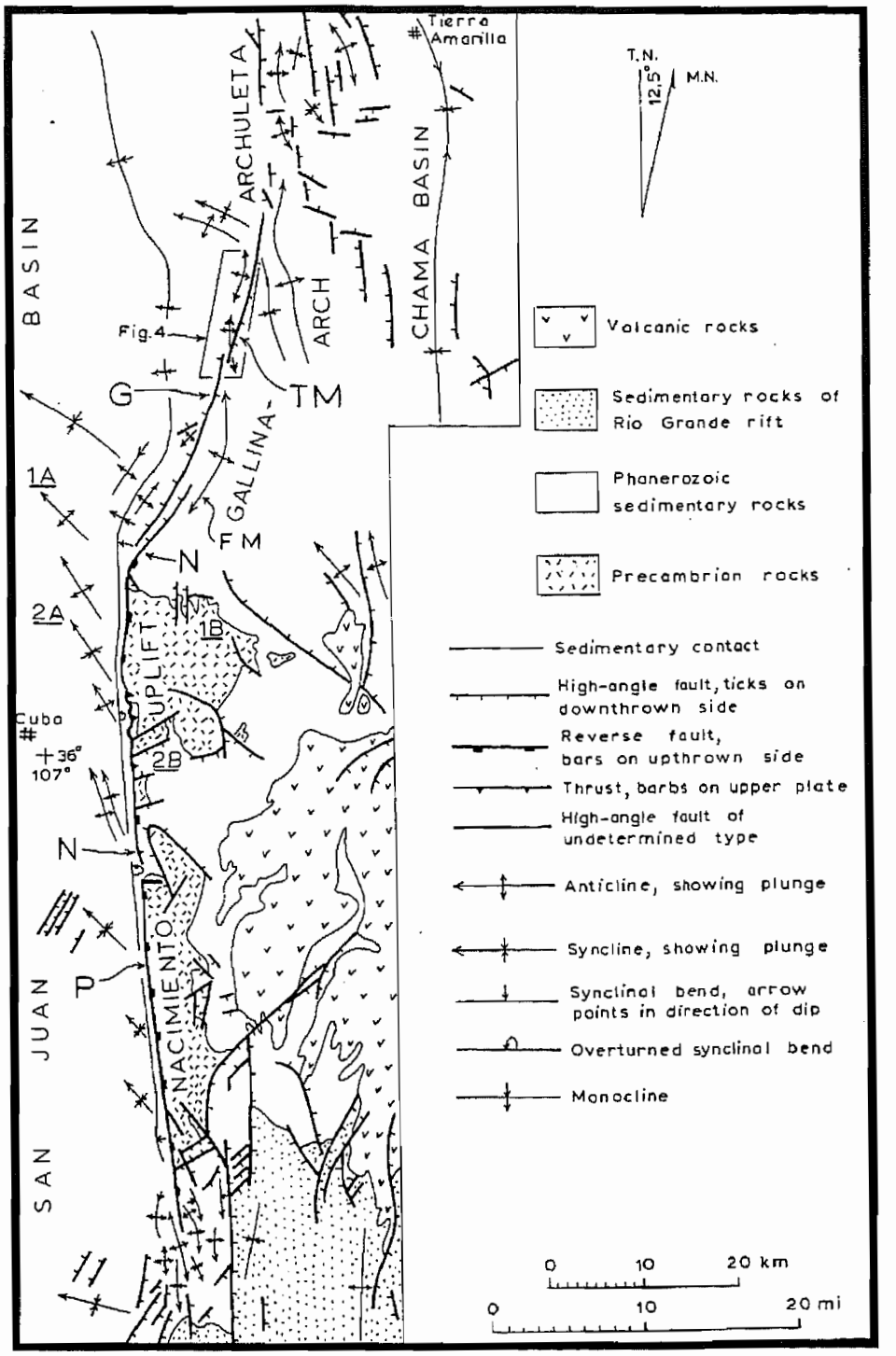

Figure 8: Tectonic map of the Nacimiento uplift area (Woodward, 1992).

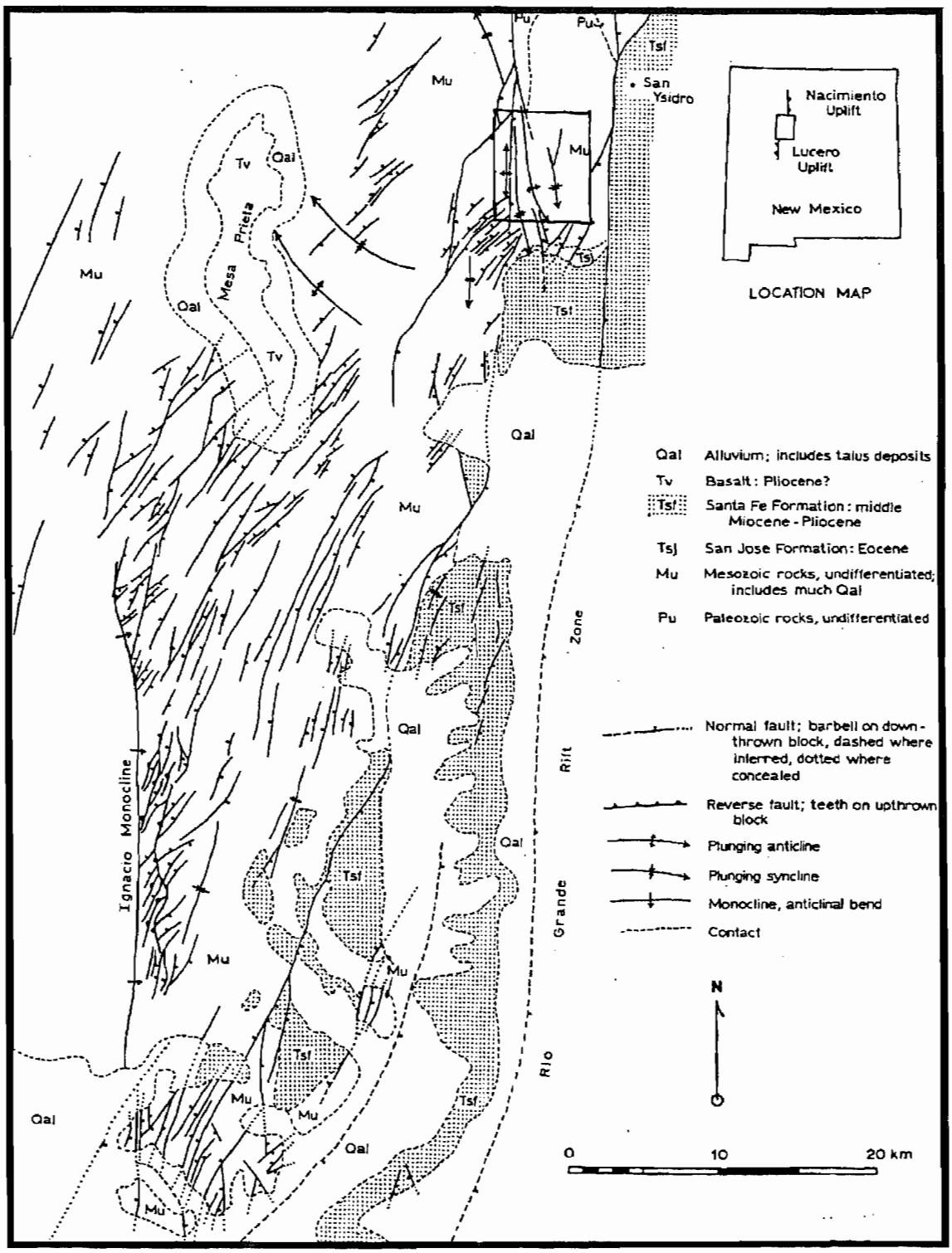

Figure 9: Tectonic map of the Rio Puerco Fault zone (Slack and Campbell, 1976).

2.13 Hogback monocline

The Hogback monocline northwest of Farmington is typically interpreted to be an eastward to southeastward-directed thrust fault. Two-dimensional seismic lines across it (Taylor and Huffman, 1988) show a downward-flattening fault with both normal and reverse senses of motion depending on the age of offset. Huffman and Taylor (1999) however, have suggested that this zone of structural weakness has also accommodated right lateral shear of unknown but important offset. The inward-dipping Hogback monocline actually extends as a traceable though discontinuous unit around much of the inner basin. Although Huffman and Taylor (1999) have published seismic cross sections showing inward-directed, sled-runner thrust planes in front of many of these monoclines, the loosely connected segments of variable dip and displacement are not the record of a single structural noose constricting the basin. Rather, we believe that they are the circumstantially aligned expressions of en echelon segments of right-lateral wrenching on the eastern and western margins of the basin, combined with southward-vergent thrust faulting from the San Juan uplift area at the northern margin of the basin.

3.0 TECTONIC MODEL

3.1 Introduction

The individual structural elements and their inferred kinematics can be incorporated into a conceptual model of the tectonic dynamics of the San Juan basin within its Laramide setting. This model can then be used to estimate Laramide stress trajectories across the basin, and ultimately used to predict the probable orientations of natural fractures that formed under these conditions. This model can be compared with the empirical fracture patterns in the outcrops and subsurface described below, and the patterns used to support and/or modify the model as necessary. The model is presented first in this report, with the supporting fracture data given later, so that the reader will have a context for the fractures when they are described.

3.2 Laramide Tectonics

The Laramide orogeny, extending from approximately 75 to 35 million years ago, was the first tectonic event to influence the San Juan basin following deposition of Dakota and Mesaverde strata. Varied phases of Laramide deformation, with or without stress rotation, have been suggested, including an early E-W oriented stress and a later stress orientation of NE-SW to nearly N-S (Kelley, 1955; Chapin and Cather, 1981; Chapin and Cather, 1983; Gries, 1983). More recent work suggests that there was no systematic geographic variation in the onset or cessation of Laramide deformation, nor significant variability in its stress orientations at crustal levels (e.g., Cross, 1986; Dickinson et al., 1988; Bird, 1998). Rather, the diverse Laramide structural trends observed around the Rocky Mountain region are inferred to have occurred contemporaneously. Although large-scale rotations of regional, Laramide, crustal-level stresses did not occur, there is evidence for a change in the intensity of deformation through time. Typically the Laramide blocks underwent an early phase of low but broad-scale uplifting during the Late Cretaceous, and a later, more intense phase of more localized uplifting in Eocene time (Bird, 1998).

The underlying mechanism for the Laramide orogeny is inferred to have been flat-plate/horizontal subduction, and traction between the top of the subducting Farallon slab and the base of the crust of the Rocky Mountain region (e.g., Dickinson et al., 1988; Bird, 1998; Lowell, 1974; Dickinson and Snyder, 1978). According to Bird, the average flow vector for the subducted slab was stable at 40° during the majority of the orogeny but changed to 55° for the last 10-15 million years.

Regional, base-of-the-crust traction provided a mechanism for both pervasive deformation across the San Juan basin and the formation of local basement-block uplifts. During the Laramide orogeny, the Colorado Plateau, encompassing the San Juan basin, was translated northeastward with respect to the Rocky Mountain foreland (Figures 10, 11), and rotated several degrees clockwise about a pole in northern Texas (Kelley, 1955; Woodward and Callender, 1977; Chapin and Cather, 1981; Woodward et al., 1997; Bird, 1998). Related northeastward yielding is evidenced by numerous northeast-facing folds of Laramide age within the Cordilleran Foldbelt of southwestern New Mexico (Corbitt and Woodward, 1973).

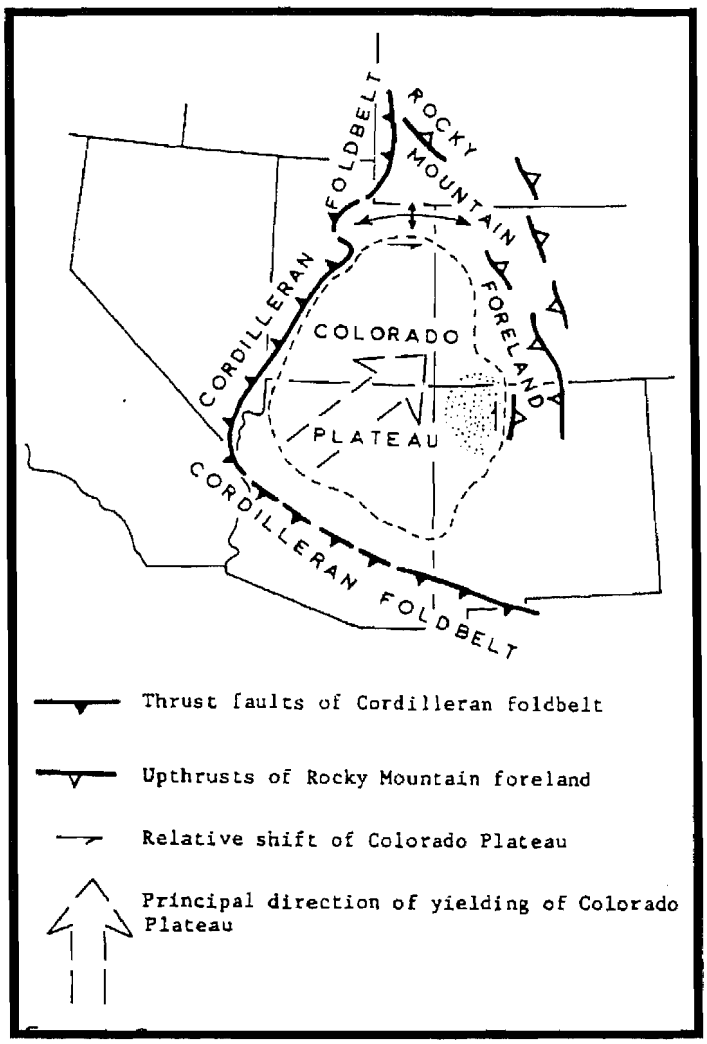

Figure 10: Map illustrating the northeastward yielding of the Colorado Plateau (Woodward et al., 1992).

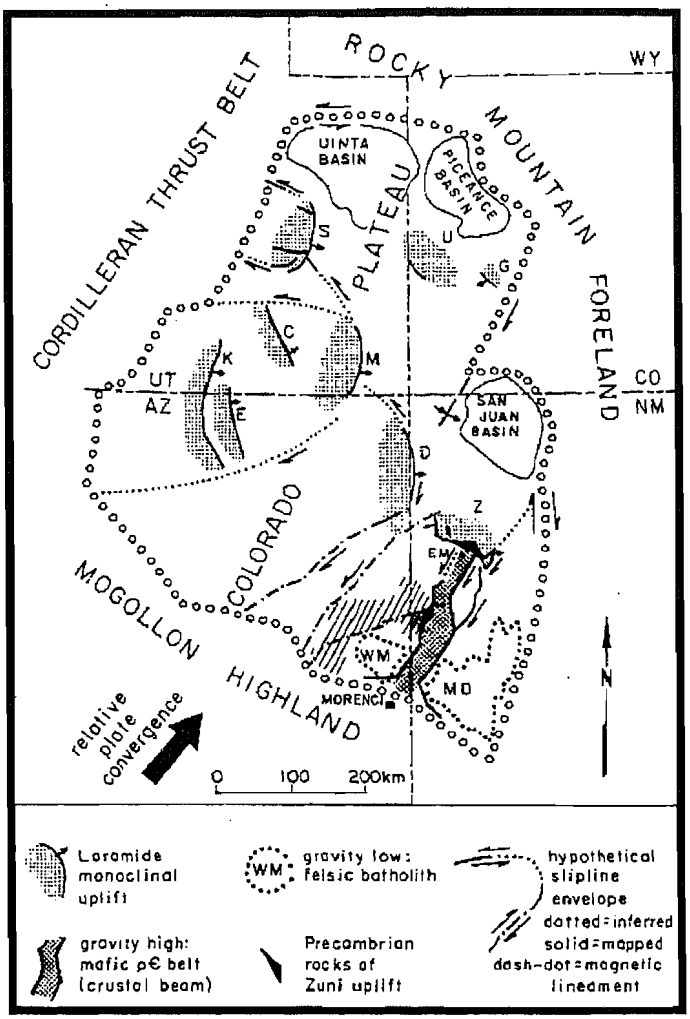

Figure 11: Map showing the location of the San Juan basin and the Zuni (Z) uplift with respect to other Laramide structures within the Colorado Plateau and the general NE yielding of the Colorado Plateau. The El Morro Gravity high (EM); S = San Rafael, C = Circle Cliffs, M = Monument, K = Kaibab, E = Echo Cliffs, U = Uncompahgre, G = Gunnison, D = Defiance, WM = White Mountains, and MD = Mogollon-Datil volcanic fields (Chamberlin and Anderson, 1989).

Thus there was a general northeastward-directed maximum horizontal stress at the deep level of the basal crust during the Laramide orogeny in New Mexico, jostling basement blocks (defined by ancient faults in the crust) against one another. Laramide structures of varied orientations reflect heterogeneous strain due to shear between the heterogeneous continental lithosphere and the low-angle subducting Farallon plate. Preexisting basement faults responding to this differential shear simultaneously produced deformation trends of varied orientation. The orientations of the pre-existing faults, more than the orientation of the deep crustal stresses or directions of subduction, dictated the geometry of the resulting structures. Plate motions, however, only indirectly controlled stresses in the shallow reservoirs described here.

Some basement blocks such as the blocks on either side of the Hogback monocline were transpressively wrench-faulted against each other. Other basement-block uplifts such as the Zuni uplift and San Juan dome were overthrust into the adjacent basins, where they impinged against and indented into the adjacent shallow basin-filling strata like bulldozers. The Nacimiento uplift apparently did both, with an early wrench-faulting and a later transpressional overthrust motion, possibly related to the late-Laramide 15° change in the plate-subduction vector.

Laramide shortening was replaced by Basin and Range extension in west-central New Mexico approximately 36 million years ago (Cather, 1989). Emplacement of the north-south trending Archuleta dike swarm in the northwestern corner of the San Juan basin occurred under these altered dynamics, but the Cretaceous reservoirs had fractured by this time and were not noticeably affected.

3.3 Major Structural Elements – San Juan and Zuni Uplifts

The major structural elements influencing the overall fracture character of the San Juan basin are the San Juan and Zuni uplifts. Both uplifts are interpreted to have been active during the Laramide formation of the basin. Kelley (1957) noted that the San Juan "basin floor is tilted northward and its deepest part generally adjoins the greater uplift of the San Juan dome as though they were counterparts of a single mechanism at depth". Over time this concept has been somewhat forgotten and the San Juan uplift considered a sort of passive dome, unconnected to the San Juan basin. However, there are Precambrian rocks at an elevation of at least 14,000 ft in the Needles Mountains and the published seismic lines show southward-directed thrust faults along and south of the Hogback monocline (Figure 12) (Taylor and Huffman, 1988; Taylor and Huffman, 1998; Huffman and Taylor, 1999).

Penecontemporaneously, the Zuni uplift was being driven northward and upward along the forefront of the El Morro indenter at the southern edge of the San Juan basin (Chamberlin and Anderson, 1989). Faults at the southern edge of the basin are aligned in a mesh array that resembles a slip-line field described by Tapponnier et al. (1986) for an indented rigid plastic media by a rigid indenter (Figure 13). Slip-line fields have been used to interpret indentation tectonics in various areas including the collision of India (rigid indenter) with Asia (plastic media) (Tapponnier et al., 1986). Thus the fault geometries observed at the southern edge of the San Juan basin support the El Morro indenter hypothesis of Chamberlin and Anderson (1989). Folds such as the Nutria monocline, Gallup sag and Chama sag were also forming laterally away from the Zuni uplift at this time as a result of the lateral escape of basement and sedimentary blocks in front of the advancing indenter.

Much of the shortening and fracturing within the San Juan basin is inferred here to have been caused by these two uplifts being displaced toward each other with the San Juan basin caught between them, all being ultimately driven by NE-SW directed, continental-scale, crustal subduction. The resultant stress trajectories within the sedimentary units are the result of the frontal configuration and orientation of these two uplifts/indenters, and only indirectly related to the subduction geometries. In general the resultant stress trajectory was N-S to NNE-SSW, as recorded by the fracture sets within the Dakota Sandstone and Mesaverde Group.

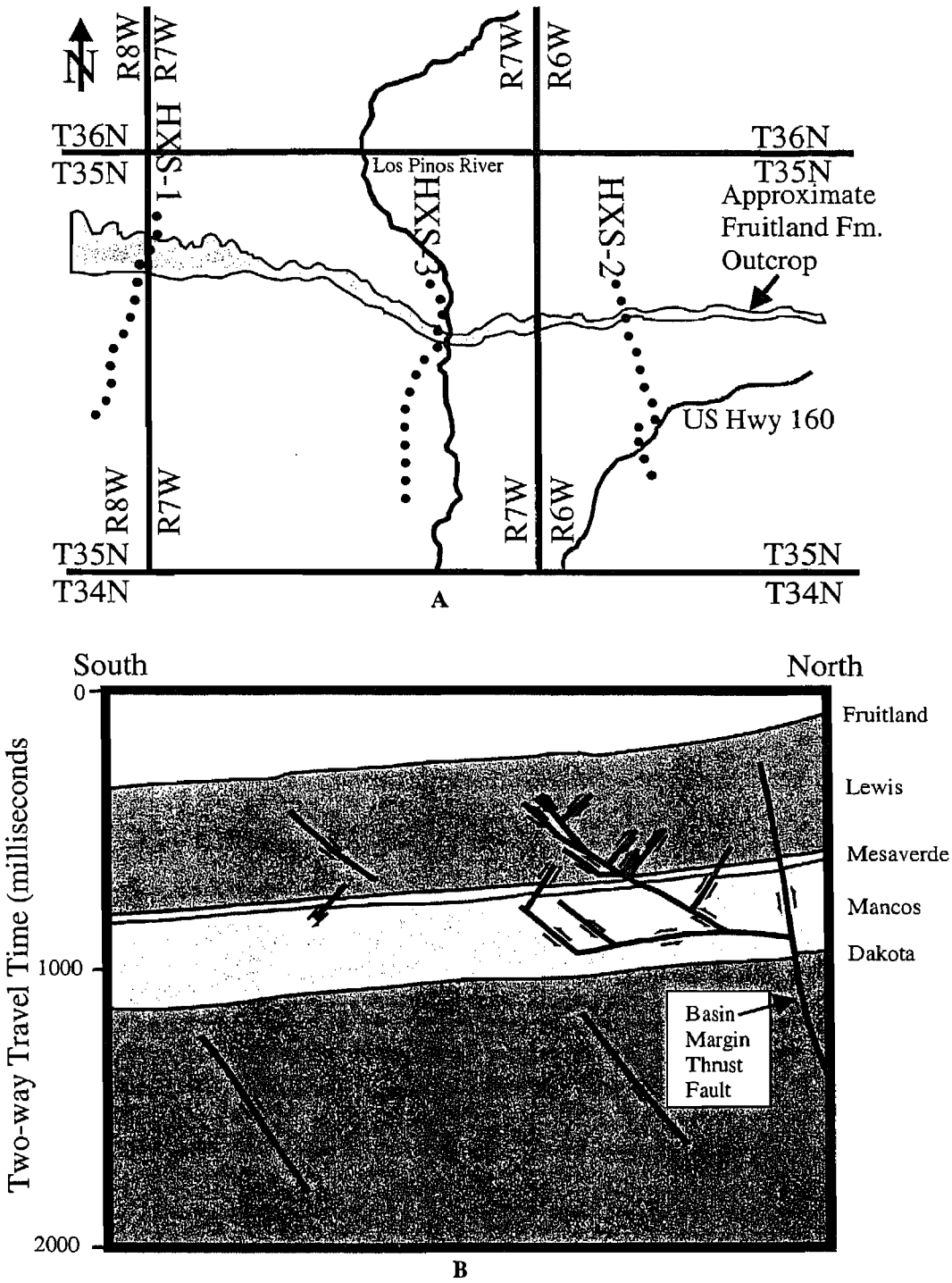

Figure 12: A) Location map of seismic lines across the Hogback monocline east of Durango, Colorado. B) Interpretation of seismic line HXS-3 (modified from Huffman and Taylor, 1999).

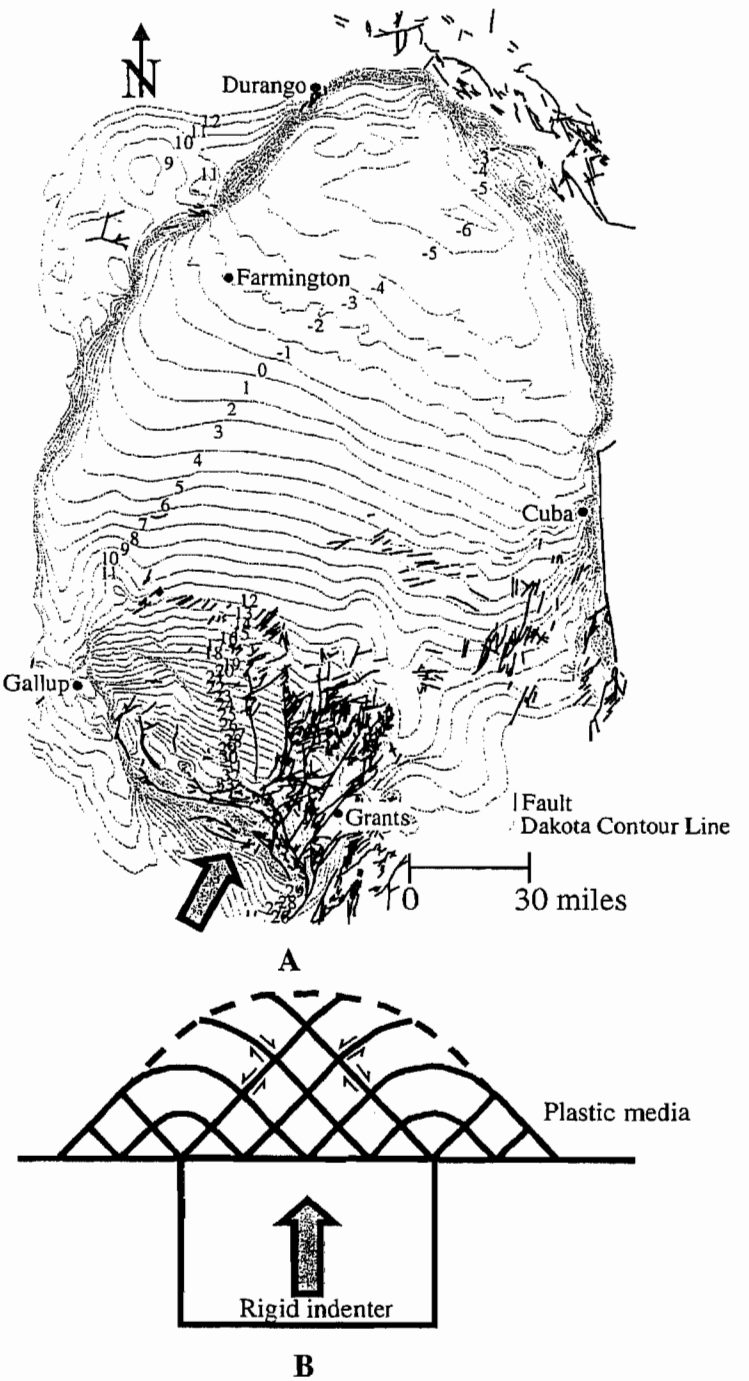

Figure 13: A) Structure map of the San Juan basin. Contours are drawn on the base of the Dakota Sandstone, intervals are meters X 100 (modified after Thaden and Zech, 1984). Faults (shown in black) along the southern margin of the basin are oriented in an array which resembles a slip-line field. Large arrow indicates direction of indentation. B) Plan-strain slip-line field, arrow indicates direction of indentation (after Tapponnier et al., 1986). The slip-line field will change with boundary conditions and indenter shape (Tapponnier and Molnar, 1976; Molnar and Tapponnier, 1977; Tapponnier et al, 1986).

3.4 Minor Structural Elements

The other tectonic elements surrounding the basin might suggest rotation of Laramide stresses if one was to simply infer the maximum horizontal compressive stress as nearly perpendicular to the trend of these tectonic elements. For example, the abrupt, faulted front of the N-S trending Nacimiento uplift would indicate E-W compression, while the sinuous Hogback monocline would suggest N-S to N-W, to even E-W compression depending on location. The general orientation of Archuleta anticlinorium would suggest NE-SW compression. However, as with the Laramide orogeny in general, rotation of stresses is not required in order to produce these geometries. For instance, the Nacimiento front has been shown to be bounded by a high-angle reverse fault (evidenced by a steep gravity gradient; Keller and Adams, 1992), but with only limited overhang on the west, and strata are disturbed only for mile or so west of the front. Therefore the Nacimiento uplift is probably the result of a preexisting basement fault responding to an oblique force. This is evidenced by right lateral motion as inferred from N-W trending en echelon folds along the fault.

This is consistent with the right-lateral shearing observed on other sub-parallel structures across the basin, including the Defiance uplift and Hogback monocline. The present configuration of the Hogback monocline has been suggested to have been a response to transpression with some component of right lateral shear between preexisting fault blocks (Taylor and Huffman, 1998; Ralser and Hart, 1999). Basement faults have been active in the region of Ute dome since well before Laramide time, with a Laramide reversal of the previous Pennsylvanian fault throws (Ralser and Hart, 1999). The flower structures associated with faults seen in seismic lines near the Archuleta anticlinorium also suggest some component of lateral movement (Figure 13) (Huffman and Taylor, 1999). Slack and Campbell (1976) have also inferred right lateral movement within the Rio Puerco fault zone.

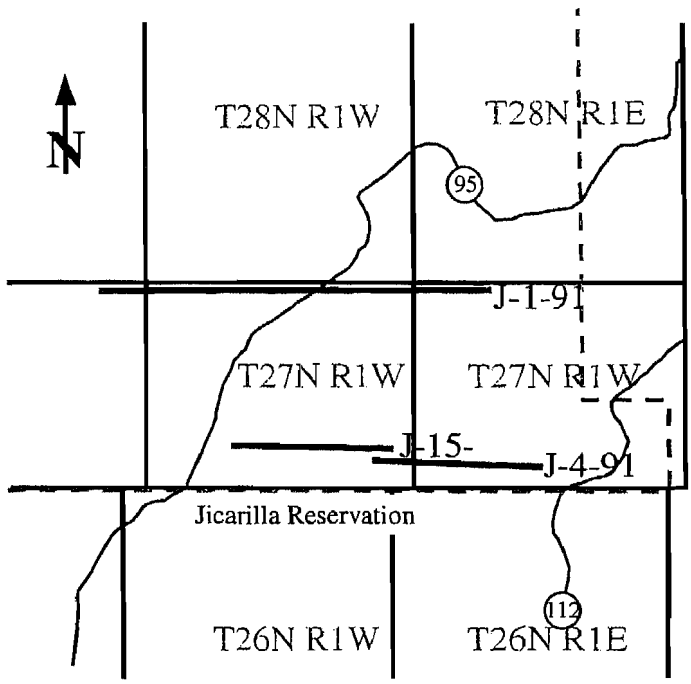

Figure 14A: Location of seismic lines across a portion of the Archuleta anticlinorium (modified from Huffman and Taylor, 1999).

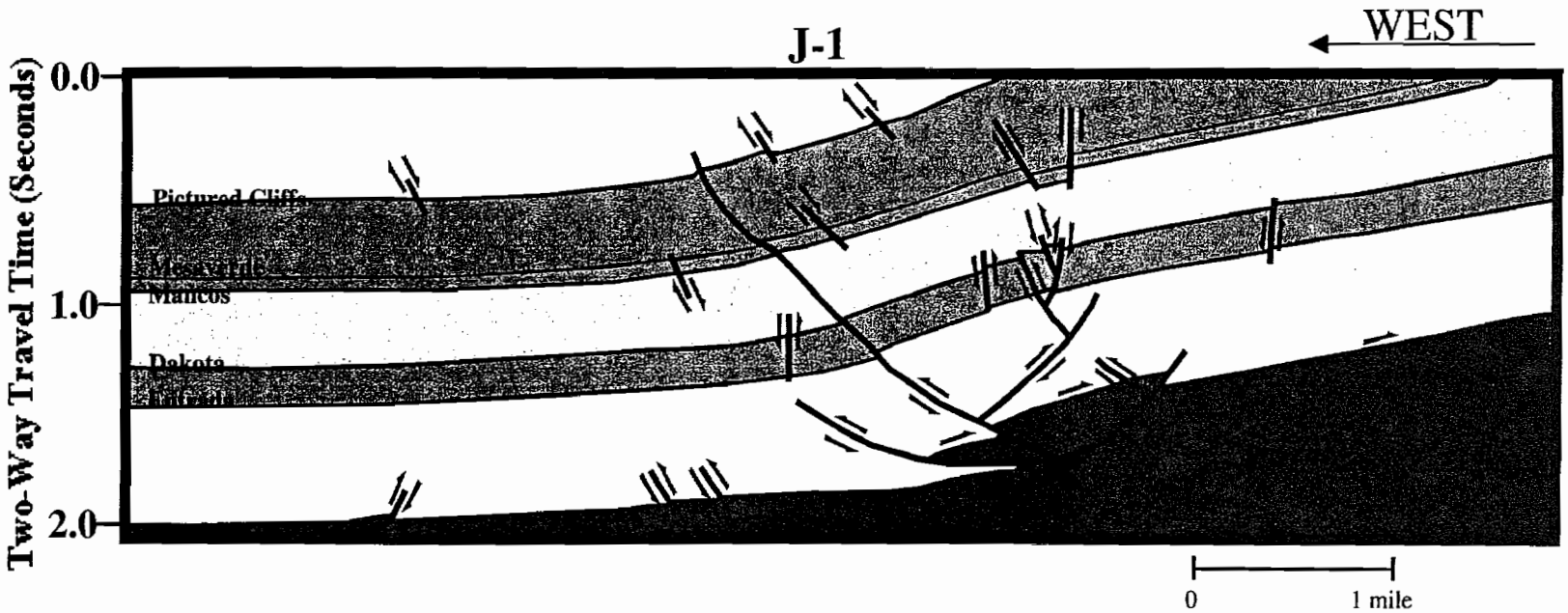

Figure 14B: Line drawing interpretation of line J-1 (modified from Huffman and Taylor, 1999).

There is overprinting of Rio Grande rift-related E-W extensional tectonics that nearly parallels N-S Laramide structures in the Rio Puerco area (Slack, 1973). This suggests that paleostress indicators such as the Tertiary Archuleta dike swarm near Dulce NM may better represent a response to Rio Grande rift extension rather than Laramide compression. Therefore, the N-S striking Archuleta dike swarm may be a Tertiary red herring and only coincidentally oriented sub-parallel to the dominant fracture trend in the basin.

3.5 Kinematic Model of Stresses and Structural Elements

Stresses and the resulting fractures in the shallow strata filling the Laramide basins were controlled more by configurations of the adjacent thrust-fault indenters than by motion vectors of subducted plates or the relative drag between them. Stress trajectories between the Laramide thrusts which formed the Zuni and San Juan uplifts were combined with northeastward yielding of the Colorado Plateau to generate a maximum horizontal compressive stress oriented roughly N-S to NNE-SSW across the basin. These two indenters are not directly opposed to each other along an north-south axis: offset impingement into the basin contributed to what appears to have been a pervasive right-lateral shearing across the basin at the scales of both fractures and faults. Clockwise rotation and/or differential motion (faster northeastward motion of the western edge than the east side: see diagrams of Bird, 1998) of the Colorado plateau would also have contributed to pervasive right-lateral shear across the San Juan basin. High horizontal stresses coupled with overpressuring in Eocene to Oligocene time (Bond, 1984) produced favorable conditions for fracturing. The shortening under these conditions is recorded by vertical extension fractures within the Mesaverde Group and Dakota Sandstone. Two pairs of conjugate shear fractures, one with a bed-parallel axis of intersection and the other with a bed-normal axis of intersection, both with a bed-parallel bisector to the acute angle, are also observed and limited to the Dakota Sandstone at the northern margin of the basin. The compressive stresses were greatest and the rocks more highly silicified in this area, leading to susceptibility to this type of fracturing. All of the observed fracture characteristics and orientations are compatible with N-S to NNE-SSW shortening within the San Juan Basin.

There is strong local evidence for NE-SW trending stresses at the southeastern corner of the basin (Yale et al, 1993; conjugate deformation bands in the San Ysidro area as described below) and in the Dakota outcrops at the northern edge of the basin (also described below). These may be related to late-Laramide, southwestward-directed overthrusting of the Nacimiento uplift and San Juan uplift respectively, due ultimately to the late-Laramide re-orientation of plate motions reconstructed by Bird (1998).

3.6 Predictions of Fracture Trends

Outcrop and core fracture data are consistent with a model wherein the San Juan basin was forming between two oppositely verging thrusts. The San Juan basin was essentially squeezed between the Zuni uplift and the San Juan dome. In addition, contemporaneous right-lateral transpressive wrench motion (due to the asymmetry of the two indenters and unequal northeastward translation of the basin as part of the Colorado Plateau) was concentrated at the basin margins (Archuleta anticlinorium, Nacimiento uplift, Hogback monocline, Defiance uplift and the Rio Puerco fault zone; Figure 14). Right-lateral motion may also have been distributed

across some of the basement faults within the basin and transmitted to the overlying Cretaceous strata.

Shear fractures within the Dakota sandstone are also consistent with a compressive force that was continuing to ramp up during the Laramide to some maximum where the horizontal compressive stress was of a greater magnitude than the overburden stress. An early phase of uplift and a later, more intense phase of deformation are evidenced by fracture abutting/age relationships observed between vertical extension and horizontal conjugate shear fractures within the Dakota Sandstone of the San Juan basin.

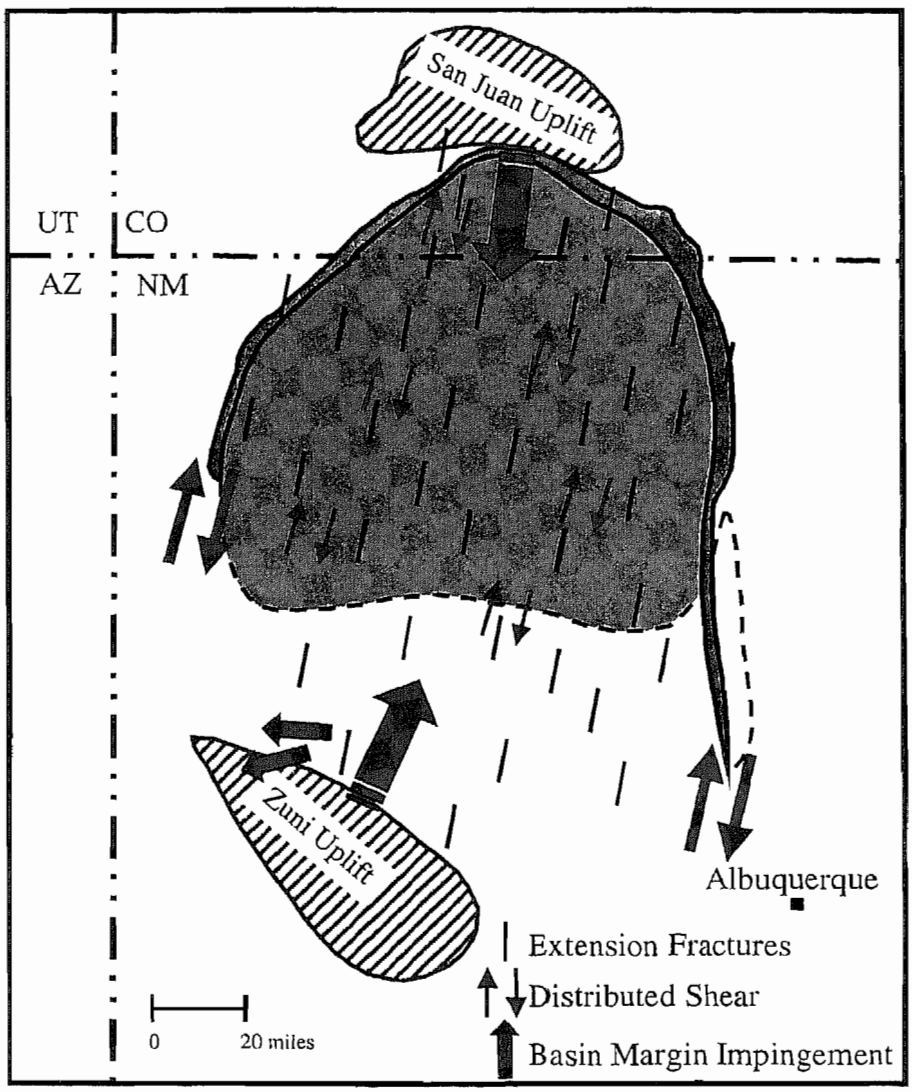

Figure 15: Tectonic fracture model of the San Juan basin. A dominant oldest set of vertical extension fractures striking primarily NNE-SSW is observed across the basin. Pervasive right lateral shear is also observed across the basin. These features are primarily the result of southward and northward indentation of the San Juan and Zuni uplifts respectively (base map after Kelley, 1957).

Although the fractures are predicted and known to have a generally N-S to NNE-SSW strike throughout the basin, there are local variations due to local structures and other heterogeneities. As fracture and/or stress orientation data have been amassed for other areas of similar size to the San Juan basin (e.g., Hillis et al., 1999), it has become apparent that gentle deviations and local anomalies within regional stress patterns are not uncommon. Thus it is apparent that while the average fracture strike for the San Juan or any basin is a reasonable first approximation for predicting local fracture strikes, it is unlikely to be an exact representation of the fracture strikes at any particular well location.

4.0 OUTCROP FRACTURE DESCRIPTIONS

4.1 Introduction

The outcrop fracture descriptions given here are presented by structural domain. Our interpretation is that the outcrop fractures that can most reliably be extrapolated into the subsurface are those that were formed prior to or during the early stages of wrench and thrust faulting that form the structural boundaries of the inner basin. However, the secondary, local fracture domains associated with the inner-basin structural boundaries were superimposed onto these regional fractures, and are commonly more numerous or "dominant" and thus obscure the earlier fractures. The secondary fracture domains related to local structure provide a reasonable basis for the following outcrop descriptions, but the theme connecting the outcrop fractures is the pre-existing set of early-formed, generally N-S to NNE-SSW striking regional fractures of Laramide age.

4.2 Indenter Margins

The northern and southern margins of the San Juan basin are very different: one- or two-degree dips characterize the southern margin whereas dips approach vertical locally on the northern margin. Nevertheless, the two areas are similar in that they have best preserved the early, pre-existing regional fractures with minimal local structural overprinting.

4.2.1 Southern Margin

The Southern margin of the San Juan Basin is defined by the gentle, essentially "non-structural" Chaco Slope of one- to two-degree dips. Dips are generally towards the NE and NNE in inner basin (arbitrarily defined here as that part of the basin lying north of the outcrops of the Cliff House sandstone member of the Mesaverde). Similar dip directions occur in the eastern part of the basin south of the inner basin, but the dip azimuths change to a northerly dip in the western part of the zone, reflecting the stronger indenter/buttress effects of the Zuni uplift in the southwestern part of the basin. Most of the fractures along the southern basin margin are extension fractures, oriented normal to bedding, although east- and west-dipping conjugate fracture and/or deformation-band shear pairs are present in some strata (notably the poorly cemented Jurassic sandstones). Fractures are most numerous and most regular in the Dakota sandstones and in the blanket marine sandstones of the Mesaverde interval.

Gilkey (1953a;b) mapped fracture patterns in the outer part of the basin, adjacent to and on the north side of the Zuni uplift between Grants and Gallup. Fracture strikes in Dakota strata in this area vary somewhat but are generally consistent in orientation over areas of tens of square miles, commonly transitioning gradually from one zone of consistent strike to the next. Exposure of Dakota pavements is good enough that Gilkey was able to trace individual fractures on aerial photographs for several miles. The dominant fracture strike is NNW-SSE, especially in the Dakota outcrops north of Grants, with local zones of NE-SW fracture strikes, and irregular abutting cross fractures.

The fracture strikes mapped by Gilkey to the west of this area, between Grants and Gallup, are less regular, with many of the fractures striking NW-SE. However, the more recent, detailed USGS Geologic Quadrangle maps of this same general area (e.g., the Oak Spring, Dalton Pass, Hosta Butte quadrangles) show very consistent, NNE-SSW to NE-SW fracture strikes in Dakota and Mesaverde strata (Figure 15). Both the Gilkey and USGS data sets show that fracture strike and fracture intensity vary significantly near the numerous faults that mark the northward indentation of the Zuni basement block into the basin.

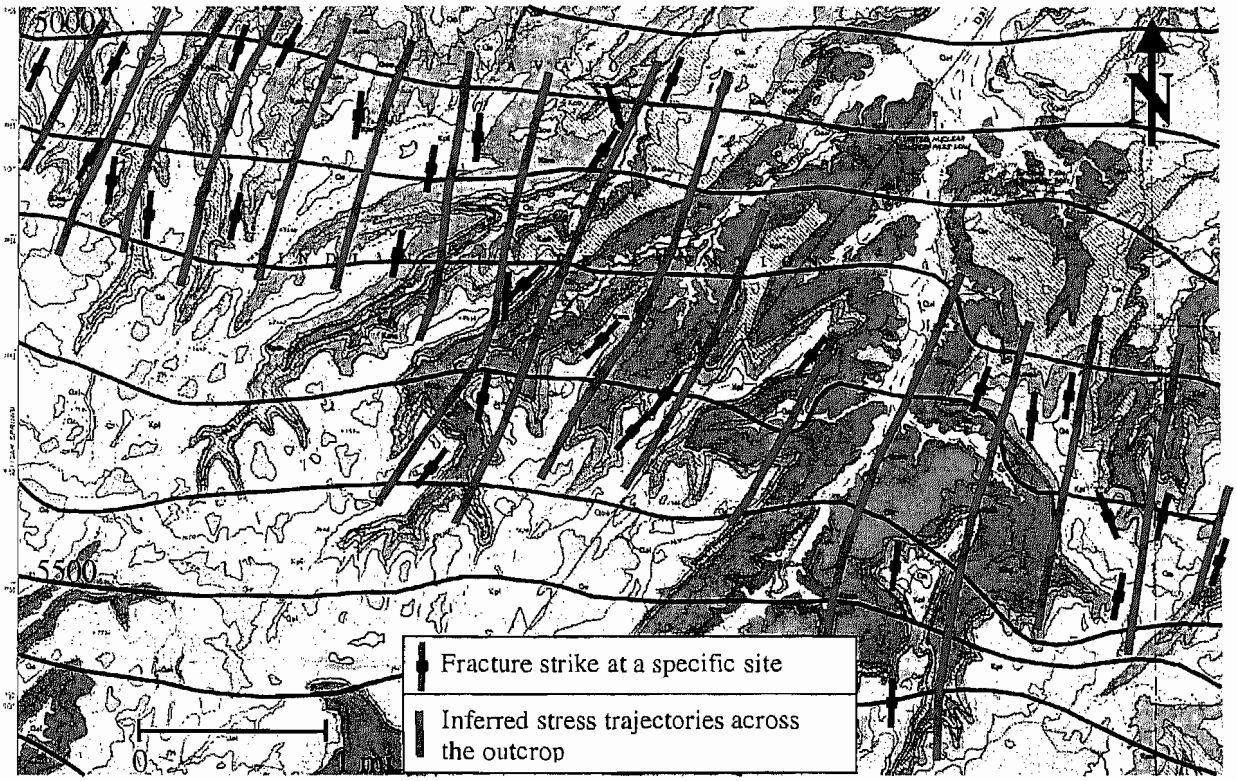

Figure 16: Pervasive NNE to NE striking natural fractures within the Cretaceous Point Lookout sandstone member of the Mesaverde Group illustrated on the geologic map of the Dalton Pass quadrangle, McKinley County, New Mexico. Structure contours are drawn on the base of the Dakota Sandstone; contour interval is 100 ft (modified from Kirk and Sullivan, 1987).

Northward, in Point Lookout sandstones at Chaco Canyon National Historical Park, the fracture pattern appears to have been influenced by the same local structure that created the east-west trending canyon in which the Anasazi dwellings were built (Figure 16). East-west striking bed-normal fractures are the dominant pattern, although a subordinate set of NNE-SSW striking fractures is also present.

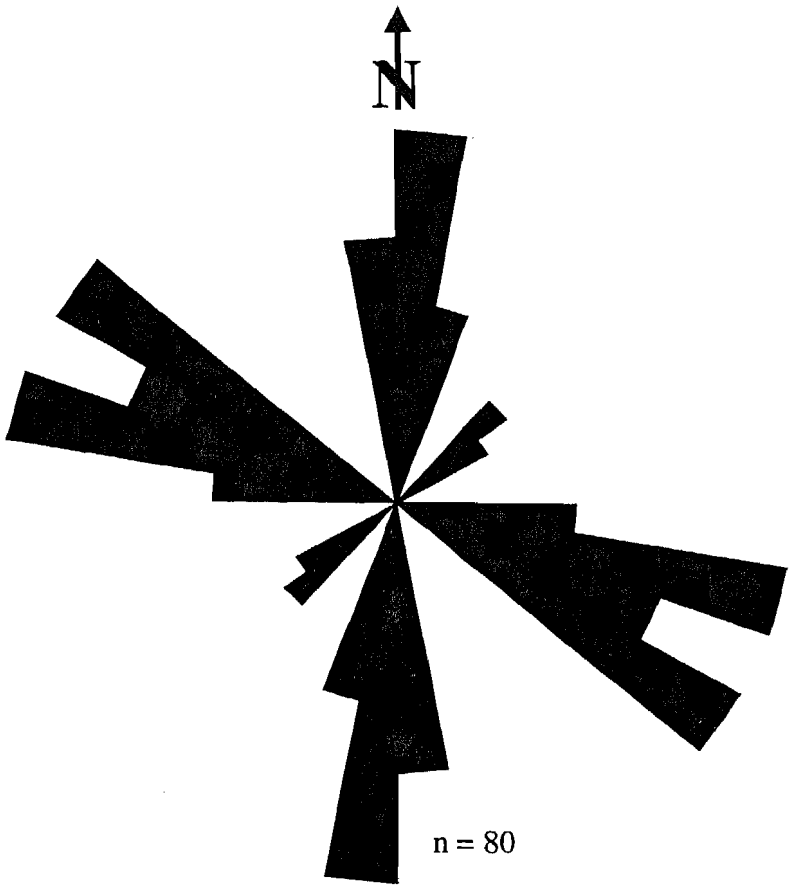

Figure 17: Rose diagram of 80 fracture orientations at Chaco Canyon National Historical Park.

East of Grants, a local fracture study by Lorenz (reported in Hallett et al., 1999) documented a NNE-SSW (15°+-15°), bed-normal, through-going natural fracture set in Dakota outcrops and near-surface cores 10 miles north of Laguna (Figure 17; Hallett et al., 1999). Fractures are spaced about 10 meters apart, spacing being approximately proportional to bed thickness. The fractures are mineralized with calcite, and locally with surface-related iron oxide. Fracture intensity increases in proximity to Cerro Negro, the local intrusive igneous plug.

In summary, the oldest, through-going fracture pattern at the southern margin of the San Juan basin displays a dominant but irregular NNE-SSW strike that varies between NE-SW and NW-SE. This regional fracture pattern is locally disrupted by faults and intrusions.

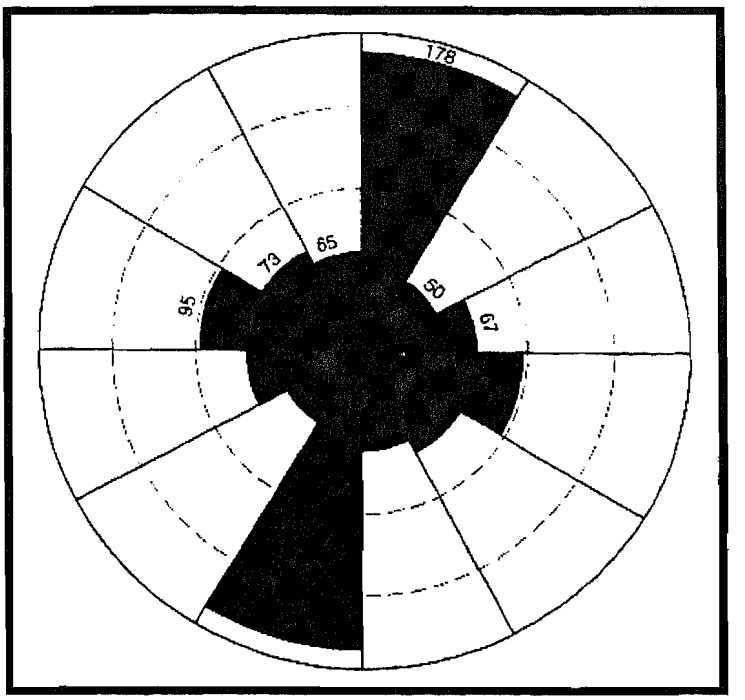

Figure 18: Rose diagram of 528 fracture orientations near Cerro Negro, New Mexico (Hallett et al., 1999).

4.2.2 Northern Margin

The northern rim of the basin, marked by the steepest dips of the Hogback, arcs eastward from the fault-valley that allows passage of the Animas river through the Hogback at Durango, through southwestern Colorado, and loses definition as it swings around back into New Mexico south of Chromo. Interruptions to the curve of the arc occur at several places, including the Animas valley and south of the local basement uplift along the Piedra River. Although not mapped, these interruptions probably mark cross faults.

East-west striking thrust faults have been mapped in outcrop north of the Hogback, and seismically in the subsurface below and immediately south of the Hogback (Taylor and Huffman, 1988; 1998). Limited subsurface data and obscured outcrops preclude the recognition of what is probably more extensive southward-directed thrust faulting in this area. The northern limits of the internal and external parts of the San Juan basin have coalesced at the Hogback along this northern margin.

A suite of approximately north-south striking, bed-normal extension fractures, similar to those found at the southern margin, is present in tilted Dakota and Mesaverde sandstones at this rim of the basin. (All fracture strikes presented in this report are the strikes the fractures have when bedding is rotated back to the horizontal). Local strike and intensity variations occur in association with local structures. This is particularly notable at breaks in the Hogback continuity that mark cross faults, such as at the Animas River valley, where the eastern outcrops are offset by a few hundred feet vertically, and possibly laterally, from the strata west of the river.

Condon (1989, 1997; personal communication 1999) mapped fractures and coal cleats around this northern edge of the basin, reporting the average strike of the earliest fractures west of the Pine River is 346° in the Pictured Cliffs sandstones and 357° in the Fruitland sandstones. East of the river the average strike is 335°. Finch (1994) reported similar NNW fracture orientations and photo-lineaments in lower Tertiary strata exposed in the Animas river valley south of Durango. Condon noted however, that the fracture strikes in the Pine river area are rotated clockwise relative to those near Durango. Irregular, abutting cross fractures trend approximately normal to these through-going fracture trends.

Condon reports that the average strike of face cleats in the associated coals, however, is oblique to fractures in the sandstones, and that the cleat strikes rotate in the *opposite* sense along the same outcrops. This suggests that the coal cleats may have an earlier and separate origin, and should not be used as equivalent data to sandstone-fracture data when reconstructing the tectonic history of the basin.

Our field data at the northern rim of the San Juan basin concur with Condon's observations: i.e., we have measured N-S to NNE-SSW strikes of bed-normal, extension fractures in both the Mesaverde and Dakota sandstones in this area (Figure 18). However, in addition to the extension fractures, conjugate shear planes oriented both normal to, and sub-parallel to bedding are present in the well-cemented, quartzitic Dakota sandstones. The two pairs of shear fractures are well exposed on the caprock of Animas Mountain immediately north of Durango, and on a bedding-plane surface exposure on the north side of Nussbaum road in Mud Springs Estates, 7-8 miles east of Durango and north off of County highway #240.

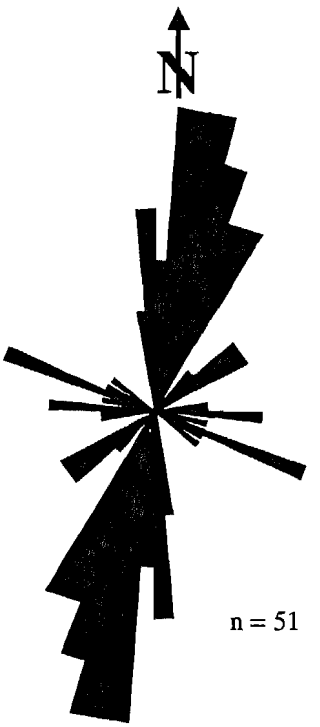

Figure 19: Rose diagram of 51 fracture orientation at Animas Mountain, Durango Colorado.

The Dakota conjugate-fracture pairs are consistently oriented 1) bed-normal with a bed-parallel, northeast-striking acute-angle bisector, and 2) oblique to bedding at shallow angles, with a bed-parallel, acute-angle bisector. The acute-angle bisectors are both bed-parallel and strike northeast when bedding is rotated back to horizontal. Shear indicators such as slickenlines and asymmetric steps suggest minor amounts of shear sub-parallel to bedding in the first instance, and parallel to the dip of the inclined surfaces in the direction of the acute-angle bisector in the second instance. These fractures record a significant bed-parallel stress oriented NE-SW. The relative ages of the conjugate fractures and the extension fractures are obscure.

Similar conjugate shear planes occur in steeply-dipping Dakota strata along Red River, north of the Colvig ranch further to the east. These shear planes are marked by millimeter-scale zones of crushed sand grains. They appear as apparently better cemented planes in the rock, but are in fact unmineralized.

The different lithologies of the Mesaverde and Dakota sandstones resulted in different mechanical properties, and dictated that the fractures in the Mesaverde and Dakota strata have significantly different characteristics. The Mesaverde sandstones contain lithic fragments and are cemented with authigenic clays and calcite, producing a somewhat ductile rock. Conversely, the Dakota sandstones are quartz-rich and are cemented with quartz, resulting in a relatively brittle rock. This resulted in the wider spacing of the N-S extension fractures in the Mesaverde strata. It also allowed the Mesaverde lithologies to strain in ductile fashion, without fracturing, under the same stress conditions that produced the conjugate shear fractures in the Dakota sandstones without an equivalent macroscopic strain structure in the Mesaverde strata.

The resulting extension fractures in Dakota strata are sub-parallel and closely spaced but short, whereas extension fractures in the Mesaverde are more widely spaced, longer, and relatively irregularly planar. Fractures in both units tend to terminate vertically at bedding boundaries, especially bedding contacts with shales, and strike generally north-south. The Dakota sandstones contain the additional sets of conjugate fractures oblique to the extension fractures, resulting in superimposed intersecting fracture sets, whereas Mesaverde strata are dominated by the unidirectional, sub-parallel, north-south fractures.

The cross faults and probable cross faults that cause breaks in the curve of the northern-rim Hogback may also cause local anomalies in fracture strikes. Condon (1997) records anomalous, east-west fracture strikes in Pictured Cliffs sandstones in the Animas River valley south of Durango. Our field data on fracture strikes in the Paleozoic strata overlying the Piedra River uplift show a variety of orientations, related as much to the local uplift as to southerly indentation of the basement block. Local fracture deviations in strike and intensity would be expected in subsurface strata south of these locations along the Hogback.

4.3 Wrench Boundaries

The eastern and western margins of the inner San Juan basin are marked by the Nacimiento Uplift and its extensions, and by the Hogback monocline, respectively. These have been suggested to be discontinuous right-lateral wrench faults with secondary transpressional thrusting directed towards the basin center (Taylor and Huffman, 1999; Lorenz et al., 1999).

This thrusting has been interpreted by other authors to have been the result of regional east-west compressional stresses, and the southward-directed thrusting at the northern rim of the basin has been largely ignored or overlooked. However, it is mechanically easier to reconstruct approximately NE-SW Laramide compression with associated transpression along the wrench-faulted eastern and western basin margins than it is to construct radial compression and thrusting along three of the four basin margins. The natural fracture data along the wrench-faulted basin margins, described below, support the former interpretation. This model is compatible with Laramide reconstructions of northward/northeastward translation of the Colorado Plateau (e.g., Corbitt and Woodward, 1973; Bird, 1998).

4.3.1 Farmington Area

The Hogback in this area is a generally northeasterly-striking, sinuous rim of southeastward-dipping rock overlying transpressional thrust faults cutting the basement and up through Paleozoic stratigraphic levels. The largest of the deviations in strike of the Hogback is caused by a localized basement uplift at Ute Dome. The Hogback becomes less well defined to the southwest, where dips decrease and where en echelon offsets of the structure occur due to lateral stepping of the deformation from fault to fault in the basement.

Multiple sets of fractures are present in Mesaverde strata along the Hogback north and northwest of Farmington. The oldest set of fractures along the Hogback and in the adjacent, less deformed strata northwest of Farmington is a set of bed-normal extension fractures that strike NNE-SSW (Figure 19). Condon (1988) reports an average strike of 15° for these fractures between the Colorado-New Mexico line and Durango, with a range of approximately plus or minus 10°. Condon also reports that fracture strikes in the strata incorporated into the Hogback seem to vary in a damped fashion congruent to the sinuous strike of the Hogback, but that this effect is not universal and not present away from the Hogback. The development of these early fractures varies: in some areas they are the dominant fracture set, in other areas their presence is obscured by younger fracture sets. However, this early-formed fracture set is always present in some degree. Face cleats in associated coals (e.g., Whitehead, 1997) do not parallel the dominant or earliest fractures in the sandstones in this area and are not considered further here. Three sets of younger fractures trend normal to, and at about 45 left and right of, the NNE-striking early fracture set.

The fractures of the four sets are not equally well developed in all areas. In fact, the early, NNE fractures are commonly the least well developed and therefore the least obvious fractures in an outcrop. The sketch presented in Figure 19 represents an anomalously high degree of development of all four fracture sets in the same area of the Hogback, about 13 miles northwest of Farmington. Typical outcrops contain only one, two, or three of these fracture sets, and the best developed sets may change both laterally and/or stratigraphically within tens of meters.

Small, sheared, cross faults cut across the Hogback monocline in this area, many trending normal to the strike of the monocline. Fracture patterns may change in the immediate vicinity of and across a fault. Some of the fractures associated with the smaller faults are micro-shear

deformation bands. Some but not all of the larger valleys across the Hogback represent cross faults for which the direct evidence has been eroded.

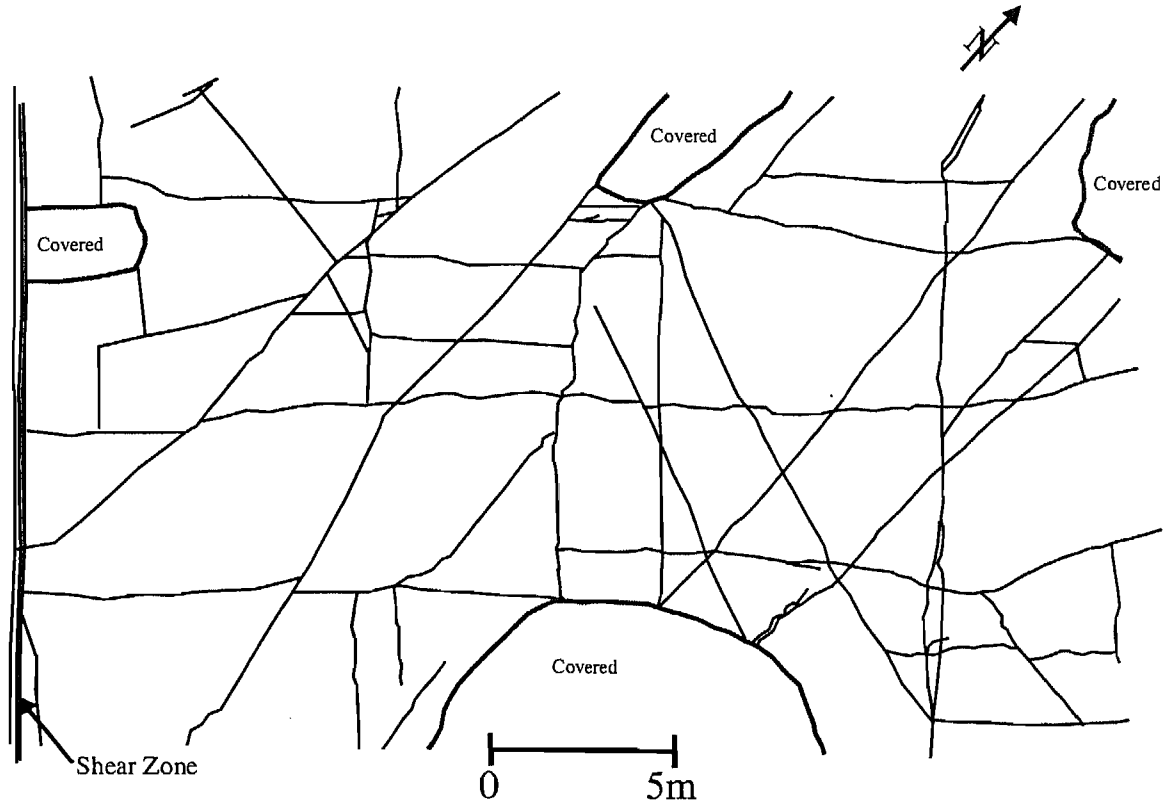

Figure 20: Plan view fracture map on the Hogback monocline east of Shiprock, New Mexico.

Although the Hogback monocline is interpreted to have formed by a transpressional, thrusted wrench fault, all fractures noted in the inclined strata incorporated into the monocline appear to be extension fractures; no shear fractures were found other than the local deformation bands associated with cross faults as noted above. However, the NNE fractures are inferred to have formed prior to monocline development, and the later fractures merely originated in extension as the strata were passively draped in a fold over the deeper fault. Thus, the absence of shear fractures does not vitiate the concept of a transpressional mechanism at depth.

The secondary sets of fractures noted in the strata along the monocline may be related to the formation of the monocline itself, and/or to surficial stress relief on uplift and exposure. However, the generally N-S striking fractures appear to be part of an early-formed, regional, extension-fracture set.

4.3.2 Ute Dome

Ute Dome is a small, local, abrupt basement uplift that interrupts the curvature of the Hogback monocline similar to the localized Piedra basement-block uplift on the north edge of the basin. Three sets of faults have been mapped in the surface and subsurface over this dome: a NNW-SSE striking set in Cretaceous strata (e.g., Barnes and Arnold, 1950; Hart et al., 1999; Ralser and Hart, 1999); a deeper NE-SW set in the Paleozoic strata (Hart et al., 1999); and a

basement-level set of faults (Taylor and Huffman, 1988). Seismic studies (i.e., Hart et al., 1999) suggest that although the fault sets overlap in plan view, they need not actually intersect vertically. The intermediate-depth faults appear to be a record of Paleozoic deformation but the ancient, NE-striking faults in the basement controlled Laramide tectonics. The shallow, WNW-trending faults probably record extension related to strain accommodation at the void created by a releasing bend. Right-lateral deformation during the Laramide wrench faulting that formed the Hogback stepped from one NE-striking basement fault to an adjacent one where Ute Dome impinged on the structure (Ralser and Hart, 1999).

Fracture patterns in the surface strata at Ute Dome are highly variable (Figure 20), although there is still a background fabric of older, N-S striking fractures at most locations. Fractures associated with some of the surface faults have very close spacing (inches) adjacent to the faults, and some of these fracture swarms, visible on the plan-view, bedding surfaces of a sandstone layer, can be traced into faults in vertical, bed-normal exposures.

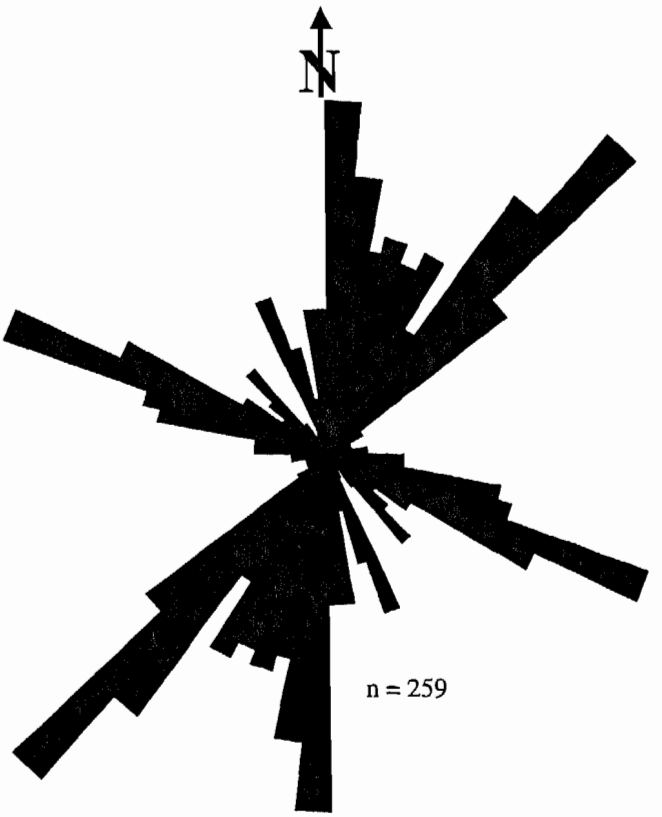

Figure 21: Rose diagram of 259 fracture orientations at Ute Dome.

Fractures are absent, replaced by conjugate and sub-parallel deformation bands in many of the exposures of less well cemented sandstones. Most of the deformation bands strike NE-SW on the eastern flank of the dome (sub-parallel to the strike of the immediately adjacent Hogback monocline), and remain vertical despite a 15° eastward dip to bedding, suggesting that this set of structures is related to monoclinal folding.

4.3.3 Nacimiento uplift

The tectonic history of the N-S striking, Precambrian-cored Nacimiento mountain range, located diagonally across the San Juan basin to the southeast from the Hogback monocline at Farmington, is a well documented transpressional structure. Baltz (1967) and Woodward, (1987) have inferred an early Laramide phase of right-lateral wrenching and a later Laramide phase of continued wrenching with associated thrusting. This has produced several broad, obliquely oriented anticlines trending NNW-SSE immediately west of the N-S mountain front, and NE-SW striking faults immediately south of the uplift.

The Cretaceous strata of interest here have been caught up in the steeply-dipping cuestas that front the western face of the northern part of uplift in this area, and thus contain high-strain deformation structures and fractures dominated by the local bulldozing effects of the overthrust uplift. However, Baltz (1967, p. 62-63) reports that the most conspicuous fractures strike 8-25° in this area, and that these fractures imprint a NNE-SSW trending grain onto the fabric of the topography. Low-altitude, oblique aerial photos confirm that this generally NNE-SSW pattern is present in the less steeply dipping Mesaverde strata west of the uplift, suggesting that it is not solely a product of flexure of the strata. Moreover, there is a pervasive and absolutely predictable, closely spaced (up to 7 fractures per foot), N-S fracture pattern, paralleling the mountain front, in the granite core of the Nacimiento uplift. This is not the fracture pattern expected in an uplift created by east-west compression, but rather it is compatible with north-south compression.

4.4 Corners

The San Juan Basin does not have definitive corners, yet there are certain structural provinces that mark the change in trend from one margin to another. The large, relatively amorphous Archuleta anticlinorium/Chama embayment is one such area, marking the transition from the eastern, wrench faulted margin to the northern, thrust-faulted margin. Another is the Rio Puerco Fault Zone, which records a transition into the younger Rio Grande extensional structural province at the southeastern limit of the basin.

4.4.1 Archuleta Anticlinorium

Fractures in the Dakota sandstones along NM route 84 and at Heron Lake, within in the Archuleta anticlinorium (Figure 21), show that the N-S to NNE-SSW theme of regional fracture strikes continues in these areas, with local deviations and overprints. The Dakota fractures are closely spaced (half to a fifth of bed thickness), bed-normal, and relatively short (Figure 22). They typically terminate vertically at bedding boundaries between mechanically dissimilar lithologies. Few fractures occur in the more highly bioturbated intervals, where clays were mixed with the sands during deposition, creating relatively ductile mechanical properties that did not fracture.

One of the major deviations from the N-S extension-fracture mode occurs in the cleanest, best-cemented, siliceous Dakota sandstones at Heron Lake. Distinctive conjugate fractures with a bed-normal acute-angle bisector and bedding-oblique fracture planes occur in these beds, and

are similar in both geometry and orientation to those found at the Mud Springs Estates outcrop east of Durango. This type of conjugate fracture geometry suggests that not only was there a compressive stress directed into the basin from the east-northeast at some time, but that the compressive/tectonic stress was large, exceeding the weight of the overburden. This may fit with the Laramide changes in motion vectors for the Colorado Plateau area reported by Bird (1998).

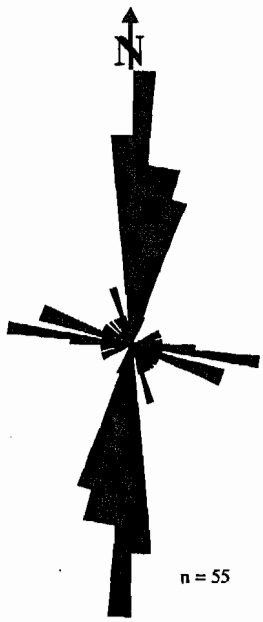

Figure 22: Rose diagram of 55 fracture orientations at Heron Lake.

Figure 23: Short, parallel, bed-normal, closely spaced extension fractures in a Dakota Sandstone bedding surface at Heron Lake. Fractures strike NNE.

4.4.2 The Rio Puerco Fault Zone

The Rio Puerco Fault Zone is a band of overlapping and en echelon, sub-parallel, relatively small normal faults that typically strike approximately NE-SW. The zone begins just west of the southern end of the Nacimiento uplift and extends southward beyond the limits of the San Juan basin to the Lucero uplift, southwest of Albuquerque. It has been described and interpreted as a Laramide right-lateral wrench fault zone by Slack and Campbell (1976), and is a southerly extension of the right-lateral strain more obvious in the Nacimiento uplift.

Faults and natural fractures in the Rio Puerco Fault Zone were studied in Dakota and the underlying Jurassic sandstones, in the normally faulted area southwest of the town of San Ysidro. This area is on BLM land and is widely accessible. There are excellent examples of the strong dependence of fracture characteristics on lithology/mechanical properties in this area, with the poorly cemented/high porosity Jurassic sandstones containing three sets of conjugate deformation bands whereas other, better cemented lithologies typically contain fractures (Olsson et al, 2001). As a further complication, due to mechanical stratigraphy considerations, some lithologies fractured under one stress regime, others fractured under a younger stress regime, and some lithologies fractured under neither or both.

Although it is not an interval of direct reservoir interest, the pattern of conjugate deformation bands in the Jurassic sandstones constrains the conditions of maximum horizontal stress during one stage of deformation to strike NE-SW. This is probably related to the late-Laramide, westward thrusting of the nearby Nacimiento block reported by Woodward et al. (1972). This pattern also documents an increase in magnitude of that stress from the intermediate compressive stress to the maximum compressive stress (see section on Tectonic Model, above). The resulting pattern of intersecting, low-permeability deformation bands compartmentalizes the sandstone into a completely unproductive reservoir (Figures 23, 24).

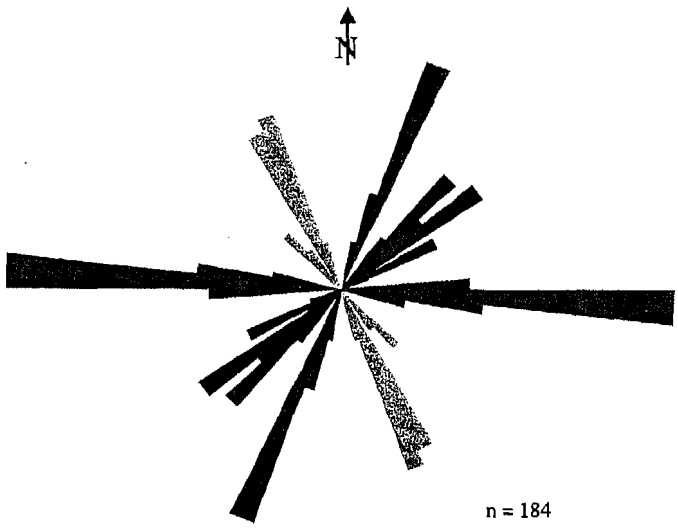

Figure 24: Rose diagram of 184 deformation band orientations near San Ysidro, New Mexico. The three grayscale colors illustrate the strike of the three different conjugate deformation band sets.

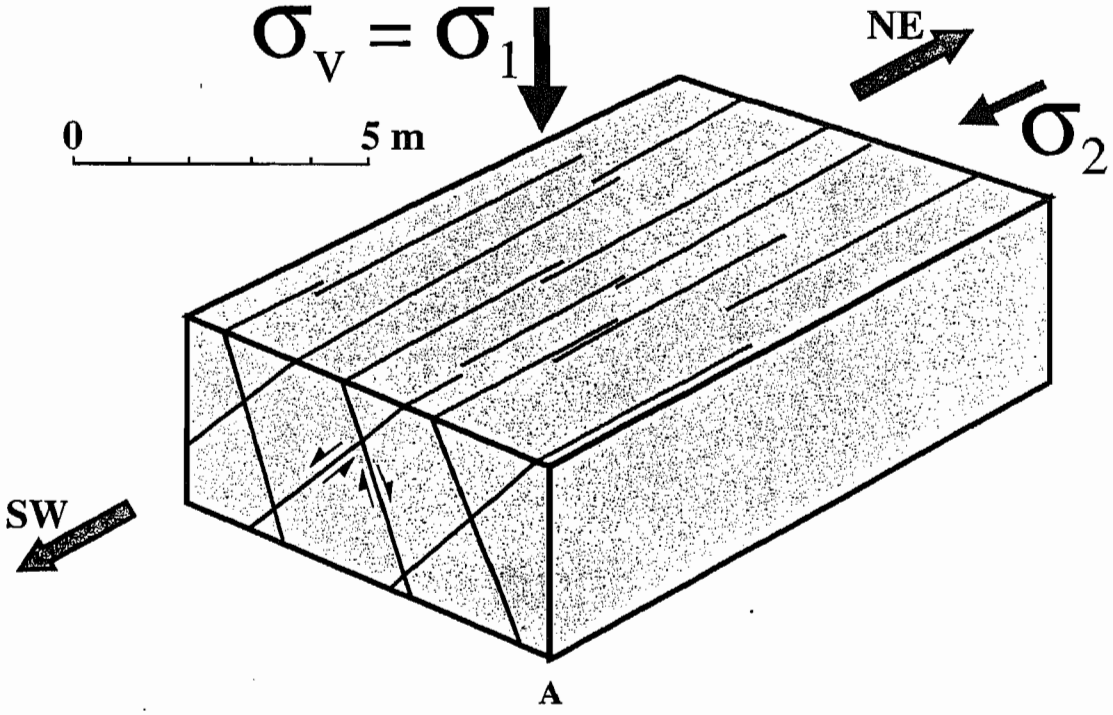
$\sigma_V = \sigma_1$
NE
σ_2
0
5 m
SW
A

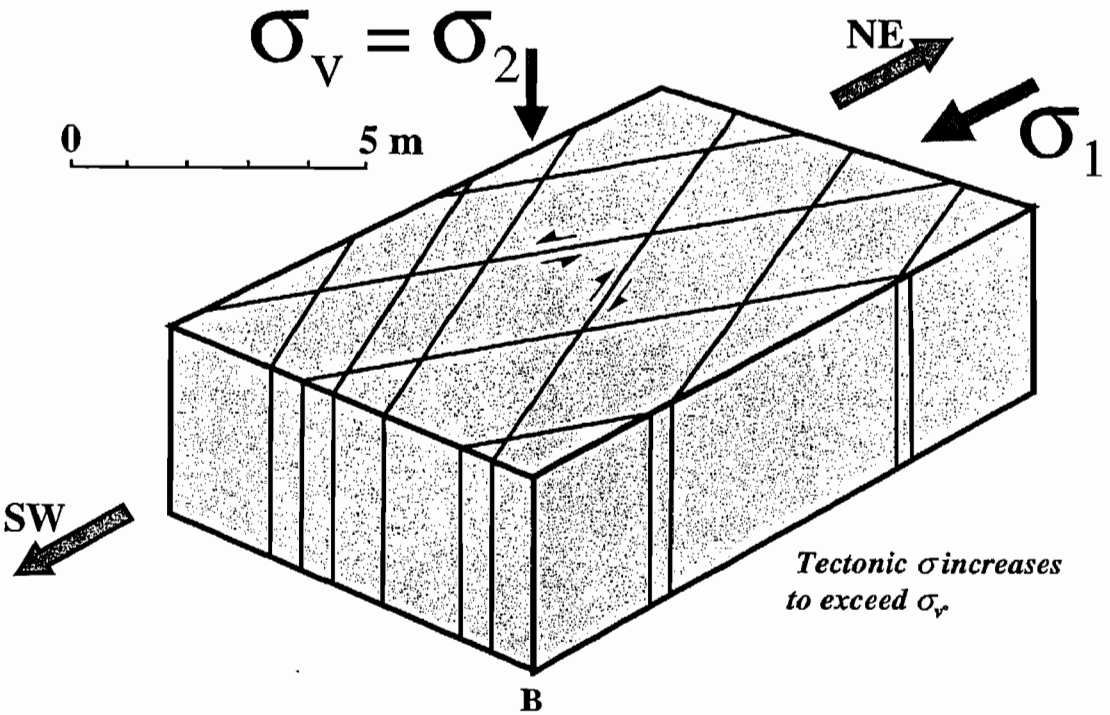
$\sigma_V = \sigma_2$
NE
σ_1
0
5 m
SW
Tectonic σ increases
to exceed σ_v
B

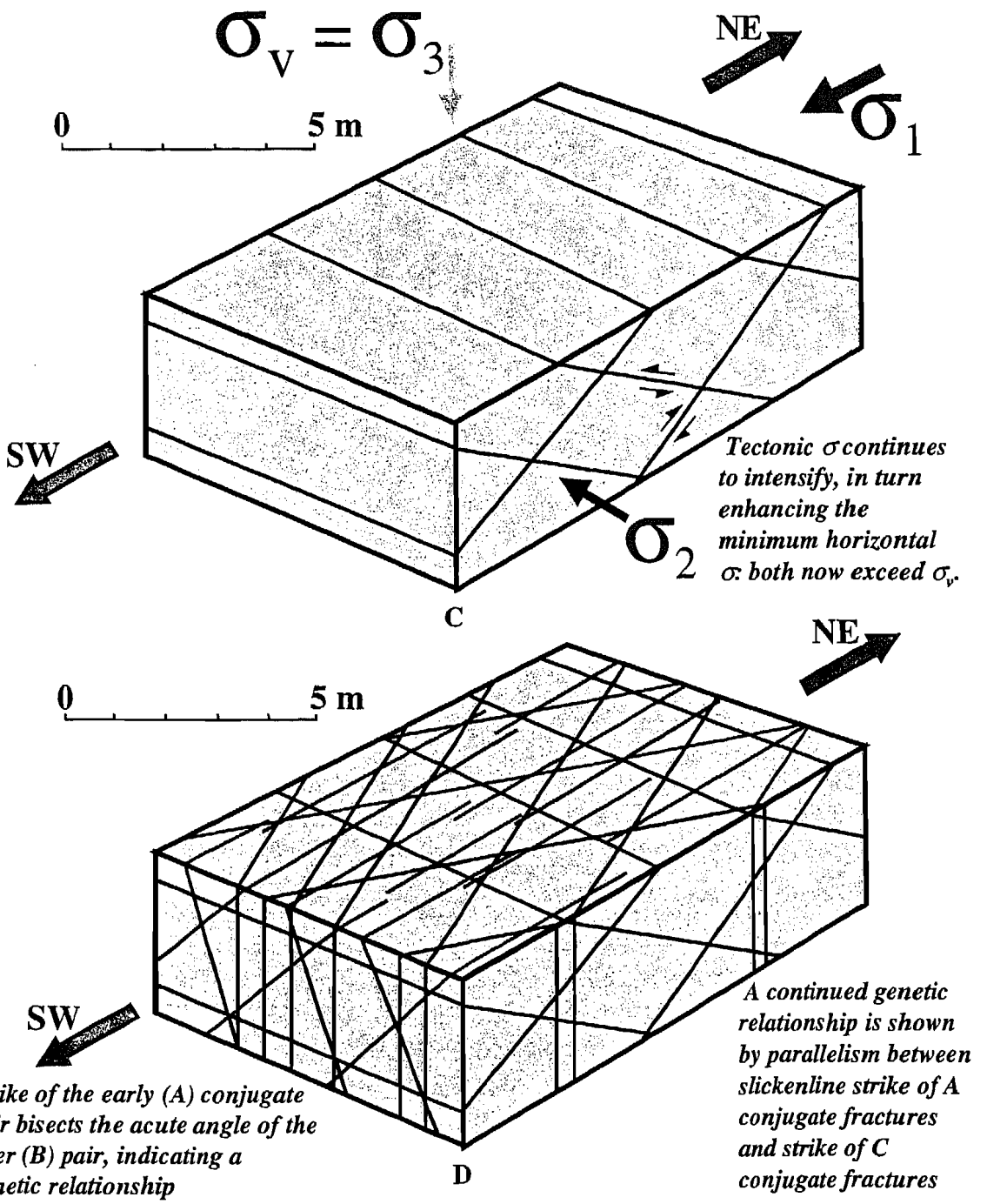

Figure 25: A) Conjugate pair of shear fractures with a vertical bisector to the acute angle at time t_1. B) Conjugate pair of shear fractures with a horizontal bisector to the acute angle at time t_2. C) Conjugate pair of shear fractures with the bisector of the acute angle in the bedding plane at time t_3. D) The superimposed result of the three sets is significant reservoir compartmentalization with permeability reduction within each shear fracture/deformation band plane.

The sandstones in the overlying Dakota interval also contain conjugate patterns, but of a significantly different nature. Few fractures are present in the heavily bioturbated, shallow-marine, muddy sandstones of the Dakota interval exposed here, except near NE-SW striking normal faults. However, where thinner, clean caprock sandstones overlie these same bioturbated sandstones just east of the compressor station, the fracture pattern is a conjugate one of N-S to NNE-SSW (10-20°) and NW-SE to ENE-WSW (60-70°) striking, bed-normal fractures. Ornamentation on the faces suggests that these fractures either originated in shear or were secondarily sheared, but offsets are minimal (a few millimeters at most).

Intersection relationships on this pavement suggest that the fractures striking 10-20° comprise an older set, imposed on the rock as extension fractures under the same conditions of NNE-SSW maximum horizontal stress seen widely elsewhere in the basin. This set was present as a background fabric, and was reactivated in shear during formation of the younger, 60-70° shear fractures. The two sets thus became a conjugate shear pair, the maximum horizontal stress having been rotated to a NE-SW orientation that bisected the conjugate angle. This was the same stress field that produced deformation bands in the Jurassic sandstones, as described above. The older set of fractures originated in extension but was reactivated in shear, having the optimum strike with respect to the re-oriented stresses to become one set of a conjugate pair while the complimentary fractures were being developed as an entirely new set in the rock. This relationship and its interpretation are widely but not universally applicable to fracture and deformation-band patterns in the San Ysidro area.

The San Ysidro area also offers an opportunity to study the relationship between fractures and faults. The northeast-striking faults in the area are relatively well exposed, being small enough that they have not allowed the obscuring erosion that commonly destroys outcrops containing larger faults. Faults in this area typically strike 35-45° and have normal offsets of 3-15 ft, although larger offsets (up to 150 ft) can be documented. These faults always have associated conjugate fractures, striking parallel to the fault and dipping both into and parallel to the fault plane, with a vertical conjugate-angle bisector. Zones containing the conjugate, fault-related fractures may be 5-30 feet wide and are typically found within the down-thrown, hanging wall. Such fractures are relatively rare in the footwall. The expression of these faults on the bedding surface consists of zones of sub-parallel fractures.

These faults zones are commonly iron stained, indicating they are permeability conduits (at least under surficial conditions.) Even where the faults cut marine, Mancos shales, abundant gypsum mineralization marks the fault zone and suggests that the fault is conductive to fluids, or at least was until plugged with gypsum.

4.5 Summary: Distributions of Fracture Intensity and Orientation in Outcrop

Most of the natural fractures in Mesaverde and Dakota outcrops are sub-parallel, approximately north-south striking extension fractures (Figure 25). Secondary cross fractures related to uplift and erosion are common in outcrop, but are not significant to the subsurface. Conjugate deformation bands (micro-shear structures) are also present in some strata in some locations, notably the less well cemented strata in the southeastern part of the basin. Fracture spacings are typically on the order of bed thicknesses, although that is an upper limit and smaller

spacings are common. Fracture swarms are commonly found as the bedding-plane manifestations of faults. The immature Mesaverde sandstones typically contain relatively long, irregular extension fractures, whereas the quartzitic Dakota sandstones contain short, sub-parallel, closely spaced, extension fractures, and locally conjugate shear planes as well (the latter oriented in any or all of the three possible conjugate geometries). Intense bioturbation has inhibited the formation of fractures in some strata of both formations. Most fractures are limited vertically by contrasts in lithology at bedding surfaces. Few of the fractures in outcrop display the calcite, quartz, and/or kaolinite mineralization that is common to fractures in the subsurface. Fractures associated with faults may have anomalously close spacings as well as anomalous strikes.

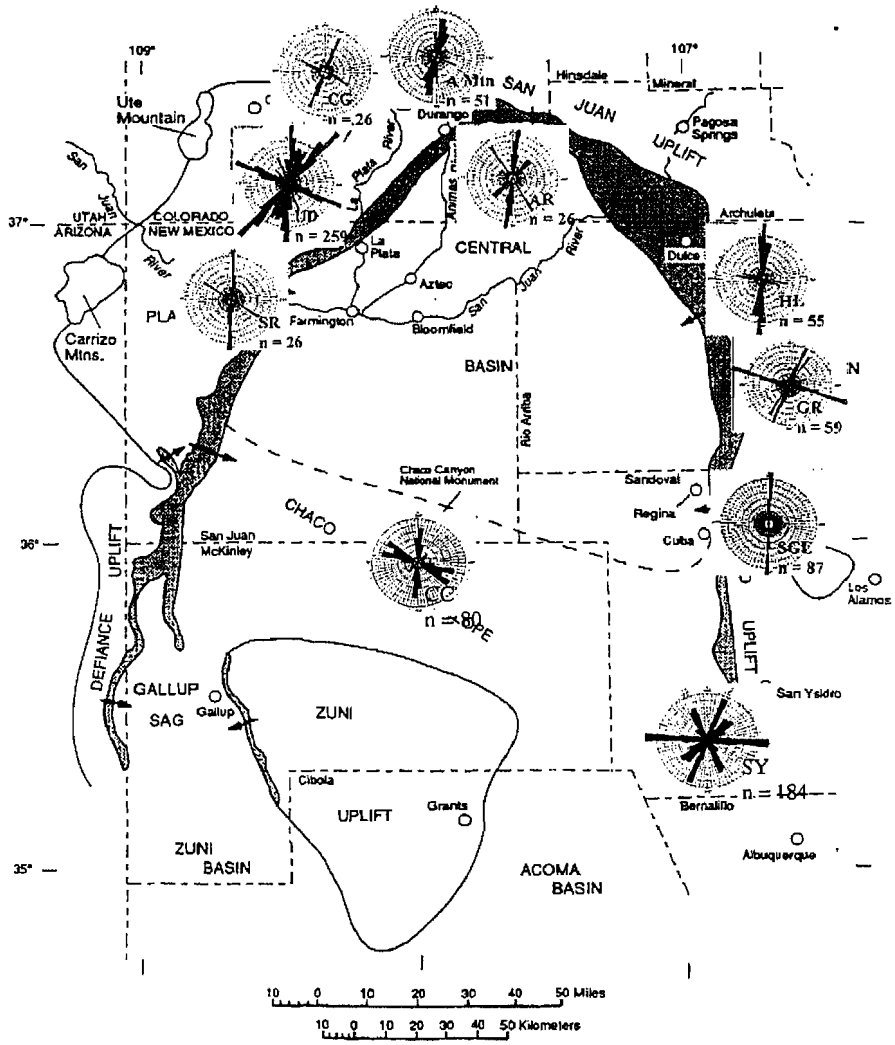

Figure 26: Rose diagrams of fracture orientations in outcrop. Diagrams are overlain on an index map illustrating the structural elements of the San Juan Basin. Areas of steep dip are shown in gray with the direction of dip indicated by arrows; CC = Chaco Canyon, SR = Shiprock, UD = Ute Dome, CG = Campground, A Mtn = Animas Mountain, AR = Animas River, HL = Heron Lake, GR = Ghost Ranch, SGL = San Gregorio Lake, SY = San Ysidro (base map modified after Fassett, 1989).

5.0 CORE FRACTURE DESCRIPTIONS

5.1 Introduction

The cores studied for this project are stored in Socorro, NM, at the New Mexico Bureau of Mines and Mineral Resources Core Library. Most of these cores were shipped to Socorro from the Amoco core facility in Tulsa, Oklahoma, as it was being dismantled. These cores were examined in order to document the subsurface fracture characteristics, to compare them with outcrop fracture characteristics, and to provide insights into the viability of extrapolating outcrop fracture data, where three-dimensional fracture characteristics can be measured, into the subsurface where wellbores provide essentially only one-dimensional data.

Well data are the only means of directly sampling a reservoir. Core provides a direct sample of a small interval, whereas logs give direct measurements of certain properties of the reservoir over larger intervals. However, the dimensions of an 8000 ft deep, 8 ¾ inch diameter wellbore drilling into a 50-ft thick, mile-wide reservoir are proportional to a piece of string 30 ft long and penetrating a table top. A core sample may be thought of as 3-inch segment of the bottom of the string. Even multiple wells represent only pinprick samples of a reservoir. Moreover, the chances of actually sampling a vertical fracture with a vertical wellbore are low. In order to have at least a 50% probability of coring (four-inch core) one fracture from a fracture set, the fractures must have an average spacing of eight inches, a ridiculously small spacing in most reservoirs. Thus the fact that a core is not fractured does not mean that there are no fractures in the reservoir.

The ribbons of slabbed cores available for this study provide even less volume for fracture study, further reducing the probability of noting and examining a fracture even if it was cored. Moreover, the slabbing and sampling processes that these cores have been subjected to preclude locking core pieces together, greatly decreasing the chances of being able to determine relative orientations of successive fractures even when they have been cored.

Cores from 19 wells were examined and characterized, and the cored fractures photographed (Figure 26). Care was taken to distinguish coring and drilling-induced fractures from natural fractures, though the latter are typically mineralized, making the distinction relatively easy. A reasonably good suite of data from different parts of the basin, and from both the Mesaverde and Dakota intervals, was provided by the available cores. However, fractures are not sufficiently numerous in any one core to support creation of quantitative, tabular data base. Rather, a verbal summary of the fractures in each well is provided below. All of the core fractures described below are vertical, extension fractures unless noted otherwise.

Several authors have indicated that San Juan reservoirs have been cored and that the cores contain fractures (e.g., London, 1972; DuChene, 1989; Emmendorfer, 1992; Gorham et al., 1979; Hawkins, 1977; Greer, 1978a,b), but in fact little information on the fracture characteristics has been published. Some of the minimalist descriptions in these reports can even be re-interpreted, given the advances in fracture understanding, to suggest that the fractures described are induced rather than natural. None of the cores examined for the present study were oriented, thus no in situ fracture orientations were obtained. However, the few published

fracture orientations for subsurface core (Ortega and Marrett, 2000; TerBest, 1997; Lorenz et al., 1999) suggest that the same NNE-SSW fracture fabric seen in outcrop is also dominant in the subsurface. The anomalous E-W fracture indications reported by Ortega and Marrett (2000) for the Sunray H Comp #6 (number 12 in section 5.2.1 Mesaverde Cores) are probably explainable by its proximity to the nearby, N-S striking Bonito dike.

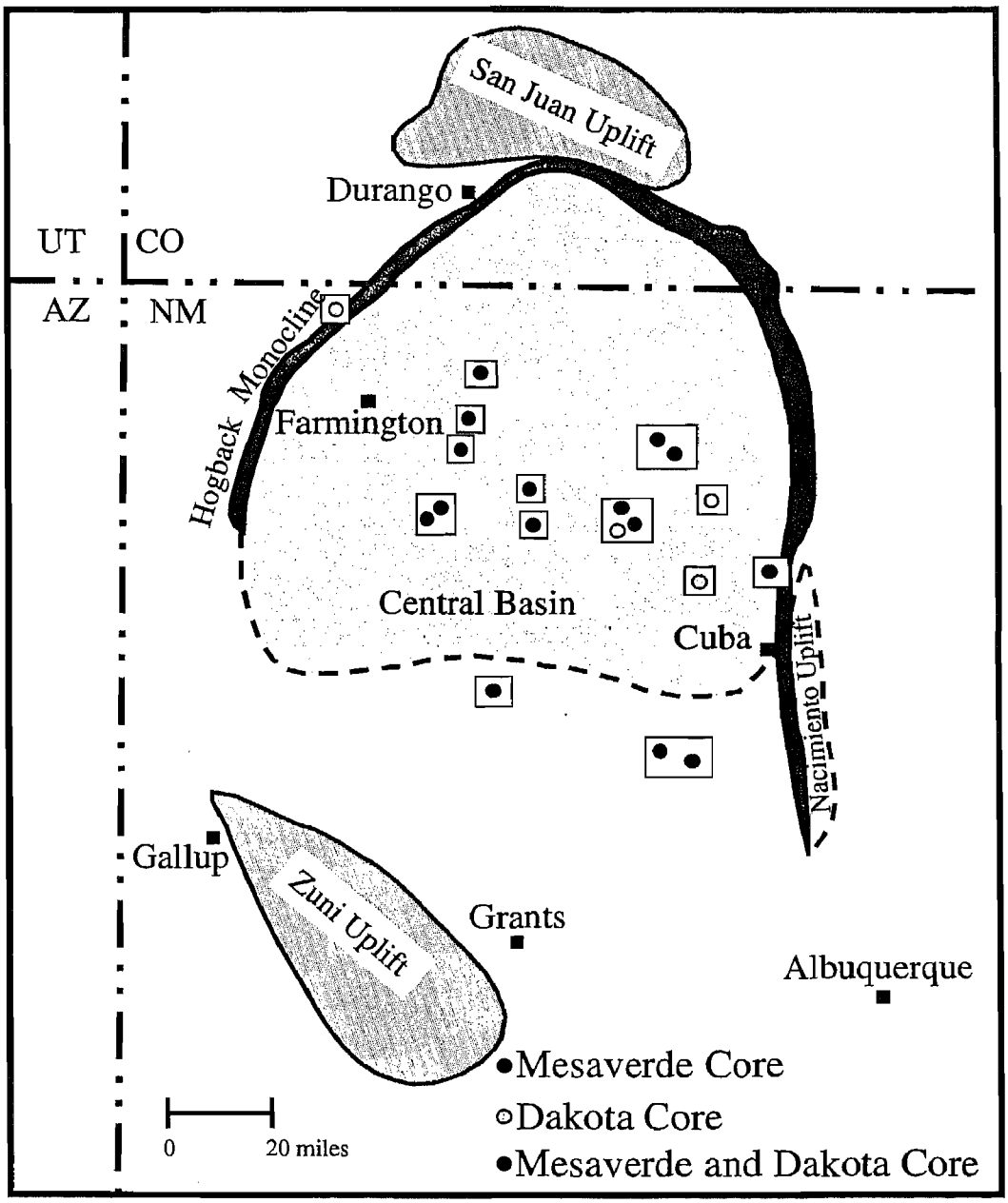

Figure 27: Map showing the locations of cores measured for this study (base map modified from Kelley, 1957).

5.2 Characteristics of Fractures in Core

5.2.1 Mesaverde Cores

1. Amoco, H.L.B. Gas Com #1, section 25, T. 24 N., R. 1 W., Rio Arriba Co., NM. This core consists of 42 ft of slab ribbons from four-inch diameter core from the Point Lookout sandstone, at a depth of 4437-4479 ft. The rock is generally high-porosity, medium-grained sandstone, with several fine-grained sandstone intervals. No fractures are present in the medium-grained interval, but one good fracture, about .5 ft high, exists in the fine-grained sandstone. This fracture is about 0.5 mm wide, with about half of this aperture mineralized with calcite (Figure 27). The vertical terminations of the fracture are in missing core. Several horizontal bedding planes display bed-parallel slickenlines, indicating horizontal shear.

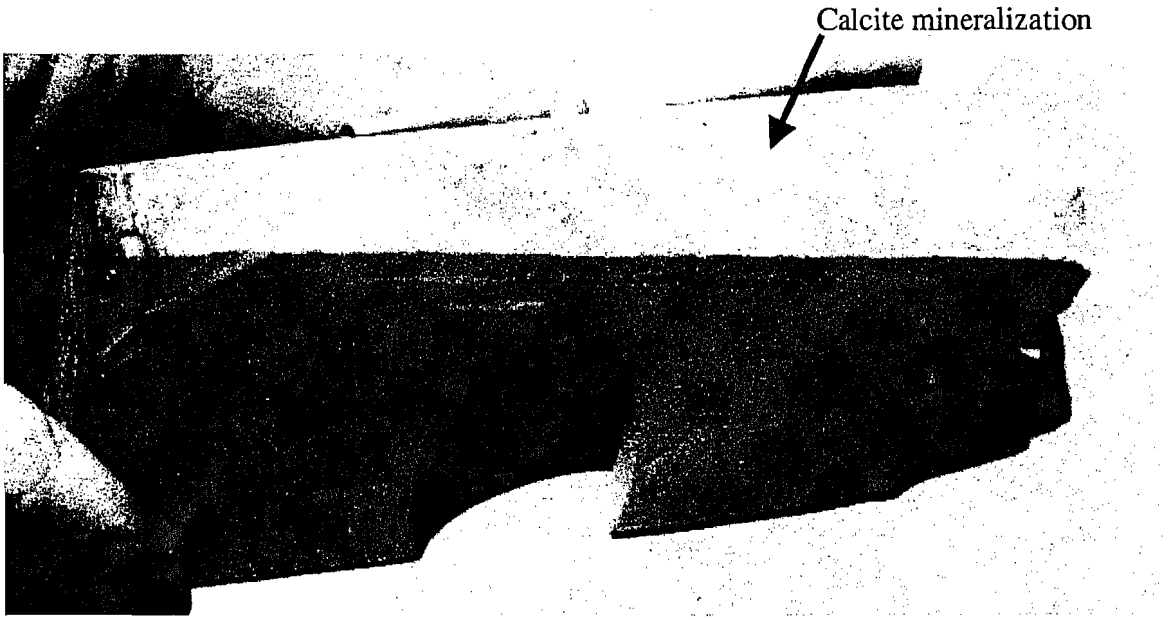

Figure 28: Photograph illustrating patchy calcite mineralization on an extension fracture.

2. Amoco, Jicarilla #146-34, section 3, T. 25 N., R. 5 W., Rio Arriba Co., NM. This core consists of 122 ft of slab ribbons from four-inch diameter core from the "Mesaverde" interval, at a depth of 5253-5275 ft. This core comes from a coarsening-upward, shallow marine facies of thin bioturbated sandstones and shales. Hairline fractures about 0.1 mm wide and almost completely mineralized with calcite are common in the lower section where the grain size approaches siltstone, but are rare (only one) in the more massively bedded sandstone. All natural fractures that can be related to each other are parallel (Figure 28), and one example is present where the natural fracture strikes sub-parallel to a coring-induced petal fracture suggesting that the fractures strike parallel to the present, maximum, horizontal compressive stress (Figure 29).

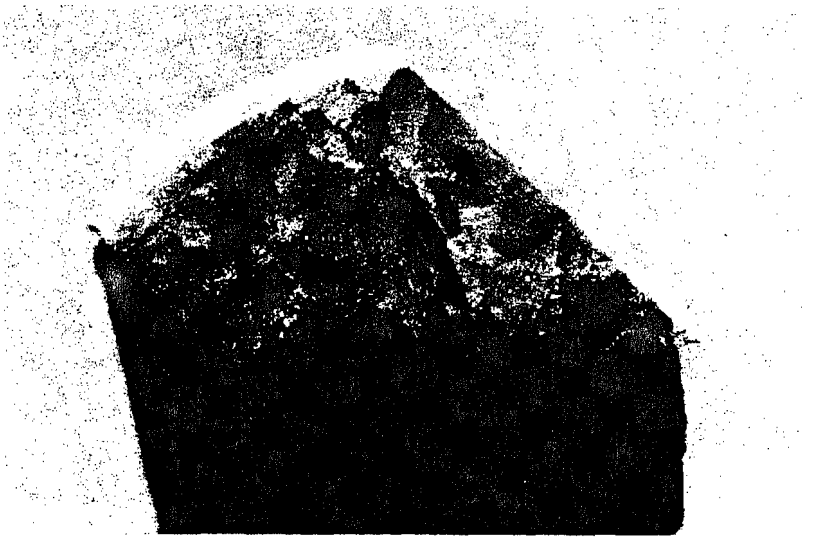

Figure 29: Parallel natural fractures (N) in core from the Jicarilla #146-34 well. The slab face is along the lower edge of the photograph.

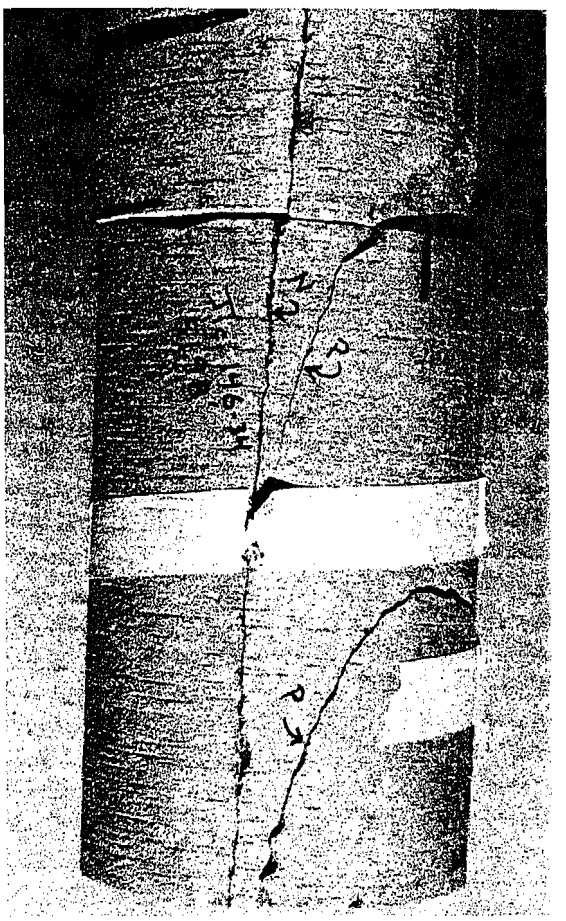

Figure 30: Orientation of the natural fracture (N) and drilling induced petal fractures (P) indicate parallelism between fracture planes and the maximum horizontal compressive stress.

3. Amoco, Jicarilla 155 A#1, section 32, T., 26 N., R. 5 W., Rio Arriba Co., NM. This core consists of the slab ribbons of 120 ft of four-inch diameter core, from depths of 5247-5367 ft. Numerous short fractures are present in this core, all apparently having the same strike, parallel to the maximum horizontal compressive stress. The vertical terminations of these fractures typically occur at minor bedding planes within the sandstones and at shale partings (Figure 30). Calcite fills or partially fills some of the hairline fractures (mineralization is more complete in the narrow-aperture regions if the fractures terminate near or at shale beds). Other fractures are apparently unmineralized. Fracture frequency increases and spacing decreases downhole into the finer-grained intervals.

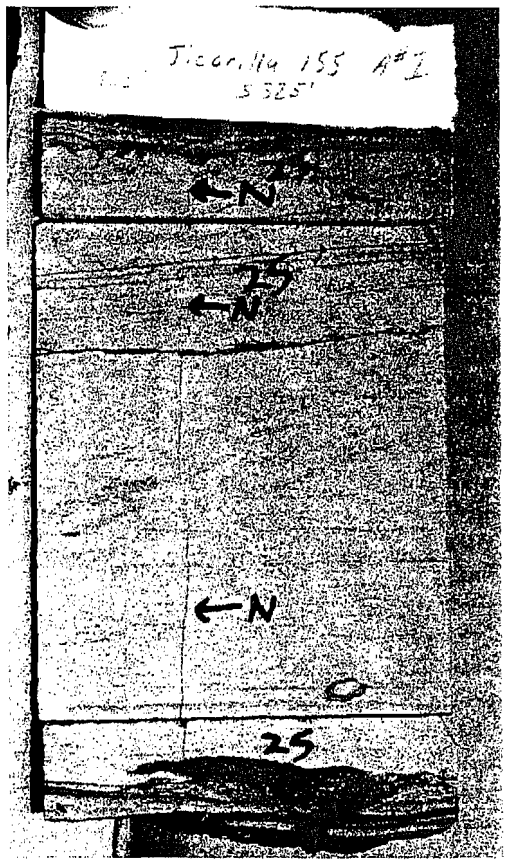

Figure 31: Photograph illustrating how the natural fracture (N) terminates at top and base at shale partings.

4. Tenneco, #7 Gallegos, section 34, T. 26 N., R. 11 W., San Juan Co., NM. This core consists of 34 ft of the butts (opposite the ribbons, which were not found) of four-inch diameter core from the Pictured Cliffs sandstones at a depth of 2190-2224 ft. The high-porosity sandstone and the bioturbated, laminated sandstone-shale facies of this core contain no fractures.

5. Valencia Canyon #13, section 22, T., 28N., R. 4 W., Rio Arriba Co., NM. This core consists of 60 ft of slab ribbons and associate butts (stored separately) from four-inch diameter core, from the Pictured Cliffs sandstone at a depth of 4260-4320 ft. Several short vertical fractures occur within the upper, coarser grained, higher porosity sandstones (Figure

31), commonly terminating vertically for no apparent reason within the sandstones but locally at shale partings. Fracture apertures are obscure, but no larger than 1 mm in width. Quartz mineralization occludes approximately half of the aperture.

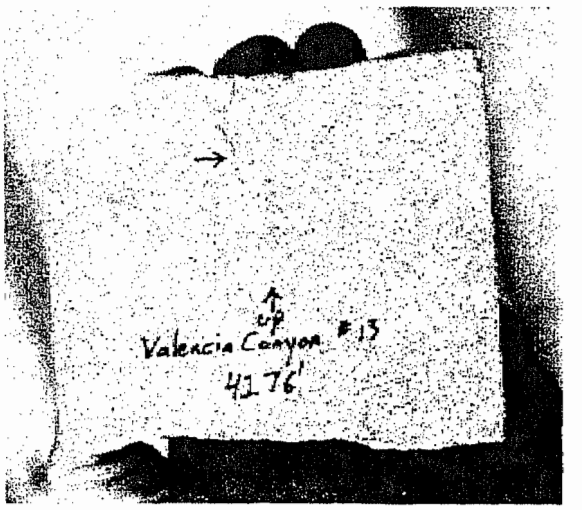

Figure 32: A small, irregular extension fracture is shown to terminate within a single lithologic unit.

6. Union Texas Petroleum, Newsom A-3E, section 4, T. 26 N., R 8 W., San Juan Co., NM. Approximately 130 ft of slab ribbons from discontinuous four-inch core are available from the Tocito sandstone (top: 6524 ft), Upper Carlisle shale (top: 6625 ft) and Juana Lopez member (top: 6639 ft). Several irregular, one-foot tall, vertical extension fractures, lined with a fine calcite druze, are present in the slightly glauconitic, calcareous sandstones and siltstones. Vertical terminations tend to be at the bedding plane lithology breaks. No fractures occur in the associated poker-chip marine shales.

7. Union Texas Petroleum, Angel Peak #37B, section 24, T., 28 N., R. 11 W., San Juan Co., NM. Slab ribbons from three-inch core are available from this well, from an undefined Mesaverde interval between 5754 and 5910 ft. The majority of the core consists of unfractured, heavily bioturbated, glauconitic sandstones and silty shales. The rare natural fractures occur in an interbedded thin, rippled, fine-grained sandstone facies (Figure 32).

8. Enerdyne, S.F. #205, section 21, T. 20 N., R. 9W., San Juan Co., NM. This is 63 ft of whole, 1.5-inch diameter core from the Menefee formation. No natural fractures are present in the core, which consists of high-porosity sandstones and carbonaceous mudstones.

9. Amoco, Romero Gas Com A-1, section 27, T. 29N., R. 10 W., San Juan Co., NM. Seventy-eight ft of core from an undefined zone of the Mesaverde formation, taken discontinuously between the depths of 2407 and 2901 ft. The majority of this core consists of unfractured, highly bioturbated, sandstone/shale in disrupted laminations (Figure 33). However, the four-ft thick interval at 2890 –2894 contains numerous irregular, unmineralized, vertical fractures, confined to the cleaner, very-fine grained sandstones unique to this zone.

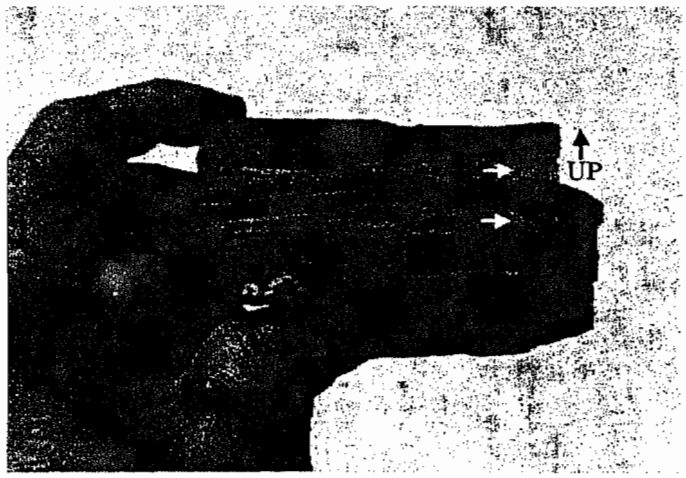

Figure 33: White arrows indicate the location of short extension fractures limited by bedding and lithology In the Angel Peak #37B well.

Figure 34: Photograph illustrating an unfractured, highly bioturbated facies within the Mesaverde Group, Romero Gas Com A-1 well.

10. Torreon Wash #C-2, section 18, T. 18 N., R.4 W., NM. Only seven feet of two-inch diameter whole core is available from this well. No fractures are present in the coaly to

carbonaceous shale interval, although the cleaner coals have a well developed face cleat system with half-inch spacing.

11. Torreon Wash #C-1, section 20, T. 18 N., R. 3 W., NM. No fractures are present in the 51 ft of two-inch diameter core, taken from a carbonaceous to coaly to shaley facies, from this shallow well (top of core at a depth of 42 ft).

12. Meridian Oil, Sunray H Comp #6, section 11, T. 30 N., R. 10 W., San Juan Co., NM. This core consists of a mixture of whole two-inch and slabs of four-inch diameter core from the Mesaverde (Fruitland) interval. A total of 185 ft of core was recovered from fluvial and marine environments, cored discontinuously between depths of 4828-5327 ft. Numerous short, vertical, hairline extension fractures, lined with quartz druze, are present in the fine-grained, unburrowed sandstones of the marine environment. These terminate vertically either at bedding plane contacts or else blindly within the rock, for no apparent reason. Several examples were noted where a natural fracture strikes parallel to a nearby coring-induced petal fracture, indicating that the maximum horizontal compressive stress trends parallel to the strikes of the fractures in this system.

13. Amoco, Carson Federal G #1, section 25, T. 28 N., R. 4 W., Rio Arriba Co., NM. Two hundred and thirty-four feet of four-inch diameter core were taken from an unspecified Mesaverde interval at a depth of 4309-4584 ft in this well; only the slab ribbons are available for study. This well was deviated about 25-30° from the vertical, therefore bedding is oriented consistently 25-30° oblique to the core axis. Extension fractures are oriented consistently normal to bedding (Figure 34). Unfortunately, a wellbore azimuth survey was either never made or has been lost, thus the strike of the fractures remains unknown. Numerous narrow (1.0-0.5 mm), calcite- and quartz-mineralized (50-95% fill of the total aperture), natural fractures are present in the very-fine grained, crossbedded sandstones of this core, more in the cleaner sandstones and fewer in the bioturbated intervals. Fracture tops and bases are typically out of the core, but can be seen locally to terminate at bedding-plane contacts, most commonly at shale beds. An estimation of fracture spacings can be obtained because the wellbore deviated across the fracture strike, with spacings ranging from inches in the thinnest beds to several feet in the thicker beds. All adjacent fractures seem have parallel strikes. Fractures are nearly absent from the higher-porosity, bioturbated, fine-grained sandstone that comprises the lower half of the core.

14. Helen Hause #1, section 8, T. 25 N., R. 8 W., San Juan Co., NM. Sixty ft of three-inch diameter core were taken from the Mesaverde interval between 5460-5723 ft: only the slabbed ribbons are available for study. A few small hairline fractures are located in the siltstones that comprise half of this core. No fractures are present in the shale facies that comprises the other half of the core.

15. Tenneco Oil, Canyon #4, section 5, T. 25 N., R. 11 W., San Juan Co., NM. Thirty-eight ft of four-inch slab ribbons are available from the Pictured Cliffs interval in this well. The facies consists almost entirely of high-porosity, white sandstone, and is totally without

vertical extension fractures. However, several low-angle, inclined thrust planes, with dip-slip oriented facial striae, suggest low-angle/reverse faulting through this interval.

Figure 35: Core from a deviated well (Carson Federal G#1) shows apparently inclined bedding and fractures.

5.2.2 Dakota Cores

The first two cores described below are from deeper intervals of the last two wells listed under the Mesaverde interval above.

1. Helen Hause #1, section 8, T. 25 N., R. 8 W., San Juan Co., NM. Slabs of 54 ft of three-inch diameter core, taken from two intervals between the depths of 6304-6574 ft are available for study in this well. Several short, narrow, calcite and quartz-mineralized vertical extension fractures are present in the clean, quartzitic sandstones in this core (Figure 35), some striking within 10^{0} of parallel to adjacent petal fractures. An additional set of short, wide fractures, mineralized with kaolinite and quartz, is also present. These fractures terminate at the common horizontal stylolites (Figure 36).

2. Tenneco Oil, Canyon #4, section 5, T. 25 N., R. 11 W., San Juan Co., NM. Fifty-eight ft of slab ribbon from four-inch diameter core, from the depths of 5802-5860 ft, is available from

this well. Numerous short, hairline fractures are present in the clean, quartzitic sandstones of this core. These fractures are lined with a quartz druze. Fewer fractures are present in the bioturbated intervals. Most of the fractures appear to be parallel to each other, but one example is present where two calcite-mineralized fractures intersect at an angle of 20° within a 0.5 ft thick calcareous siltstone.

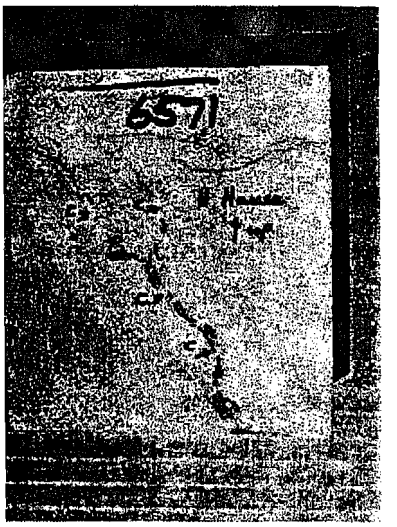

Figure 36: Calcite (C) mineralization in extension fractures. Most of the apparent irregularity is due to near parallelism between fracture surface and slab face.

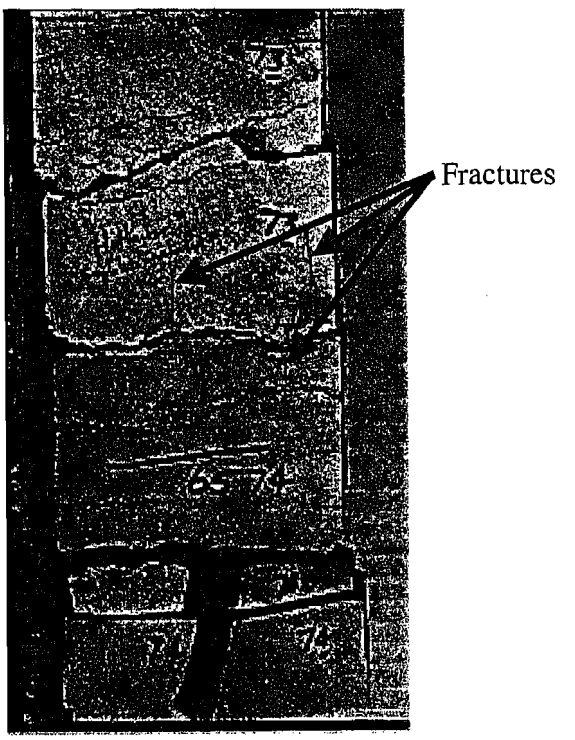

Figure 37: Suite of stylolite-related fractures within the Helen Hause # 1 well.

3. Amoco, Ute Indians A-15, section 36, T. 32 N., R. 14 W., NM. This core consists of 175 ft of unslabbed, four-inch diameter whole core, intersecting the Dakota sandstone from 2433-2608 ft. Three fracture 'facies' are present in the clean sandstones of this, the most highly fractured of any of the cores examined: 1) abundant stylolite-related fractures, associated with (originating at?) and bounded by stylolites, these fractures contain patchy kaolinite and/or druzy quartz mineralization. Most but not all of these have parallel strikes. 2) fault-related fractures (Figure 37), occur within a brecciated zone, probably ten feet thick, of re-cemented, fault-derived rubble, but commonly with poor recovery of the core. 3) Parallel vertical fractures with locally great height (up to 5 ft), crossing numerous lithologic boundaries and mineralized with both kaolinite and quartz (Figures 38, 39). Synsedimentary faults and miscellaneous compaction faults are also present. Unfractured lithologies are also present, typically the bioturbated and high-porosity sandstones, and the shales.

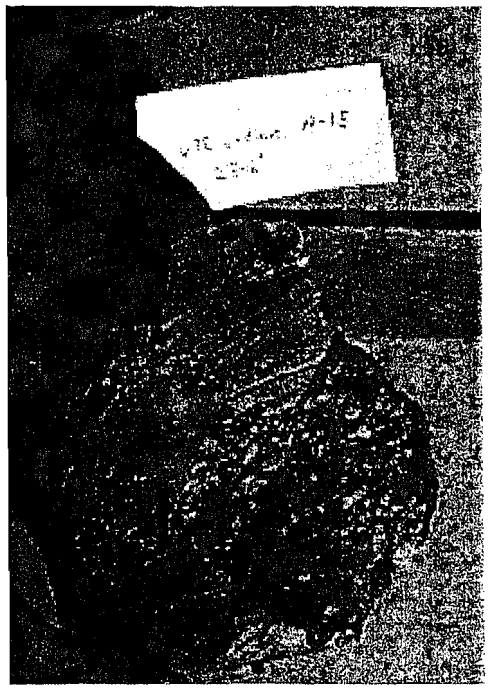

Figure 38: Core of fault breccia from the Ute Indians A-15 well.

4. Amoco, Jicarilla Apache 118 #14, section 36, t. 26 N., R. 3 W., Rio Arriba Co., NM. Approximately 400 ft of 3.5-inch diameter core were recovered from the Dakota interval at depths of 7109-7639 ft. The ribbons from slabbing were available for study. Fractures in this core have a uniform dip 10-15° oblique to the core axis. However, since bedding is not also oblique but remains normal to the core axis, the fracture dips are probably real rather than an artifact of a deviated borehole as is the case with the Carson Federal G #1 well (#13 above). Numerous hairline fractures (0.1 mm total width, occluded to 50% filled with calcite mineralization) are present in the massive shale/siltstone facies. Spacing normal to the fracture planes ranges from 0.5-2.0 ft, and fracture faces are ornamented with plumes. These fractures strike parallel to each other as well as to the associated drilling-induced fractures. Smaller fractures with rougher, quartz-druze-lined faces cut across the thinly laminated sand-shale bedding in other depositional facies.

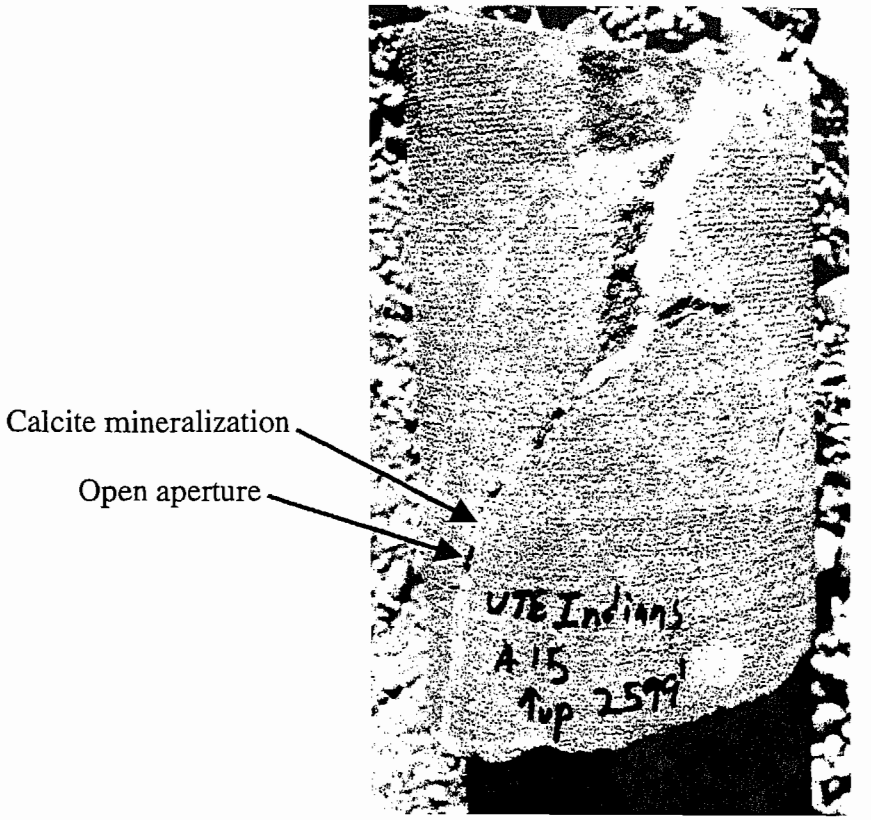

Figure 39: Large calcite mineralized fractures with obvious porosity. When viewed end on the parallel nature of fractures in this core can be observed (Figure 39).

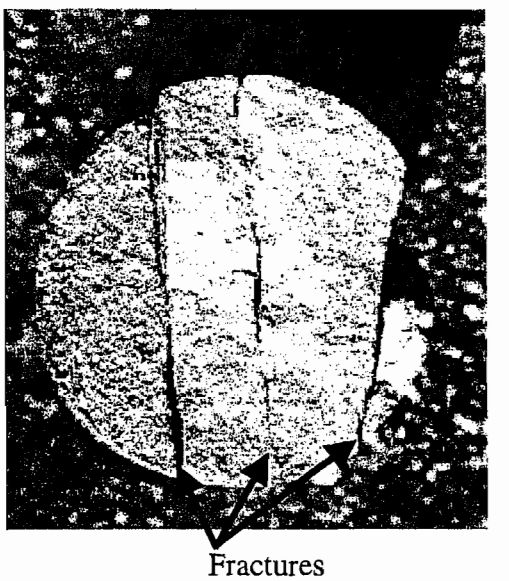

Figure 40: End view of the same core shown in Figure 38 illustrating the parallel nature of the natural fractures.

5. Getty, Jicarilla B20-E, section 31, T. 25 N., R. 5 W., Rio Arriba Co., NM. 234 ft of four-inch diameter core was recovered from the Dakota interval between 5984-6280 ft; ribbons from slabbing are available for study. Only two, small, obscure natural fractures are present in this entire core: one in the siltstone-shale laminated facies and one in the shales. The dearth of fractures is attributed to the high degree of bioturbation present in the sandstones, and to the fact that much of the rest of the core consists of black, clay, shale.

6. Amoco, Jicarilla 396 #8, section 17, T. 23 N., R. 3 W., NM. 263 ft of four-inch diameter core was taken from between 7368 and 7481 ft. Only the slab ribbons are available for study. Few fractures are present in the highly bioturbated sandstones or in the highly porous, massive sandstones. Natural fractures are only common where the siliceous white sandstone is well cemented, in the lower core interval (top at 7481 ft). Mineralization on these hairline fractures is obscure, probably consisting of a very fine quartz druze.

5.3 Core Fracture Summary

Natural fractures in the Mesaverde interval are primarily vertical, extension fractures, filled to partially filled with calcite and locally quartz. Quartz may in fact be an early phase that's present but obscured under later calcite mineralization. The narrower fractures (less than half a millimeter) are typically those that are more completely occluded by mineralization. The data suggest that there is one, sub-parallel set of fractures that strikes parallel to the maximum in situ horizontal compressive stress. The orientation of that stress is poorly constrained by the data presented here, but other indicators and published data (see below) suggest a generally north-south strike with local variations. Vertical extents of the fractures are variable; smaller fractures tend to terminate within sandstones and/or at internal bedding boundaries whereas the larger fractures terminate at the major bedding boundaries such as at contacts with bounding shales. The majority of the cored fractures are less than 1 mm in total width, as would be expected in a standard population or regional extension fractures (i.e., with significant numbers of small fractures and much fewer large fractures). A few bedding-parallel shear fractures are also present in Mesaverde sandstones.

Mesaverde fracture spacings are poorly constrained by the subsurface data, although the few data points from deviated wells suggest that spacings of inches to several feet are common in the fractured lithologies. By analogy to outcrops, the fractures are expected to be more closely spaced in thinner beds, with spacings typically equivalent to or less than bed thicknesses. Larger and more closely spaced fractures with more variable strikes are present in association with fault zones. The more highly fractured lithologies include the well cemented, well sorted, unburrowed sandstones and siltstones: few fractures are present in high-porosity sandstones, in highly bioturbated sandstones, in glauconitic sandstones, or in the clay shales and carbonaceous shales. Numerous hairline fractures are present, however, in calcareous shales.

Natural fractures in the Dakota sandstones are similar in many respects to those in the Mesaverde. Most of the Dakota fractures are vertical extension fractures, and the meager data support a set of parallel fractures that also strike parallel to the maximum in situ horizontal compressive stress. Several variable fracture strikes were also noted among the Dakota

fractures, however, and more than one set of intersecting fractures may be present. This type of variability was also reported in cored Dakota fractures by Lorenz et al. (1999).

Fault zones enhance fracture variability and intensity. Mineralization in the Dakota fractures includes quartz and calcite, as seen in the Mesaverde fractures, but a phase of kaolinite precipitation may also be present. Dakota fractures are significantly more numerous in the cleaner, better cemented, siliceous sandstones, and are notably absent in the highly bioturbated intervals. A set of short, wide fractures is exclusive to a facies consisting of well-cemented sandstones containing numerous horizontal stylolites, and these fractures typically originate at the stylolite peaks.

Little can be determined about the lateral distribution and variability of fracture characteristics from the cores, in part because cores represent such a miniscule sampling of the lateral dimensions of the formations. This also due in part to the fact that the available cores come from different, non-correlative zones within the overall Mesaverde and Dakota intervals, making it difficult to eliminate that axis of variability and normalize observations to permit meaningful detailed observations. However, it can be said with certainty that a generally N-S to NNE-SSW striking set of natural fractures is pervasive in all parts of the subsurface basin.

Ouenes et al. (1998) have indirectly addressed such variabilities in development of the San Juan fracture systems by using neural networks to compare estimated ultimate recovery (EUR) with subtle structures. They have reported that minor anticlines, with presumably enhanced fracturing, correlate to higher EUR's. Ortega and Marrett (2000) claim a degree of success in the use of microfractures to predict the strikes, frequencies, connectivity and degree of cementation of macrofractures in the San Juan basin. In the absence of coring on 1 acre spacing, and until fracture identification on 3D seismic studies has been more fully quantified, such indirect means of fracture study may be useful in complementing conceptual models of fracture characterization such as that presented here.

6.0 COMPARISON OF SUBSURFACE AND OUTCROP FRACTURE CHARACTERISTICS

A set of vertical extension fractures, striking N-E to NNE-SSW but with local variations, is present in both the outcrop and subsurface in both Mesaverde and Dakota sandstones. Additional sets of conjugate shear fractures have been recognized in outcrops of Dakota strata and may be present in the subsurface (e.g., Lorenz et al., 1999), but the deformation bands prevalent in outcrops in parts of the basin as yet have no documented subsurface equivalent. Outcrops typically display secondary cross fractures. These are rare in the subsurface, which suggests, along with their morphology, that they are related to surficial processes and irrelevant to subsurface studies. However, oblique fractures associated with local structures such as the Hogback monocline may be present in similar strata in the subsurface.

Spacings of the bed-normal extension fractures would appear to be on the order of or less than the thicknesses of the beds in which they formed in both outcrop and subsurface. Fracture intensities increase in association with faults, where there is a gradation from intense fracturing into fault breccia.

Bioturbation and minimal cementation seems to have inhibited fracture development in both domains, and there are similarities in the vertical limitation of fracture growth by bedding/lithology contrasts. Fracture mineralizations have been largely dissolved or replaced in outcrops, but local examples of preserved mineralization show that quartz and calcite were originally common to subsurface fractures and those now found in outcrop.

7.0 SUBSURFACE STRESSES

The permeability of a fracture system is not controlled entirely by parameters such as aperture, frequency, and connectivity. Stress magnitudes, differentials, and orientations will also influence the degree of control natural fractures have on permeability and permeability anisotropy (e.g., Lorenz, 1999). Pore pressures will also be a contributing factor in the stress equation.

Pore pressures in the San Juan basin are typically less than hydrostatic at present, thus the weight of the overburden as well as any active and/or locked–in tectonic stresses dominate the stress regime. Few data points have been collected on the in situ stress orientations within the San Juan basin, and even fewer on stress magnitudes. The large, N-S striking Tertiary dikes that cluster in the northeastern part of the basin and that are scattered sparsely elsewhere suggest that the maximum in situ horizontal stress at crustal levels was oriented N-S during the time of intrusion. However, this is not necessarily the orientation of the stresses under current conditions or at the shallower Mesaverde and Dakota stratigraphic levels.

The only published results of a study designed specifically to determine the present-day stress orientations (Yale et al., 1993) found a consistently NE-SW trend for the maximum horizontal compressive stress in four wells in one field. This field is located near Cuba, in the southeastern corner of the basin (Yale, personal communication, 1998). It is probable that this the local stress orientation has been influenced by the nearby Nacimiento uplift, similar to that recorded by the family of conjugate deformation bands slightly farther to the south, near San Ysidro (see discussion on the Rio Puerco Fault Zone above). This stress field therefore should not be extrapolated to the entire basin.

Other markers for the present-day stress orientation include coring-induced petal fractures in oriented core (e.g., Lorenz et al., 1999) and wellbore breakouts seen in oriented caliper or wellbore image logs. Unpublished company reports note several such indicators in the San Juan basin, with the maximum horizontal compressive stress striking consistently N-S to NNE-SSW.

8.0 PROBABLE EFFECTS OF FRACTURES ON RESERVOIRS

8.1 Introduction

Fractures can increase effective porosity and permeability and introduce permeability anisotropy, particularly in rocks with low matrix permeability such as the tight-gas sandstone reservoirs of the San Juan Basin (e.g., Rice, 1983; Nelson, 1985; Fassett, 1991; Teufel and

Farrell, 1992). Mineralized fractures and deformation bands, however, are characterized by significant permeability reduction (Nelson, 1985; Antonellini and Aydin, 1994; Antonellini et al., 1994). Faults can also function as fluid migration pathways, barriers, or a combination of both (Caine et al., 1996). For modeling and production purposes it is important to document directions of preferred fracture and fault orientations within hydrocarbon reservoirs. By quantifying the controls on fracture and fault orientation and distribution in a given reservoir the accuracy of fluid flow modeling can be improved, thereby increasing primary and secondary hydrocarbon recovery.

8.2 Permeability Anisotropy

Fractures, deformation bands and faults can influence permeability and fluid flow within an aquifer or petroleum reservoir. In general, these features influence fluid flow by introducing a horizontal permeability anisotropy. One can calculate the aspect ratio of a drainage ellipse around a production well within a fractured reservoir. Harstad et al. (1998) calculates the aspect ratio as the square root of the permeability ratio.

$$a/b = (k_{max}/k_{min})^{1/2}$$

If the permeability ratio were 100 to 1 then using this formula the aspect ratio would be 10:1. Field observations suggest that large permeability anisotropies and aspect ratios are not uncommon (Elkins and Skov, 1960; Lorenz and Finley, 1989). Lorenz, et al. (1989) reported permeability anisotropies of up to 100 to 1 in a Mesaverde reservoir in Colorado. A 1000 to 1 permeability anisotropy within the Spraberry trend of west Texas has also been reported (Elkins and Skov, 1960). A 10:1 permeability anisotropy was measured in pressure interference tests within Mesaverde sandstones in the San Juan Basin (Harstad et al., 1998). Measured values were 0.348 md maximum horizontal permeability and 0.035 md minimum horizontal permeability. The direction of maximum permeability was determined to be approximately N4°E (Harstad et al., 1998). This is consistent with the observed outcrop and core fracture data.

8.3 Influence of Matrix Porosity and Permeability on Fracture Related Permeability Anisotropy

Matrix porosity and permeability can influence permeability anisotropy. Ute Dome, located on the eastern edge of the Four Corners platform and west of the Hogback monocline, will be used to help illustrate this point. Porosity data (15%) and permeability data (10 millidarcies) (Tezack, 1978) indicate that the Dakota sandstone reservoir at Ute Dome is a conventional reservoir rock with respect to matrix permeability. This contrasts with published data from the central part of the San Juan basin, where the Dakota is low-permeability reservoir (e.g. porosity between 5-15% and matrix permeabilities less than 1 millidarcy: DuChene, 1989). Open fractures should have less influence in reservoirs with 10 md matrix permeabilities than in areas where the permeability is significantly less. Qualitatively, as matrix permeability increases the permeability anisotropy associated with open fractures will decrease. The influence on permeability is dependent upon the following fracture variables: 1) trace length, 2) aperture width, 3) interconnectivity of the fracture system, and 4) number of fractures intersecting the well bore.

Deformation bands are barriers to flow, but may also create permeability anisotropy in a reservoir. In this scenario, the direction of maximum permeability would be parallel to deformation band strike but flow would be contained primarily within the matrix between bands rather than along and within them. The result would be a drainage pattern where maximum elongation is parallel to major fracture/deformation band trends. Therefore, in low permeability rocks, fractures will be the primary pathways for fluid flow. In contrast, in the high porosity sandstones that host deformation bands, the matrix will provide the main pathway for fluid flow.

8.4 Summary

This study shows that the primary fracture set within the San Juan basin strikes N-S to NNE-SSW. The direction of maximum permeability should parallel the strike of these fractures. Studies by Harstad (1998) and Hammoud (2000) have, in fact, documented significant permeability anisotropy in Mesaverde reservoirs in different parts of the inner San Juan basin, with maximum permeability oriented in the N-S to NNE-SSW direction (10°).

Our observations suggest that fracture permeability would not enhance the system permeability over matrix permeability in either the vertical direction or the direction normal to fracturing in either formation. This is because fractures did not propagate through most shale breaks within reservoir sandstones and cross fractures appear to be rare in Mesaverde strata in the subsurface, thus horizontal permeability orthogonal to the main fracture set would be near matrix values for Mesaverde reservoirs. However, secondary fracturing may enhance orthogonal horizontal permeabilities in the Dakota interval, where the larger numbers and orientations of fractures dictate a less anisotropic permeability system. Numerous small fractures are present in both systems that would be capable of feeding larger fractures.

Most of the natural fractures strike parallel to the maximum horizontal compressive stress, therefore a hydraulic fracture would propagate parallel to, without intersecting, the natural fracture system. Significant variations in fracture strike and intensity may occur at and near local geologic structures such as anticlines, synclines, monoclines and faults, providing secondary cross fractures or fractures oriented oblique to the in situ stresses and therefore more amenable to hydraulic fracturing.

9.0 RECOMMENDATIONS FOR FUTURE WORK

Although a new tectonic framework for, and general characteristics of, the natural fractures in Mesaverde and Dakota strata in the San Juan basin are delineated here, specific subsurface attributes such as spacing and variations in orientations, and their correlations to subsurface structures, are still only partially constrained. Oriented core and wellbore image data, especially from deviated wells, would help tremendously in refining these parameters, particularly the in situ spacing of conductive fractures. Deviated wells may not be economically feasible production mechanisms for such relatively shallow, layered reservoirs. However, a few research-oriented, deviated, cored, and logged wells would provide information on the in situ fracture characteristics such as spacings and range of apertures that can never be obtained from vertical wells, leading to better placement and completion practices for the more common, vertical production wells.

Core fracture data from shalier Cretaceous intervals such as the Lewis and Niobrara, units that have relatively poor outcrop exposures, would help in extrapolation of the fracture model presented here to these reservoirs.

In most intervals less is known about in situ stresses than about the subsurface fractures. Data from mini hydraulic fractures, Anelastic Strain Recovery techniques, as well as from wellbore-image logs, would help refine knowledge of the orientations and magnitudes of the in situ stresses.

The fracture permeabilities are probably sensitive to changes in stress during reservoir pressure drawdown/production, but this is not a known factor. A compilation of the known pore pressure data and rock mechanical property data in the Cretaceous reservoirs should be undertaken in order to construct a quantitative model of the dynamics of the fractures under changing stress conditions.

Characteristics of the stresses and natural fractures in potential Paleozoic reservoirs are virtually unknown, thus even a limited number of cores from these intervals would provide a multifold increase in knowledge.

10.0 CONCLUSIONS

Characterizing the subsurface fracture pattern in the San Juan basin on the basis of the core and outcrop fracture characteristics reported here is somewhat like playing the game "battleship", where each player tries to sink the other's invisible ships with random hits on a gridwork. In this version of the game, however, the grid is many miles across and the squares are eight-inch wellbores. The outcrop patterns, filtered to exclude surficial effects, provide the player with a conceptual idea of the types and numbers of ships (fractures) to expect in the invisible subsurface, laying out the framework of the game. The cores provide pinprick data points in parts of the basin, telling about hits and misses, with which to reconstruct the pattern and sink the whole fleet. Once the fleet has been sunk or the whole basin cored, the complete pattern is obvious. Unfortunately, the myriad of uncored wellbores in which a minimal log suite was run add little if anything to the player's knowledge of the subsurface fracture pattern. In addition, Mother Nature doesn't always play by the rules, invariably throwing in an unexpected fault, anticline, or submarine. Nevertheless, the conceptual model constructed from the outcrop and subsurface data provides a rationale for drilling and exploiting the fractured reservoirs in the San Juan basin.

Our conceptual model reconstructs north-south trending compressive stresses created by southward indentation of the San Juan dome area (where Precambrian rocks are exposed at an elevation of 14,000 ft) and northward indentation of the Zuni uplift, controlled Laramide-age fracturing. Contemporaneous right-lateral transpressive wrench motion (due to the asymmetrical arrangement of the two indenters and/or northeastward translation of the basin) was both concentrated at the basin margins (Nacimiento uplift and Hogback monocline on east and west edges respectively) and distributed across the strata depth. These shallow, basin-scale stresses were the indirect product of continental-scale, Laramide crustal dynamics.

Within this framework, a set of vertical extension fractures, striking N-E to NNE-SSW but with local variations, was formed in both Mesaverde and Dakota sandstones. Additional sets of conjugate shear fractures have been recognized in outcrops of Dakota strata and may be present in the subsurface. Fractures in the immature Mesaverde sandstones typically formed as relatively long, irregular extension fractures, whereas the quartzitic Dakota sandstones contain short, sub-parallel, closely spaced, extension fractures. Outcrops typically display secondary cross fractures which are rare in the subsurface, although oblique fractures associated with local structures such as the Hogback monocline may be present in similar subsurface structures.

Spacings of the bed-normal extension fractures are approximately equal to or less than the thicknesses of the beds in which they formed, in both outcrop and subsurface. Fracture intensities increase and fracture strikes deviate from the regional trends in association with faults. Fracture development was minimal where bioturbation and minimal cementation altered the mechanical properties of the sandstones to limit fracture susceptibility. Quartz and calcite, and locally kaolinite, are the common mineralization phases that incompletely fill the subsurface fractures.

Maximum permeability has been observed to parallel the N-S to NNE-SSW primary extension fracture set. These fractures strike parallel to the maximum horizontal compressive stress. Therefore, induced hydraulic fractures may parallel the primary fracture set in many locations. Variations in fracture strike will occur on and near local geologic structures. The secondary fractures associated with these structures may allow for interconnected drainage of a reservoir that could be further enhanced through hydraulic fracturing

11.0 ACKNOWLEDGMENTS

This work has been supported by the National Energy Technology Laboratory, Morgantown, West Virginia, as part of the Geotechnology for Low-Permeability Reservoirs contract to Sandia National Laboratories. Our thanks to Tom Mroz, NETL contract manager for this project, and to Jim Ammer, project manager for the San Juan basin study, for their support. We would also like to thank the New Mexico Library of Subsurface Data, (New Mexico Bureau of Mines and Technology), for access to the core data reported on here. Sandia is a multiprogram laboratory operated by Sandia Corporation, a Lockheed Martin Company, for the United States Department of Energy under contract DE-AC04-94AL85000.

12.0 REFERENCES

Antonellini, M., and Aydin, A., 1994, Effect of faulting on fluid flow in porous sandstones: Petrophysical properties: American Association of Petroleum Geologists Bulletin, v. 78, p. 355-377.

Antonellini, M., Aydin, A., and Pollard, D.D., 1994, Microstructure of deformation bands in porous sandstones at Arches National Park, Utah: Journal of Structural Geology, v. 16, p. 941-959.

Ayers, W.B., Jr., Kaiser, W.R., and Laubach, S.E., 1991, Geologic and hydrologic controls on the occurrence and producibility of coalbed methane, Fruitland Formation, San Juan

Basin: The University of Texas at Austin, Bureau of Economic Geology, topical report prepared for Gas Research Institute under contract No. 5087-214-1544, 314 p.

Baltz, E.H., 1967, Stratigraphy and regional tectonic implications of part of upper Cretaceous and Tertiary rocks, east-central San Juan basin, New Mexico: Washington, U.S. government printing office, 101 p.

Barnes, F.C., and Arnold, E., 1950, Proved and potential oil and gas traps of the San Juan Basin, San Juan Basin New Mexico and Colorado, New Mexico Geological Society First Field Conference Guidebook, p. 90-100.

Bird, P., 1998, Kinematic history of the Laramide orogeny in latitudes 35° - 49°N, western United States: Tectonics, v. 17, p. 780-801.

Bond, W.A., 1984, Application of Lopatin's method to determine burial history, evolution of the thermal gradient, and timing of hydrocarbon maturation in Cretaceous source rocks in the San Juan basin, northwestern New Mexico and southwestern Colorado, Hydrocarbon Source Rocks of the Greater Rocky Mountain Region, Rocky Mountain Association of Geologists, p. 433-447.

Caine, J.S., Evans, J.P., and Forster, C.B., 1996, Fault zone architecture and permeability structure: Geology, v. 24, p. 1025-1028.

Cather, S.C., 1989, Post-Laramide tectonic and volcanic transition in west-central New Mexico, *in* Anderson, O.J., Lucas, S.G., Love, D.W., and Cather, S.W., eds., Southeastern Colorado Plateau, New Mexico Geological Society 40th Field Conference Guidebook, p. 91-97.

Cather, S.M., 1999, Implications of Jurassic, Cretaceous, and Proterozoic piercing lines for Laramide oblique-slip faulting in New Mexico and rotation of the Colorado Plateau: Geological Society of America Bulletin, v. 111, p. 849-868.

Chamberlin, R.M., and Anderson, O.J., 1989, The Laramide Zuni Uplift, southeastern Colorado Plateau: A microcosm of Eurasian-style indentation-extrusion tectonics?, *in* Anderson, O.J., Lucas, S.G., Love, D.W., and Cather, S.M., eds., Southeastern Colorado Plateau, New Mexico Geological Society 40th Annual Field Conference Guidebook, p. 81-90.

Chapin, C.E., and Cather, S.M., 1981, Eocene tectonics and sedimentation in the Colorado Plateau-Rocky Mountain area, *in* Dickinson, W.R., and Payne, M.D., eds., Relations of tectonics to ore deposits in the southern Cordillera: Arizona Geological Society Digest, Volume 14, p. 173-198.

Chapin, C.E., and Cather, S.M., 1983, Eocene tectonics and sedimentation in the Colorado Plateau - Rocky Mountain area, *in* Lowell, J.D., and Gries, R., eds., Rocky Mountain foreland basins and uplifts: Rocky Mountain Association of Geologists, p. 33-56.

Condon, S.M., 1988, Joint patterns on the northwest side of the San Juan basin (Southern Ute Indian Reservation), southwest Colorado, *in* Fassett, J.E., ed., Geology and Coal-Bed Methane Resources of the Northern San Juan Basin, Colorado and New Mexico, Rocky Mountain Association of Geologists, p. 61-68.

Condon, S.M., 1997, Fracture studies on the upper Cretaceous Pictured Cliffs Sandstone and Fruitland Formation, northern San Juan basin, La Plata county, Colorado, *in* Close, J.C., and Casey, T.A., eds., Natural Fracture systems in the Southern Rockies: Four Corners Geological Society Guidebook, p. 85-96.

Corbitt, L.L., and Woodward, L.A., 1973, Tectonic framework of Cordilleran foldbelt in southwestern New Mexico: American Association of Petroleum Geologists Bulletin, v. 57, p. 2207-2216.

Cross, T.A., 1986, Tectonic controls of foreland basin subsidence and Laramide style deformation, western United States, *in* Allen, P.A., and Homewood, P., eds., Foreland basins: International Association of Sedimentologists Special Publication no. 8, p. 15-39.

Dickinson, W.R., Klute, M.A., Hayes, M.J., Janecke, S.U., Lundin, E.R., McKittrick, M.A., and Olivares, M.D., 1988, Paleogeographic and paleotectonic setting of Laramide sedimentary basins in the central Rocky Mountain region: Geological Society of America Bulletin, v. 100, p. 1023-1039.

Dickinson, W.R., and Snyder, W.S., 1978, Plate tectonics of the Laramide orogeny, *in* Matthews, V., III, ed., Laramide folding associated with basement block faulting in the western United States: Geological Society of America Memoir 151, p. 355-365.

DuChene, H.R., 1989, Fracture reservoirs in the San Juan Basin, Colorado and New Mexico, *in* Lorenz, J.C., and Lucas, S.G., eds., Energy frontiers in the Rockies, Albuquerque Geological Society, p. 101-109.

Elkins, L.F., and Skov, A.M., 1960, Determination of fracture orientation from pressure interference: Petroleum Transactions, American Institute of Mining Engineers, v. 219, p. 301-304.

Emmendorfer, A.P., 1992, Tectonic dolomitization in the Gavilan Mancos oil pool, Rio Arriba county, New Mexico, *in* Lucas, S.G., Kues, B.S., Williamson, T.E., and Hunt, A.P., eds., San Juan Basin IV, New Mexico Geological Society Guidebook, 43rd Field Conference, p. 123-131.

Fassett, J.E., 1989, Coal-bed methane - A contumacious, free-spirited bride; The geologic handmaiden of coal beds, *in* Lorenz, J.C., and Lucas, S.G., eds., Energy Frontiers in the Rockies, Albuquerque Geological Society, p. 131-146.

Fassett, J.E., 1991, Oil and gas resources of the San Juan basin, New Mexico and Colorado, *in* Gluskoter, H.J., Rice, D.D., and Taylor, R.B., eds., Economic Geology, U.S., Volume P-2: The Geology of North America, Geological Society of America, p. 357-372.

Fassett, J.E., and Hinds, J.S., 1971, Geology and fuel resources of the Fruitland Formation and Kirtland Shale of the San Juan Basin, New Mexico and Colorado: United States Geological Survey Professional Paper 676, 76 p.

Fassett, J.E., Molenaar, C.M., Aubrey, W.M., Ridgley, J.L., Zech, R.S., Leckie, M.R., and Dunbar, R.W., 1990, Cretaceous stratigraphy of the San Juan basin, New Mexico and Colorado: American Association of Petroleum Geologists Bulletin, v. 74, p. 1323.

Finch, S.T., Jr., 1994, Fracture and methane-contamination study Animas River valley from Bondad, Colorado to Cedar Hill, New Mexico, Gas Research Institute Topical Report Contract No. 5091-253-2160, p. 1-45.

Gilkey, A.K., 1953, Fracture Pattern of the Zuni Uplift: Oak Ridge, United States Atomic Energy Commission, p. 34.

Gilkey, A.K., and Duschatko, R.W., 1953, Progress report for June 15 to December 15, 1952, Part 1: Fracture patterns of the Zuni Uplift, Part 2: Fracture studies of the Lucero Uplift, Columbia University, p. 24.

Gorham, F.D., Jr., Woodward, L.A., Callender, J.F., and Greer, A.R., 1979, Fractures in Cretaceous rocks from selected areas of San Juan Basin, New Mexico - Exploration implications: American Association of Petroleum Geologists Bulletin, v. 63, p. 598-607.

Greer, A.R., 1978a, Puerto Chiquito Mancos, east, *in* Fassett, J.E., Thomaidis, N.D., Matheny, M.L., and Ullrich, R.A., eds., Oil and Gas Fields of the Four Corners area, Volume II; Four Corners Geological Society, p. 464-467.

Greer, A.R., 1978b, Puerto Chiquito Mancos, west, *in* Fassett, J.E., Thomaidis, N.D., Matheny, M.L., and Ullrich, R.A., eds., Oil and Gas Fields of the Four Corners area, Volume II; Four Corners Geological, p. 468-471.

Gries, R., 1983, North-south compression of Rocky Mountain foreland structures, *in* Lowell, J.D., and Gries, R., eds., Rocky Mountain foreland basins and uplifts, Rocky Mountain Association of Geologists, p. 9-32.

Hallett, R.B., Long, P.E., Lorenz, J.C., and Bjornstad, B., 1999, Geology and thermal history of the Pliocene Cerro Negro volcanic neck and adjacent Cretaceous sedimentary rocks, west-central New Mexico, *in* Pazzaglia, F.J., Lucas, S.G., and Austin, G.S., eds., Albuquerque Geology, New Mexico Geological Society Guidebook, 50th Field Conference, p. 235-245.

Harstad, H., Teufel, L.W., and Lorenz, J.C., 1998, Drainage efficiency in naturally fractured tight gas sandstone reservoirs, SPE paper number 39974, Gas Technology Symposium: Alberta, Canada, Society of Petroleum Engineers, p. (not consecutively numbered).

Hart, B., Herrin, M., Nicolaissen, K., Ralser, S., Balch, B., and Cooper, S., 1999, Is the Pennsylvanian play in the San Juan Basin a fractured reservoir play? Lessons from Ute Dome, Petroleum Technology Transfer Council Symposium on Fractured Reservoirs: Characterization and Production: Farmington, New Mexico, Petroleum Technology Transfer Council Southwest Region, p. (not consecutively numbered).

Hawkins, J.M., Snyder, R.W., and Pahwa, S.B., 1977, How well logs were used to improve evaluation of a gas storage project: Journal of Petroleum Technology, p. 1550-1558.

Hilpert, L. S., 1969, Uranium resources of northwestern New Mexico, United States Geological Survey Professional Paper 603, 166 p.

Huffman, C., and Taylor, D., 1999, Relationship of hydrocarbon resources to basement faulting in the San Juan basin, *in* Cather, M., ed., Fractured Reservoirs: Characterization and Production, Petroleum Technology Transfer Council: Farmington, NM, p. not consecutively numbered.

Jentgen, R.W., 1977, Pennsylvanian rocks in the San Juan Basin, New Mexico and Colorado, *in* Fassett, J.E., ed., San Juan Basin III,, New Mexico Geological Society, 28th Field Conference, p. 129-132.

Keller, G.R., and Adams, D., 1992, Gravity and magnetic anomalies in the San Juan basin area, *in* Lucas, S.G., Kues, B.S., Williamson, T.E., and Hunt, A.P., eds., San Juan Basin IV, New Mexico Geological Society Guidebook, 43rd Field Conference, p. 133-134.

Kelley, V.C., 1950, Regional structure of the San Juan Basin, San Juan Basin, New Mexico and Colorado, New Mexico Geological Society Guidebook, First Field Conference, p. 101-108.

Kelley, V. C., 1955, Regional tectonics of the Colorado plateau and relationship to the origin and distribution of uranium, University of New Mexico Publications in Geology, Number 5: Albuquerque, New Mexico, 120 p.

Kelley, V.C., 1957, Tectonics of the San Juan basin and surrounding areas, *in* Little, C.J., ed., Geology of the San Juan Basin: Second Field Conference, Four Corners Geological Society, p. 44-52.

Kelley, V.C., 1963, Tectonic setting, *in* Kelley, V.C., ed., Geology and Technology of the Grants Uranium Region: New Mexico Bureau of Mines and Mineral Resources Memoir 15, p. 19-20.

Kelley, V.C., 1967, Tectonics of the Zuni-Defiance region, New Mexico and Arizona, *in* Trauger, F.D., ed., Defiance-Zuni-Mt. Taylor Region Arizona and New Mexico, New Mexico Geological Society, 18th Field Conference, p. 28-31.

Kelley, V.C., and Clinton, N.J., 1960, Fracture systems and tectonic elements of the Colorado plateau: Albuquerque, University of New Mexico Press, 104 p.

Kirk, A.R., and Condon, S.M., 1986, Structural control of sedimentation patterns and the distribution of uranium deposits in the Westwater Canyon Member of the Morrison Formation, northwestern New Mexico -- A subsurface study, *in* Turner-Peterson, C.E., Santos, E.S., and Fishman, N.S., eds., A Basin Analysis Case Study: Morrison Formation, Grants Uranium Region, New Mexico, Volume A179: Tulsa, Energy Minerals Division of The American Association of Petroleum Geologists, p. 105 - 143.

Kirk, A. R., and Sullivan, M. W., 1987, Geologic map of the Dalton Pass quadrangle, McKinley County, New Mexico, MAP GQ - 1593: United Sates Geological Survey, scale 1:24,000.

Laubach, S.E., 1992, Fracture networks in selected Cretaceous sandstones of the Green River and San Juan basins, Wyoming, New Mexico, and Colorado, *in* Schmoker, J.W., Coalson, E.B., and Brown, C.A., eds., Geological Studies Relevant to Horizontal Drilling; Examples from Western North America, Rocky Mountain Association of Geologists, p. 115-127.

London, W.W., 1972, Dolomite in Flexure-Fractured Petroleum Reservoirs in New Mexico and Colorado: American Association of Petroleum Geologists Bulletin, v. 56, p. 815-821.

Long, J.C.S., Aydin, A., Brown, S.R., Einstein, H.H., Hestir, K., Hsieh, P.A., Myer, L.R., Nolte, K.G., Norton, D.L., Olsson, O.L., Paillet, F.L., Smith, J.L., and Thomsen, L., 1997, Rock Fracture and Fluid Flow: Washington, D.C., National Academy Press, p. 551.

Lorenz, J.C., 1999, Stress-Sensitive Reservoirs: Journal of Petroleum Technology, p. 61-63.

Lorenz, J. C., Basinski, P. M., Head, C. F., and Peabody, W. W., 1999, Complex natural fracture patterns in Dakota Sandstone reservoirs of the San Juan Basin: American Association of Petroleum Geologists 1999 Annual Meeting Expanded Abstracts, April 11 - 14, 1999, San Antonio, TX: American Association of Petroleum Geologists Bulletin, v. 83 (1999), no. 13 (Supplement), (not consecutively numbered).

Lorenz, J.C., and Finley, S.J., 1989, Differences in fracture characteristics and related production: Mesaverde Formation, Northwestern Colorado: Society of Petroleum Engineers Formation Evaluation, v. 4, p. 11-16.

Lorenz, J.C., Finley, S.J., and Warpinski, N.R., 1990, Significance of coring-induced fractures in Mesaverde core, Northwestern Colorado: American Association of Petroleum Geologists Bulletin, v. 74, p. 1017-1029.

Lorenz, J.C., and Hill, R.E., 1991, Subsurface fracture spacing: comparison of inferences from slant/horizontal core and vertical core in Mesaverde reservoirs: Society of Petroleum Engineers Paper 21877: Joint Rocky Mountain Section Meeting and Low-Permeability Reservoir Symposium, p. 705-716.

Lorenz, J.C., and Hill, R.E., 1992, Measurement and Analysis of fractures in core, *in* Schmoker, J.W., Coalson, E.B., and Brown, C.A., eds., Geological studies relevant to Horizontal drilling: Examples from Western North America, Rocky Mountain Association of Geologists, p. 47-59.

Lorenz, J.C., Warpinski, N.R., Branagan, P.T., and Sattler, A.R., 1989, Fracture characteristics and reservoir behavior of stress-sensitive fracture systems in flat-lying lenticular formations: Journal of Petroleum Technology, v. 41, p. 615-622.

Lowell, J.D., 1974, Plate tectonics and foreland basement deformation: Geology, v. 2, p. 275-278.

Molenaar, C.M., 1977, Stratigraphy and depositional history of Upper Cretaceous rocks of the San Juan Basin area, New Mexico and Colorado, with a note on economic resources, *in* Fassett, J.E., ed., Guidebook of San Juan Basin III, northwestern New Mexico, Volume 28, New Mexico Geological Society, p. 159-166.

Molenaar, C.M., 1988, Stratigraphic cross section showing upper Cretaceous rocks across the San Juan Basin, New Mexico and Colorado, *in* Fassett, J.E., ed., Geology and Coal-Bed Methane Resources of the Northern San Juan Basin, Colorado and New Mexico, Rocky Mountain Association of Geologists, p. 21.

Molnar, P., and Tapponnier, P., 1977, The relation of the tectonics of eastern Asia to the India-Eurasia collision: an application of slip line field theory to large scale continental tectonics: Geology, v. 5, p. 212-216.

Muehlberger, W.R., 1967, Geology of Chama Quadrangle, New Mexico: New Mexico Bureau of Mines and Mineral Resources Bulletin, v. 89, p. 114.

Nelson, R.A., 1985, Geologic analysis of naturally fractured reservoirs: Houston, Gulf Publishing Company, 360 p.

Olsson, W. A., Lorenz, J. C., and Cooper, S. P., 2001, Multiply-Oriented Conjugate Deformation Bands: Effects On Reservoirs And Constraints On Stress History: American Association of Petroleum Geologists 2001 Annual Meeting Abstracts, June 3-6, 2001, Denver, Colorado.

Ortega, O., and Marrett, R., 2000, Prediction of macrofracture properties using microfracture information, Mesaverde Group sandstones, San Juan basin, New Mexico: Journal of Structural Geology, v. 22, p. 571-588.

Ouenes, A., Zellou, A., Nova, T., Basinski, P.M., and Head, C.F., 1998, Practical use of neural networks in tight gas fractured reservoirs: Application to the San Juan basin: paper number SPE 39965, SPE Rocky Mountain Regional/Low Permeability Reservoirs Symposium and Exhibition: Denver, Colorado, April 5-8, 1998, Society of Petroleum Engineers, p. 573-580.

Owen, D.E., 1966, Nomenclature of Dakota Sandstone (Cretaceous) in the San Juan Basin, New Mexico and Colorado: American Association of Petroleum Geologists Bulletin, v. 50, p. 1023-1028.

Owen, D.E., and Siemers, C.T., 1977, Lithologic correlation of the Dakota Sandstone and adjacent units along the eastern flank of the San Juan Basin, New Mexico, *in* Fassett, J.E., ed., Guidebook of San Juan Basin III, northwestern New Mexico, Volume 28, New Mexico Geological Society, p. 179-183.

Powell, J.S., 1973, Paleontology and sedimentation of the Kimbeto Member of the Ojo Alamo Sandstone, *in* Fassett, J.E., ed., Cretaceous and Tertiary of the southern Colorado Plateau: Four Corners Geological Society, p. 222-224.

Ralser, S., and Hart, B. S., 1999, Structural evolution of Ute Dome, NW New Mexico: implications for the development of the Hogback Monocline, Abstract 51730, Geological Society of America Annual Meeting Abstracts with Programs, Denver, Colorado, p. A131.

Rice, D.D., 1983, Relation of natural gas composition to thermal maturity and source rock type in San Juan basin, northwestern New Mexico and southwestern Colorado: American Association of Petroleum Geologists Bulletin, v. 67, p. 1199-1218.

Santos, E.S., and Turner-Peterson, C.E., 1986, Tectonic setting of the San Juan Basin in the Jurassic, *in* Turner-Peterson, C.E., Santos, E.S., and Fishman, N.S., eds., A Basin Analysis Case Study: Morrison Formation, Grants Uranium Region, New Mexico, Volume A179: Tulsa, Energy Minerals Division of The American Association of Petroleum Geologists, p. 27 - 33.

Sears, J. D., 1925, Geology and coal resources of the Gallup-Zuni basin, New Mexico, United States Geological Survey Bulletin 767, 53 p.

Sikkink, P.G.L., 1986, Lithofacies relationships and depositional environment of the Tertiary Ojo Alamo Sandstone and related strata, San Juan Basin, New Mexico and Colorado, *in* Fassett, J.E., and Rigby, J.K., Jr., eds., The Cretaceous-Tertiary boundary in the San Juan and Raton Basins, New Mexico and Colorado: Geological Society of America Special Paper 209, p. 81-104.

Slack, P. B., 1973, Structural geology of the northeast part of the Rio Puerco fault zone, Sandoval County, New Mexico, University of New Mexico unpublished M.S. thesis, 74p.

Slack, P.B., and Campbell, J.A., 1976, Structural Geology of the Rio Puerco fault zone and its relationship to central New Mexico Tectonics, *in* Woodward, L.A., and Northrop, S.A., eds., Tectonics and Mineral Resources of Southwestern North America, New Mexico Geological Society Special Publication No. 6, p. 46-52.

Steven, T.A., 1975, Middle Tertiary volcanic field in the southern Rocky Mountains, Cenozoic history of the southern Rocky Mountains, Geological Society of America Memoir 144, p. 75-93.

Tapponnier, P., and Molnar, P., 1976, Slip line field theory and large-scale continental tectonics: Nature, v. 264, p. 319-324.

Tapponnier, P., Peltzer, G., and Armijo, R., 1986, On mechanics of the collision between India and Asia, *in* Coward, M. P., and Ries, A. C., eds., Collision Tectonics, Geological Society Special Publication No. 19, p. 115-157.

Taylor, D.J., and Huffman, A.C., Jr., 1988, Overthrusting in the northwestern San Juan basin, New Mexico - A new interpretation of the Hogback monocline: United States Geological Survey Research on Energy Resources - Program with Abstracts, p. 60-61.

Taylor, D.J., and Huffman, A.C., Jr., 1998, Map showing inferred and mapped basement faults, San Juan basin and vicinity, New Mexico and Colorado, United States Geological Survey Investigation Series I-2641.

TerBest, H., Jr., 1997, Open apertures, fracture orientations, and their correlation to production in the Mesaverde Group in the San Juan Basin, Natural Fracture Systems in the Southern Rocky Mountains, Four Corners Geological Society, p. 147.

Teufel, L. W., and Farrell, H. E., 1992, Interrelationship between in situ stress, natural fractures, and reservoir permeability anisotropy: A case study of the Ekofisk Field, North Sea, In Proceedings of Fractured and Jointed Rock Conference, Lake Tahoe, Ca, June 3-5, 1992, (not consecutively numbered).

Tezack, M.A., 1978, Ute Dome Dakota, *in* Fassett, J.E., ed., Oil and gas fields of the Four Corners area, Volume 2, Four Corners Geological Society, p. 543-545.

Thaden, R.E., and Zech, R.S., 1984, Preliminary structure contour map on the base of the Cretaceous Dakota Sandstone in the San Juan Basin and Vicinity, New Mexico, Arizona, Colorado, and Utah: United States Geological Survey Miscellaneous Field Studies Map MF-1673.

Tremain, C.M., Laubach, S.E., and Whitehead III, N.H., 1991, Coal fracture (cleat) patterns in Upper Cretaceous Fruitland Formation, San Juan Basin, Colorado and New Mexico - implications for coalbed methane exploration and development, *in* Schwochow, S.D., ed., Coalbed methane of western North America: Rocky Mountain Association of Geologists, 1991 guidebook, p. 49-59.

Turner-Peterson, C.E., 1989, Recent geologic studies in the San Juan Basin: Highlights and new directions, *in* Lorenz, J.C., and Lucas, S.G., eds., Energy Frontiers in the Rockies, Albuquerque Geological Society, p. 177-188.

Whitehead, N.H., III, 1997, Fractures at the surface, San Juan Basin, New Mexico and Colorado, *in* Hoak, T.E., Klawitter, A.L., and Blomquist, P.K., eds., Fractured Reservoirs: Characterization and Modeling Guidebook, Rocky Mountain Association of Geologists, p. 27-42.

Woodward, L.A., 1983, Potential oil and gas traps along the overhang of the Nacimiento uplift, northwestern New Mexico, *in* Lowell, J.D., and Gries, R., eds., Rocky Mountain Foreland Basins and Uplifts, Rocky Mountain Association of Geologists, p. 213-218.

Woodward, L. A., 1987, Geology and mineral resources of Sierra Nacimiento and vicinity, New Mexico, Memoir 42, New Mexico Bureau of Mines and Mineral Resources, Memoir 42, 85 p.

Woodward, L.A., Anderson, O.J., and Lucas, S.G., 1997, Tectonics of the Four Corners region of the Colorado Plateau, Mesozoic Geology and Paleontology of the Four Corners Region, New Mexico Geological Society Guidebook, 48th Field Conference, p. 57-64.

Woodward, L.A., Hultgren, M.C., Crouse, D.L., and Merrick, M.A., 1992, Geometry of Nacimiento-Gallina fault system, northern New Mexico, *in* Lucas, S.G., Kues, B.S., Williamson, T.E., and Hunt, A.P., eds., San Juan Basin IV, New Mexico Geological Society Guidebook, 43rd Field Conference, p. 103-108.

Woodward, L.A., Kaufman, W.H., and Anderson, J.B., 1972, Nacimiento fault and related structures, northern New Mexico: Geological Society of America Bulletin, v. 83, p. 2383-2396.

Woodward, L.E., and Callender, J.F., 1977, Tectonic framework of the San Juan Basin, *in* Fassett, J.E., ed., San Juan Basin III, New Mexico Geological Society, 28th Field Conference, p. 209-212.

Yale, D.P., Strubhar, M.K., and El Rabaa, A.W., 1993, Determination of hydraulic fracture direction, San Juan basin: paper number SPE 25466, Production Operations Symposium: Oklahoma City, Oklahoma, March 21-23, 1993, Society of Petroleum Engineers, p. 543-553.